Faculté des sciences économiques,
sociales, politiques et de communication
École des sciences politiques et sociales (PSAD)

Integrating demographic and epidemiological transitions into climate impact projections

A case study with temperature-mortality association in Antananarivo

Auteur : Kuijt Emmanuelle
Promoteur : Masquelier Bruno
Lecteur : Bocquier Philippe
Année académique 2023-2024
Master en sciences de la population et du développement - Finalité Démographie

Preface

"The principle of common but differentiated responsibilities underscores the unfairness of climate change impacts on Africa. While African nations have historically emitted minimal greenhouse gases, they are now facing the brunt of climate-related disasters, leading to increased mortality rates and exacerbating poverty and inequality." - Prof. Saleemul Huq, Director, International Centre for Climate Change and Development (ICCCAD)

Acknowledgments

I would first like to thank the promoter of this thesis, Bruno Masquelier, for his trust, invaluable assistance, constructive feedback, and generous time. I also thank him for being one of the most inspiring lecturers I have encountered during my studies.

I would also like to express my gratitude to Philippe Bocquier, the reader of this thesis, for his insightful lectures and for encouraging me to pursue the EDSD program. His guidance has greatly helped me, and I hope this program will enable me to continue my journey in research.

Furthermore, I extend my thanks to all the other teachers from whom I have had the privilege to learn from during this master's degree. Finally, a special acknowledgment goes to Alice Rees for her bright and cheerful presence, which has made my two years as a student in DEMO even more enjoyable.

Many thanks also go to the members of the CRED for their feedback on the advancement of my work, a special thought goes to Emilie Castin for her availability.

I would also like to thank Benjamin Schlüter for his valuable knowledge on code debugging and guidance regarding the mastering of this tutorial.

A special thank you goes to my incredible mother, Mary, for her meticulous proofreading, nurturing my passion for learning, and raising me with a strong foundation in English. I am equally grateful to Manon Decroly, whose support made the thesis-writing process significantly easier and thinking about the future more reassuring. Lastly, I thank Mathieu Santacreu for his companionship during our quality breaks and climbing sessions, which provided much-needed relief and a chance to clear my mind.

Ethical Declaration

"I solemnly declare that this dissertation has been written by me alone, without soliciting any illicit external assistance, that it is not a reproduction of work submitted to another institution for evaluation, and that it has never been published, in whole or in part. All information (ideas, sentences, graphs, maps, tables, etc.) borrowed from or referencing primary or secondary sources are properly referenced according to the prevailing academic method. I declare that I have read and adhere to the Code of Ethics for students regarding borrowing, quoting, and using various sources, and understand that plagiarism constitutes a serious offense."



Contents

1 Introduction **1**

1 Background . . . 1
2 Literature review . . . 3
2.1 Climate change and adverse health effects . . . 3
2.1.1 The effects of climate change on health . . . 3
2.1.2 The climate change paradox . . . 7
2.2 Defining and choosing exposure . . . 8
2.2.1 Defining the exposure-response association . . . 8
2.2.2 Diverse exposures . . . 9
2.3 Empirical findings . . . 9
2.3.1 The association between health and temperature in SSA . . . 9
2.3.2 Factors influencing the exposure-response association . . . 11
2.4 Methods for measuring the exposure-response association . . . 12
2.5 Gap in literature in LLMICs . . . 13
2.5.1 Scarcity in existing studies . . . 13
2.5.2 Interactions between health-related effects of climate change and epidemiological transitions . . . 15
3 Research context : Antananarivo, Madagascar . . . 18
3.1 Antananarivo, Madagascar: current climate profile . . . 18
3.2 Antananarivo, Madagascar: projected climate profile and associated health risks . . . 21
3.3 Antananarivo's epidemiological transition . . . 22
4 Research question and hypotheses . . . 25

2 Data and Methods **29**

1 Data . . . 29
1.1 Exposure : daily mean temperature . . . 29
1.1.1 Dataset for the 2000-2015 period : NOAA data . . . 29
1.1.2 Dataset for the 2016-2100 period : ISIMIP data . . . 31
1.2 Outcome : daily deaths . . . 33
2 Methods . . . 35

2.1 Distributed Lag Non-linear Models 35
2.1.1 Steps for the model 35
2.1.2 Modelling choices 38
2.2 Sensitivity analyses 40
2.2.1 Sensitivity test 1: Allowing for age-specific relative risks . . . 41
2.2.2 Sensitivity test 2: Allowing for changes in the age composition of deaths in the future 42
2.2.3 Sensitivity test 3: Allowing for cause-specific relative risks . . 44
2.2.4 Sensitivity test 4: Sensitivity to control for seasonality 45
2.2.5 Sensitivity test 5 : Controlling for the effect of modelled exposure data 45

3 Results **47**
1 Allowing for age-specific relative risks 47
1.1 Main results: models disaggregated by age 47
1.1.1 Age-specific relative risks and seasonality 48
1.1.2 Projected temperature and calibration 52
1.1.3 Age-specific projected health outcomes 56
1.2 Comparing age-specific and overall models 61
2 Allowing for changes in the age composition of deaths in the future 63
2.1 Comparing mortality due to heat and cold: constant and projected . . 63
3 Allowing for cause-specific relative risks 72
3.1 Trends in cause-of-death distribution 72
3.2 Cause-specific relative risks 74
3.2.1 Cardiovascular diseases 74
3.2.2 Infectious diseases 77
3.2.3 Nutritional deficiencies 80
3.2.4 Respiratory system diseases 82
3.3 Cause-specific health outcomes 83
4 Sensitivity to control for seasonality 85
5 Controlling for the effect of modelled exposure data 86

4 Discussion **89**
1 Main results 89
1.1 Age-disaggregated models 90
1.2 Associations between temperature and mortality by cause 91
1.3 The lagged temperature-mortality association 93
1.4 Projecting the burden of non-optimal temperatures 94
1.5 High seasonality of deaths for children 94

1.6 Measured risk using modelled and measured data 95
2 Study limits 96
3 Conclusions 98

References **100**
List of Figures 117
List of Tables 122

Figure appendix **123**

Table appendix **127**

Code appendix **129**
0.1 Retrieving data 129
0.2 DLNM and Projections - The Vicedo-Cabrera et al. (2019) method . . 129
0.3 Exponential Projections 146
0.4 Recoding ICD 9 codes to larger groups 151

Introduction

1 Background

Climate change is recognised as an existential threat to humanity, in the words of UN Secretary-General Antonio Gutierrez. Before 2070, between 1 and 3 billion people will find themselves outside the climatic conditions that we have experienced for at least 6000 years under the worst-case scenario (Xu et al., 2019). Yet, it is equally crucial to grasp the paradoxical reality: those who have contributed the least to climate change are the ones experiencing its most severe impacts (Allafta and Opp, 2024). Presently, Sub-Saharan Africa (SSA) contributes the least to anthropogenic emissions, yet it is estimated to face the highest burden of climate change (Amegah et al., 2016). In light of these changes the region records an increasing number of extreme climatic events such as heat waves (Engdaw et al., 2022), hurricanes and floods (Serdeczny et al., 2017). SSA also faces other challenges such as alterations in patterns of vector-borne diseases (Giesen et al., 2020) and poorer air quality (Abera et al., 2021).

Despite growing awareness, research on the impacts of global warming in SSA remains scarce, and this is aggravated by the region's limited capacity to mitigate these changes (Haines et al., 2006; Saeed et al., 2023). Moreover, the scarcity of existing studies limits the conclusions that can be drawn, particularly given the inconsistencies in methods and results (Pradyumna and Sankam, 2022; Amegah et al., 2016). Given the plethora of existing outcomes, this thesis tackles one of the effects of climate change : the increase in ambient temperature. For the analysis of projected temperatures, Distributed Lag Non-Linear Models (DLNMs) are emerging as the preferred method for analysing exposure-response associations, offering the ability to project mortality outcomes in the face of further climate warming. This method accounts for lagged and potentially non-linear effects of exposures on health outcomes, offering a comprehensive understanding of the exposure-response relationship (Gasparrini,

2011). But this method demanding robust, long term and timely data (Gasparrini et al., 2015), has rarely been applied in Sub-Saharan Africa due to lacking data.

In the case of Antananarivo, Madagascar, where mortality and temperature data are available, there is a promising opportunity to apply DLNMs in a context where this association has never been studied before, despite the region's high vulnerability to climate change. With a population of 1.28 million, Antananarivo faces significant risks from climate variations, particularly due to its population's dependence on rice harvests and the condition of its healthcare and sanitary systems (Rousseau et al., 2023; Waltisperger et al., 2005). However, the city grapples with a dual burden of communicable and noncommunicable diseases (Schlüter et al., 2020), coupled with a progressively aging population (see the diminishing pyramid base for children under 5 and the increase in older age groups in figure 1), which complicates the task of determining its sensitivity to climate in this evolving landscape.

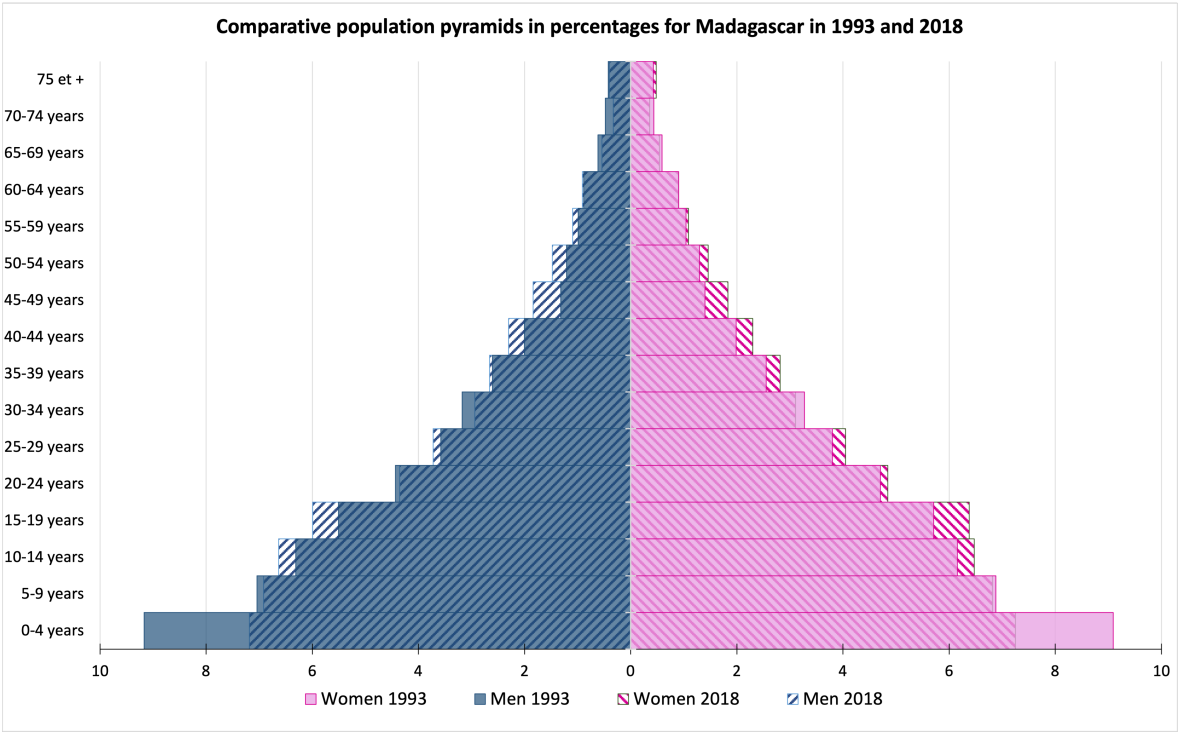


Figure 1: **Population pyramids for the Malagasy population in 1993 and 2018.** *The data was extracted from the INSTAT (Institut National de la Statistique) reports from the General Population and Housing Census of 1993 and 2018. The data was accessed on* `https://www.instat.mg/thematique/population`.

Therefore, the aim of this thesis is to use the available data and understanding of Antananarivo's population to asses the current exposure-response association and develop context-specific projections of the future impacts of global warming in the city. Our research questions

are as follows: **what are the prevailing relationships between mortality and temperatures in Antananarivo today, and how might they change in the future?** Answering this question also brings up the following : **how effectively do DLNMs apply to LLMICS in subtropical climate contexts?** And **how does incorporating shifts in epidemiological and demographic transitions into the model improve its relevance and accuracy?**

To address these questions, we will use DLNMs, more precisely the tutorial developed by Vicedo-Cabrera et al. (2019) and disaggregate our analysis by age group to accommodate variations in vulnerability across different age brackets. We will assess the outcomes of various projections, comparing those with and without adjustments for changes in population structure, and examine the varying sensitivities of different causes of death. Then, we will assess the impact of considering the mediating effect of seasonality. Finally, we will test the outcomes of using modelled temperatures instead of measured temperatures. Our analysis will use the death notification data collected from 2000 to 2015 by the Municipal Bureau of Hygiene across five districts of the city, along with mean daily temperatures sourced from the Natinoal Oceanic and Atmospheric Administration (NOAA) database.

This thesis is structured as follows: We begin with a review of existing methodological and empirical findings on the subject, followed by a descriptive overview of Antananarivo and an explanation of why we selected this case study. Next, we outline the thesis objectives along with our hypotheses. In the second part, we introduce our data and the methodology we have chosen to analyse them, outlining how we intend to address our research questions. Subsequently, we present our findings. Finally, we discuss the results, address the limitations of this study, and draw conclusions.

2 Literature review

2.1 Climate change and adverse health effects

2.1.1 The effects of climate change on health

Climate change, which we will be using interchangeably with the notion of global warming, constitutes a major challenge for human populations, notably in regard to human health. This change in ambient temperatures is partly due to greenhouse gas emissions, which are attributable to the growing anthropogenic activities. This phenomenon is widely recognised by the scientific community (McMichael et al., 2006).

In this context rises an increasing interest in the understanding of the driving forces, the levels of action and the different health outcomes of such changes in climate. Hence, the World Health Organisation (WHO) has developed the Driving forces, Pressure, State, Exposure, Effect and Action (DPSEEA) framework to allow for efficient monitoring, help and support on environmental health (WHO, 1999). This framework presented in figure 2 highlights the various scales on which one can focus when it comes to environmental and human health.

Moreover, when we look into how the environment impacts human health, researchers have uncovered various ways in which climate can affect population well-being. To outline these pathways, McMichael et al. (2006) developed a schematic summary, depicted in figure 3. There, the authors include the notion of mitigation which refers to prevention (the reduction of greenhouse gas emissions) and adaptation which entails intervention to diminish adverse health effects. The addition of these terms allows to understand the levels at which one can act to reduce climate change, or later, the effects of these changes on health.

In more details, other authors have led research on the specific outcomes of climate change on human health. Generally, figure 4 built by Ebi et al. (2021) represents the paths through which warm weather can affect health (such as through cardiovascular strain or critical organ failure for example). Furthermore, increased temperatures also affect human well-being as it increases the risks of dying from many causes such as cardiovascular diseases, respiratory diseases, cerebrovascular diseases, genitourinary diseases, diabetes, dehydration, hypertension etc... (Ebi et al., 2021).

Through many possible pathways, global warming affects many lives, and is projected to affect many more in the future. In the case of exposure to heat in Africa, Marcotullio et al. (2021) have studied future urban heat-waves and have shown that by the 2100 horizon 300 million Africans may be exposed to 15-day heat waves of at least 42°C without the UHI (Urban Heat Island) effect[1]. This is projected to be much higher (950 million) if the effect of UHIs is considered.

[1]The Urban Heat Island effect corresponds to the phenomenon by which temperatures are higher in urban areas due to human constructions and activities (Yang et al., 2016).

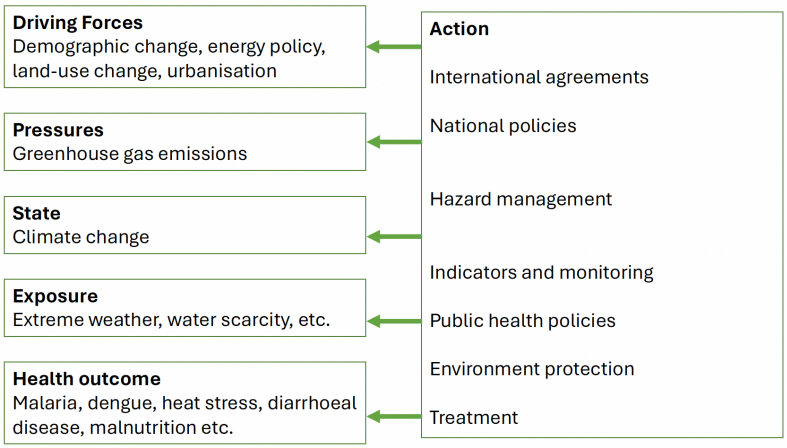


Figure 2: **The DPSEEA framework for environmental health risk assessment, applied to climate change.**
Source : Kovats et al. (2005)

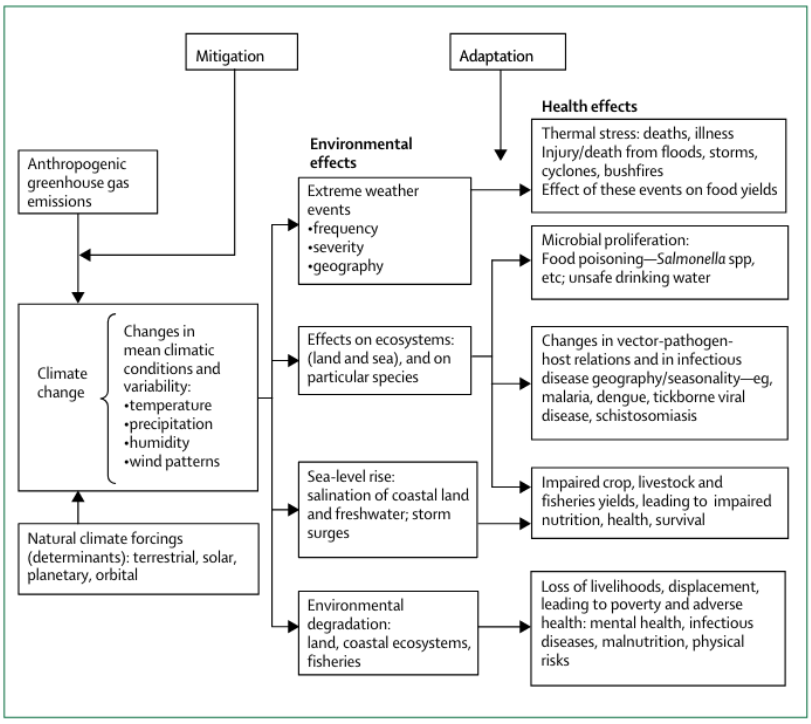


Figure 3: **Schematic summary of main pathways by which climate change affects population health.**
Source : McMichael et al. (2006).

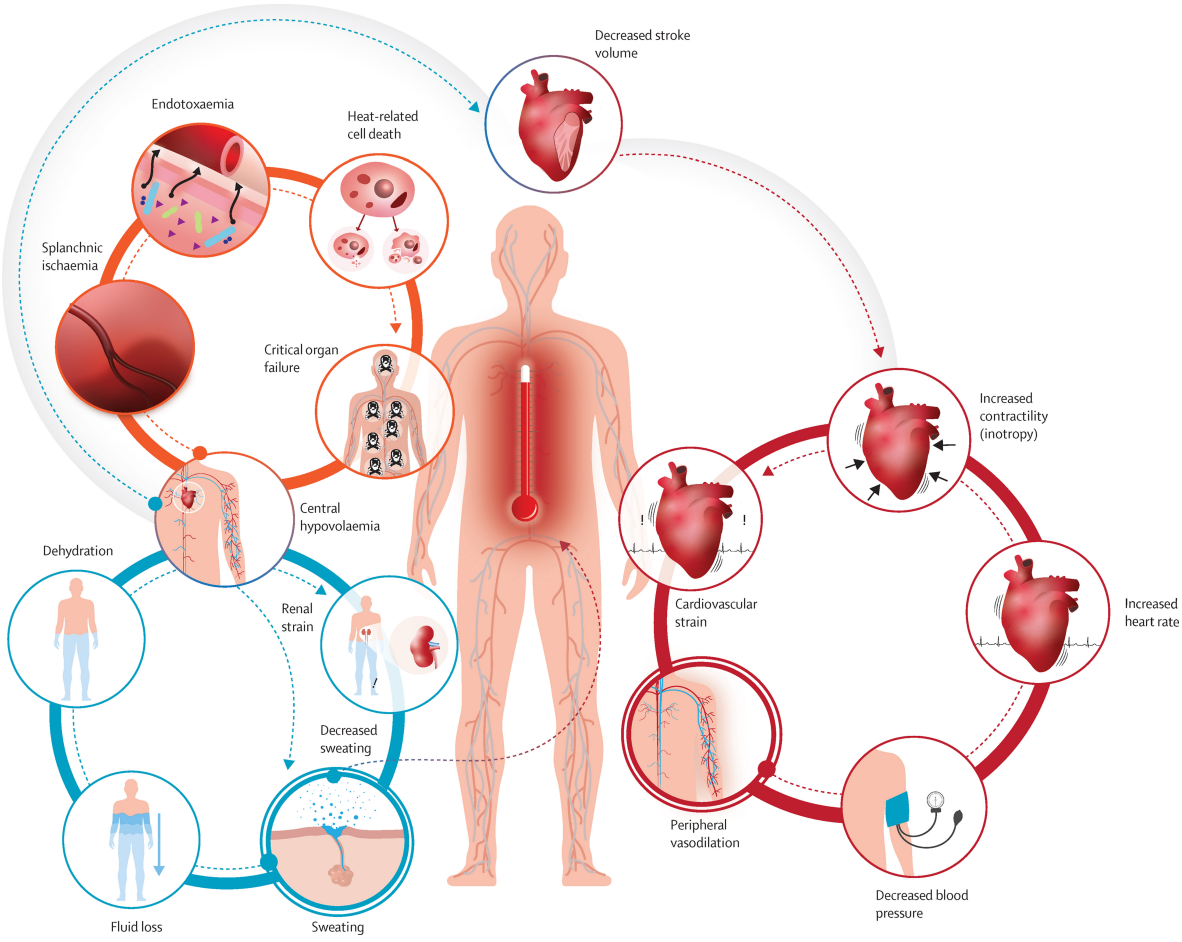


Figure 4: **Illustration of the physiological pathways of human heat strain.**
Source : Ebi et al. (2021).

2.1.2 The climate change paradox

While we now have a broad understanding of the pathways through which climate affects health, further research is required to delve deeper into the specifics, especially in local contexts. The need for specific case studies stems from the disparate effects of climate change globally and the paradox according to which those who emit the less are those who suffer from the highest burden of disease due to climate change (Allafta and Opp, 2024). This paradox which highly concerns LLMICS (Low and Lower Middle Income Countries) can be observed with the analysis of figures 5 and 6, where we observe that those who emit the least are often those who are projected to carry the highest burden in the future.

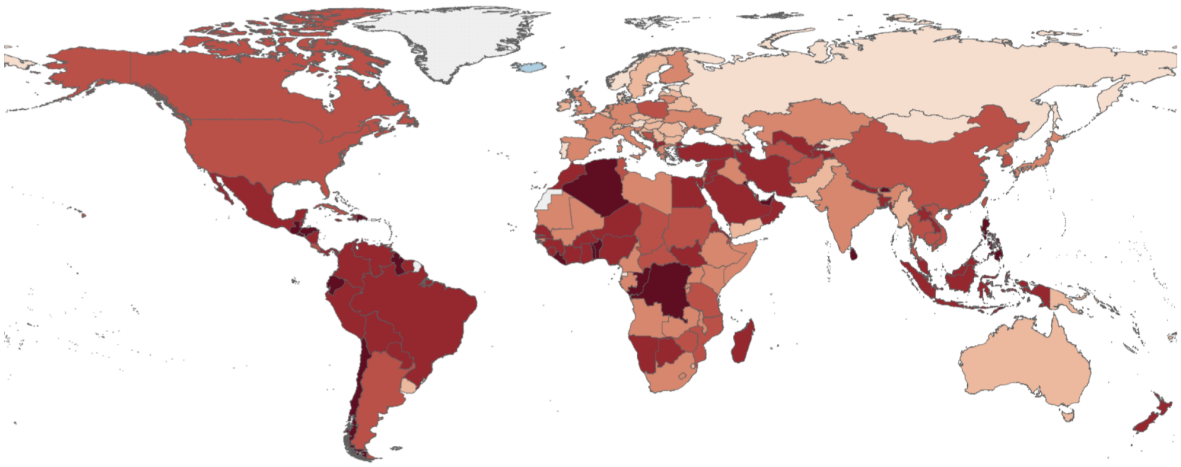


Figure 5: **Heat-related Mortality.**
Percent change in annual deaths[2]: Blue corresponds to negative change whereas red represents positive changes (which go up to 200%).
Source : (Romanello et al., 2023).

[2]Percent change in annual heat-related deaths of adults over 65 years old in 2018-2022 compared to 2000-2004. Compares with counterfactual scenario in which temperatures are unchanged from baseline values.

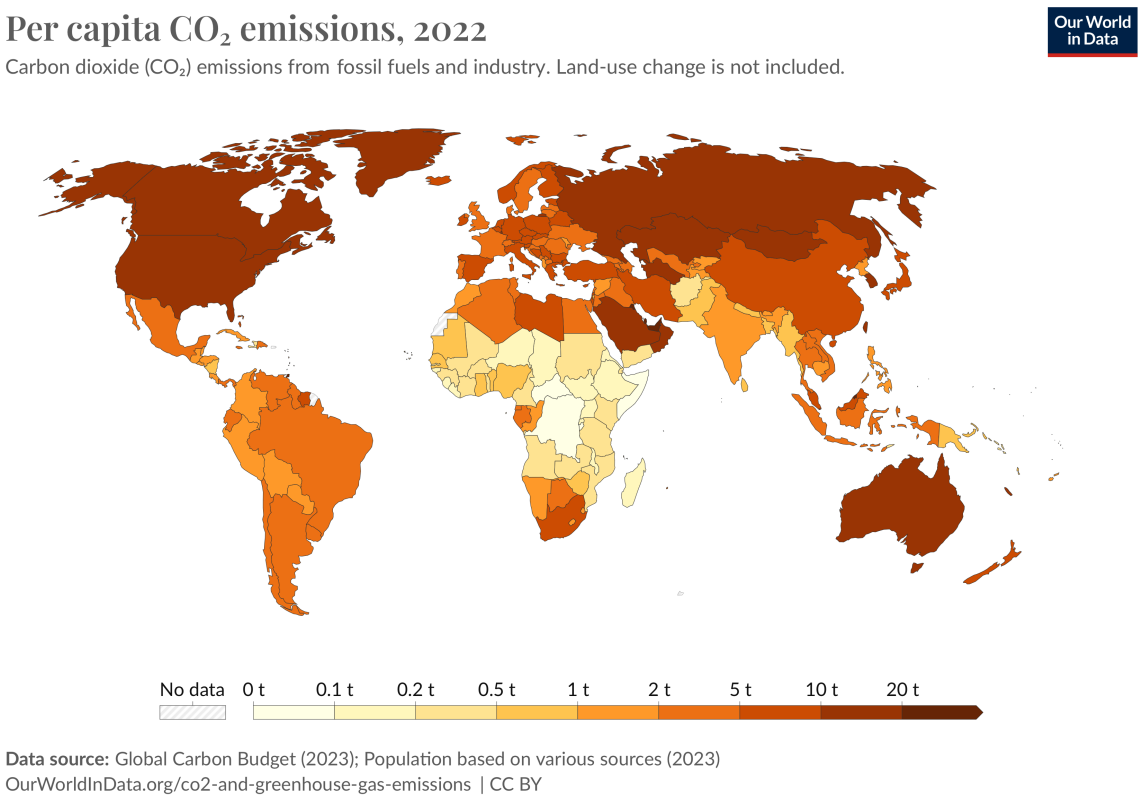


Figure 6: **Per capita CO2 emissions in 2022.**
Extracted from : https://ourworldindata.org/co2-emissions.

2.2 Defining and choosing exposure

2.2.1 Defining the exposure-response association

The references mentioned above have outlined general pathways through which global warming can impact human health. In this thesis, our goal is to quantify the effects of a specific exposure on health outcomes. For context, exposure is defined as the "*presence of people; livelihoods (. . .) in places that could be adversely affected by a climate hazard*" (O'Neill et al., 2014) (p. 392) and will be examined in relation to the measured sensitivity or responsiveness to the predetermined exposure. Given the uncertainty surrounding the precise effects of climate change on health, focusing on a specific exposure allows us to explore specific relationships between the exposure and observed events. Focusing on a single exposure also enhances the interpretability of the measured relationship and facilitates refinements when seeking explanations for the pathways between exposure and events.

2.2.2 Diverse exposures

When analysing the impacts of environmental changes on health, researchers have explored various exposure variables, including ambient temperatures (both indoors and outdoors) (Anderson and Bell, 2009; Barreca et al., 2016; Vicedo-Cabrera et al., 2019; Levy et al., 2016), humidity (Armstrong, 2006), rainfall (Motlogeloa and Fitchett, 2024), and air pollution (Bhaskaran et al., 2013; Shirinde and Wichmann, 2023). Reviewing existing studies underscores the importance of justifying the choice of exposure based on factors like data availability, relevance to the study area, and comparability with other research. Among these exposure variables, ambient temperature emerges as a prioritised exposure due to its ease of monitoring, relevance for global warming studies, and detectable changes. Conversely, changes in rainfall, while also indicative of changes in climate and potential impacts on population health, are less favoured due to the difficulty of detecting their variations (Nematchoua et al., 2018). When it comes to combining exposure events, the literature has shown that different climatic variables often highly interfere with one another which often makes the model more complicated to analyse but not less relevant nonetheless (Motlogeloa and Fitchett, 2024; Armstrong, 2006).

Additionally, the literature diverges on how to measure these exposures. While some studies consider long-term exposure encompassing all variations in the exposure variable (Vicedo-Cabrera et al., 2019), others focus on specific events such as heatwaves (Xu et al., 2019; Ncongwane et al., 2021a). Studies focusing on specific events tend to suggest higher mortality increases during heatwaves compared to those examining broader time frames. For instance, studies on temperature analysis during heatwaves report increases in mortality ranging from 8.9% to 12.1%, while studies covering longer time frames document lower attributable mortality rates ranging from 1.6% to 2% (Gasparrini et al., 2015).

2.3 Empirical findings

2.3.1 The association between health and temperature in SSA

Now that we have discussed the general impacts of climate change on health and outlined our chosen exposure (temperature), we focus on specific health-temperature associations that make empirical sense in Sub-Saharan Africa. It is important to note that not all potential associations have been empirically verified due to limited research in this area. This aspect is discussed comprehensively by Amegah et al. (2016), who provide an in-depth analysis of the potential health outcomes linked to climate change in SSA. Therefore, this section aims to highlight the documented causes that have been measured or are likely associated with

climate change in this region.

First, Amegah et al. (2016) express that changes in climate are expected to highly increase the occurrence of infectious diseases in the region. Even though evidence remains quite sparse for Sub-Saharan Africa, many studies point towards this. These studies explain that changes in temperatures should expand the time frame for pathogen replication (Huq et al., 1983) or favor the replication of food spoilage microorganisms (Amegah et al., 2016). Hence, increased temperatures are expected to increase the prevalence of infectious diseases such as water borne diseases like cholera (Lipp et al., 2002) or diarrhoeal diseases (Klein and Rasoanomenjanahary, 2023; Kolstad and Johansson, 2011; Naumova et al., 2007). Additionally, it must be said that these infectious diseases do not affect all age groups equally. Indeed, there is a tendency for infectious diseases to mostly affect younger population subsets. This has been shown in the case of malaria (Carneiro et al., 2010) and diarrhoeal diseases for example (Walker and Black, 2010). But the relevance of studying the effects of climate on infectious diseases is highly relevant for older age groups in SSA where authors have shown that with a dual burden of communicable and non-communicable diseases (Gavazzi et al., 2004; Dalal et al., 2011), it is important to study the effects of these diseases for older population subsets too (Carneiro et al., 2010; Walker and Black, 2010).

Another temperature related cause of death in Sub-Saharan Africa is under-nutrition (Amegah et al., 2016). This is even more a concern given the impact of variations in climate and temperature extremes on crop yields which are significantly associated with undernourishment (Phalkey et al., 2015). But this threat, even though it is significantly associated to changes in climate mostly affects child health. Indeed, Smith and Haddad (2015) have shown that 40% of children (under 5 years old) are stunted in SSA, and Baker and Anttila-Hughes (2020) have further demonstrated that warmer temperatures are associated with poorer child nutrition.

Then, given the double burden of communicable and non-communicable diseases in SSA, we outline the importance of studying climate sensitive NCDs. First, Dalal et al. (2011) have shown that the growing prevalence of NCDs in SSA requires more studies towards the effects of climate change on these causes of death. In this context, cardiovascular diseases and respiratory diseases are presented as the most common associated causes of death with temperature variations (Campbell and Woodruff, 2006). But the lack of empirical evidence of this association in SSA makes it difficult to draw substantive conclusions (Amegah et al., 2016). Indeed, Michelozzi et al. (2009) and Ye et al. (2012) have shown the effects of heightened temperatures on cardiovascular mortality, but there remains lacking evidence of this association in SSA, underlining the need to conduct further studies. D'Amato et al. (2014) and Michelozzi et al. (2009) have also shown that increased temperatures are positively as-

sociated to increases in chronic respiratory diseases, but again there is insufficient empirical evidence to underpin any findings. These NCDs, even though they mostly intervene in older age groups, also affect children (Dalal et al., 2011).

Empirical evidence on causes of mortality specifically temperature-related in SSA highlights the importance of focusing on specific causes, which affect different age groups differently. Before describing available methods, we present the factors which have been measured to affect the association between temperature and health outcomes.

2.3.2 Factors influencing the exposure-response association

To assess the impacts of climate on health, various outcome variables can be considered, such as mortality (Gasparrini and Leone, 2014), hospitalisation rates (Xu et al., 2019), or the measured incidence of a disease (Motlogeloa and Fitchett, 2024). The selection of outcome variables hinges firstly on their availability and secondly on their susceptibility to correlate with the exposure. In this section, we focus on the effects of ambient outdoor temperatures on diverse health outcomes to establish a foundation for our research.

Firstly, researchers emphasise the need for localised studies on the effects of climate on health. Nonlinear relationships between health and climate tend to vary significantly by region due to factors such as health strategies, adaptation, and demographic structures (Motlogeloa and Fitchett, 2024; Anderson and Bell, 2009).

Secondly, studies considering the possibility of a delay (lag) between exposure and outcome show that the cold effect tends to manifest over a week or more after exposure, while the heat effect is more immediate (Armstrong, 2006; Anderson and Bell, 2009). Consequently, authors have found that including different lag periods when measuring the dose-response association significantly affects results (Motlogeloa and Fitchett, 2024; Armstrong, 2006; De Troeyer et al., 2020).

Thirdly, it is widely observed that the effects of temperature on health vary across different age groups. Children, with lower thermoregulatory capacity, and the elderly are particularly susceptible to temperature changes. These nonlinear relationships vary by geographical location, underscoring the importance of context-specific studies (Green et al., 2019).

Finally, the impacts of temperature on human health vary greatly depending on type of disease. Even though multiple causes of death are affected by temperatures, the nature of this association varies greatly. For instance, the incidence of acute respiratory diseases is negatively associated with maximum and minimum temperatures (Motlogeloa and Fitchett, 2024). Weather conditions influence pathogen cycles and transmission to humans, as well as

human behaviours and immune system performance (D'Amato et al., 2014; Bi et al., 2007). Conversely, cardiovascular disease-related mortality is positively correlated with ambient temperatures (Huang et al., 2011), while hospitalisations related to diabetes increase with every 5°C rise in temperature in Brazil (Xu et al., 2019). Additionally, a scoping review of literature reveals a positive association between ambient temperatures and diarrheal diseases in six regions of the world[3](Kolstad and Johansson, 2011).

2.4 Methods for measuring the exposure-response association

The available methods for assessing the relationship between climate variables and human health vary in complexity. However, when analysing the effects of environmental exposure on human health, time series regression studies are often favoured. This preference stems from the regular variations in exposure and health outcomes over time, such as hourly, daily, or monthly fluctuations. Bhaskaran et al. (2013) outlined the main options for conducting time series regressions in environmental epidemiology.

The first option, time stratified models, divides time into intervals and assigns different baseline risks for each interval using indicator variables. While this approach is straightforward and effective at capturing main long-term patterns, it assumes sudden changes in risk between intervals, limiting its ability to analyse specific biological links. The second option, periodic functions, models long-term patterns smoothly using Fourier terms, representing periodic cycles within the data. Although less complex than the third option, it assumes a consistent seasonal pattern each year. Finally, flexible spline functions fit smooth curves composed of polynomial segments to represent long-term patterns. While flexible, this method is more mathematically complex and requires decisions on the number of knots, affecting its flexibility and interpretation (Bhaskaran et al., 2013).

When timely data is available to analyse the exposure-response relationship, flexible spline functions are recommended. However, the addition of timely data raises questions about the delay between exposure and health outcomes, known as lag. This consideration led to the development of Distributed Lag Non-linear Models (DLNMs), adapting Distributed Lag Models (DLMs) from econometrics.

DLNMs are valuable not only for quantifying current and past exposure-response associations but also for extending these associations to future time periods while considering changes in population demographics. Projections are essential for assessing and managing the effects of climate change, and DLNMs allow for scenario-based projections, enhancing their relevance and applicability (Huang et al., 2011). Antonio Gasparrini and colleagues

[3]South America; North Africa; Middle East; equatorial Africa; southern Africa & Southeast Asia.

have developed a comprehensive method utilising DLNMs, incorporating various functions such as flexible natural spline functions to assess attributable fractions (AF) of deaths due to non-optimal temperatures (Gasparrini and Leone, 2014; Vicedo-Cabrera et al., 2019). This method, which we will elaborate on in our dedicated section, has been selected for this thesis due to the availability of documented code explained in a tutorial (Vicedo-Cabrera et al., 2019) and its potential for analysing the weather-mortality relationship within a specified, well-documented, and evolving context.

2.5 Gap in literature in LLMICs

2.5.1 Scarcity in existing studies

Globally, there has been a slow growth in scientific publications focusing on the effects of global warming on human health, with most studies conducted outside Low and Lower Middle Income Countries and even fewer on the African continent (Ncongwane et al., 2021a; Green et al., 2019) (see figure 7). Despite having lower capacity to adapt to higher temperatures, LLMICs, particularly in Africa, have been relatively understudied (figure 8). Moreover, existing studies use simplistic approaches to analyse the relationship between warmer temperatures and health, while studies have clearly shown the non-linear delayed effect of the climate-health relation (Armstrong, 2006; Gasparrini, 2011). These findings highlight the need for more complex methods that consider long-term effects rather than just specific heat events, for example (Green et al., 2019). In this context, we face a lack of studies on the African continent, especially concerning the use of complex methods. Following our review of available methods to measure and project the associations between climate and human health, DLNMs emerged as an interesting option. However, while DLNMs have been used in various climates, including continental Europe, Latin America, Central Asia, and Oceania (Australia), there has been limited application of this method focusing solely on LLMICs or Africa, apart from a multi-location study in South Africa (Motlogeloa and Fitchett, 2024). The scarcity of applications of this method in other contexts is likely due to a lack of long-term outcome and exposure data required to run the model (Dinku, 2019). DLNMs demand extensive data, which explains the authors' need to compromise between location-specific associations and pooled associations from different sites to address uncertainty arising from small sample sizes in some locations (Gasparrini et al., 2015). However, while this approach reduces confidence intervals, it eliminates some location-specific variations in the model, which have been found to contribute significantly to heterogeneity compared to factors such as initial temperature range or mean temperature (Gasparrini et al., 2015).

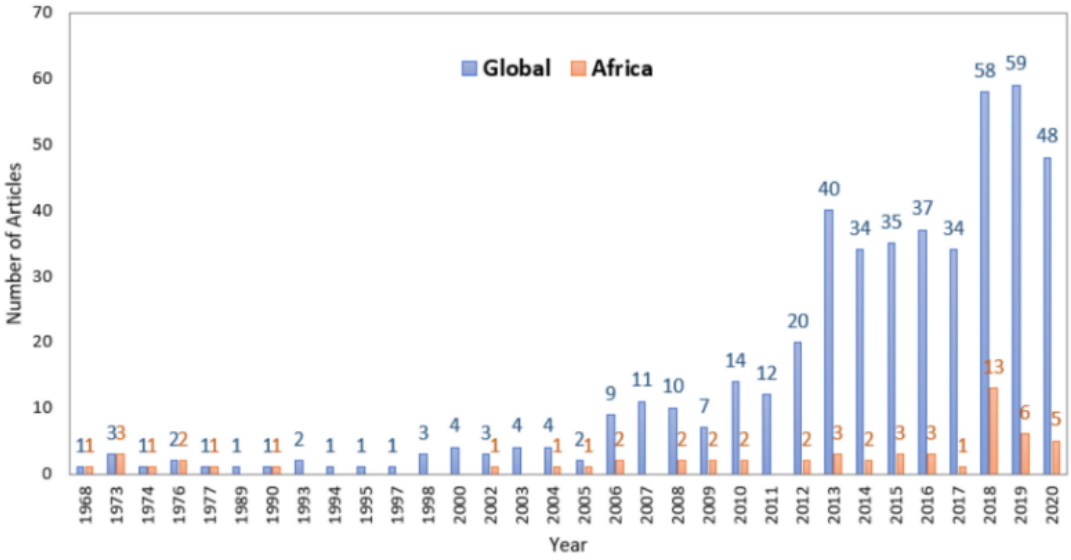


Figure 7: **Annual scientific production on the effects of heat on human health (globally and for Africa): research from 1968–2020.**
Source: Ncongwane et al. (2021a)

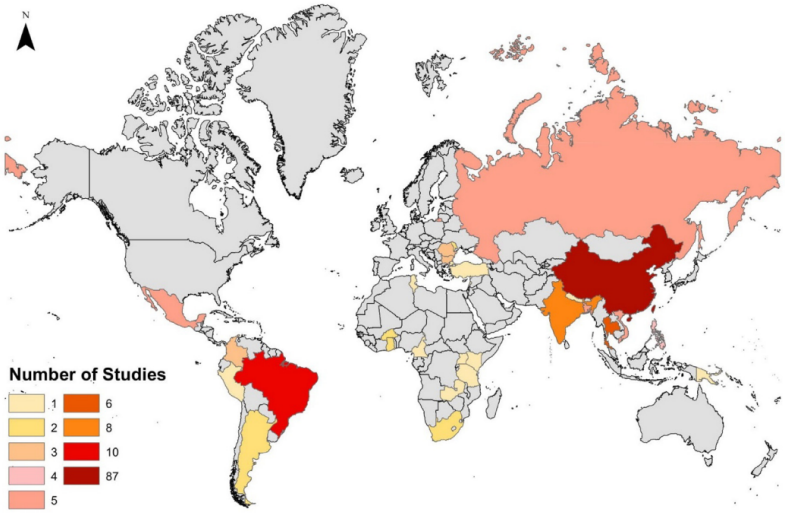


Figure 8: **Map representing the number of studies conducted on the relation between high temperatures and health in the world.**
Source: Green et al. (2019)

2.5.2 Interactions between health-related effects of climate change and epidemiological transitions

While DLNMs have primarily been used in locations that are at advanced stages of their epidemiological and demographic transitions, their implications in different epidemiological contexts where such transition is less advanced remain unexplored in the literature. This gap is highly significant, particularly when considering the importance of factors such as age and the main causes of death in understanding the association between weather and population health.

For reference, epidemiological and demographic transitions are concepts developed to describe the stages through which populations evolve over time. On one hand, the demographic transition (DT) was initially thought by Notestein in 1945 to describe the passage from a regime of high mortality and fertility to a regime of low mortality and fertility (Kirk, 1996). This concept was based on the analysis of high-income societies and was then described as a universal trajectory. In more details, the DT has been attributed to two driving forces : at first a decline in mortality later initiating a decline in fertility. The gap between the occurrence of these decreases is attributed to be the main driver for population growth (Diggs, 2008). On the other hand, the epidemiological transition (ET) describes changes in mortality and cause-of-death patterns which was described by Omran as an inherent change faced when going from a regime of high mortality to a lower mortality regime. In his theory, Omran describes a gradual shift away from communicable diseases to non-communicable diseases (Omran, 2001).

While these concepts are still highly relevant in some countries in transition (such as Iran and parts of India for example) (Moradabadi et al., 2023; Ahsan Karar et al., 2009), their application in Sub-Saharan Africa must be cautious due to different challenges faced by the continent, such as conflicts, instability, economic factors, and prevailing health contexts like HIV/AIDS. Indeed, evidence shows that Africa, which faces distinctly different challenges compared to now-developed countries, is facing a double burden of communicable and non-communicable diseases. Furthermore, countries which experience a protracted mortality transition (Agyei-Mensah and de Graft Aikins, 2010) are highly dependent on imported anti-microbial and anti-parasitic treatments to decrease the burden of infectious diseases (Easterlin, 1999; Preston, 1975).

Despite this protracted transition, ET and DT serve as necessary tools for our analysis, providing insights into expected changes in demographic trends and epidemiological structures. To vindicate this idea we present in figure 10 the representation of mortality by cause of death in Madagascar for the years 2000 and 2015. When comparing the two figures it is

clear that even though communicable diseases still represent a big part of mortality, there is an increase in the burden of non-communicable diseases. In regard to the analysis of DT in the country, our analysis of the population pyramids in figure 1 detail the ongoing changes in population structure. Figure 9 also shows the burden of mortality for different age groups in Antananarivo. On the one hand, it suggests that there has been a constant decrease in yearly numbers of deaths for the under 15 years old age group. On the other hand, the number of deaths between 15 and 59 and over 60 years old have increased during the 1990-2015 period. These changes are indicative of an ongoing DT in the region, pointing to the need to consider these changes in the analysis of mortality in Antananarivo. Hence, this thesis will use these terms to enhance our understanding of the temperature-mortality relation in our case study of Antananarivo, recognising the potential changes in mortality patterns and age structures over time.

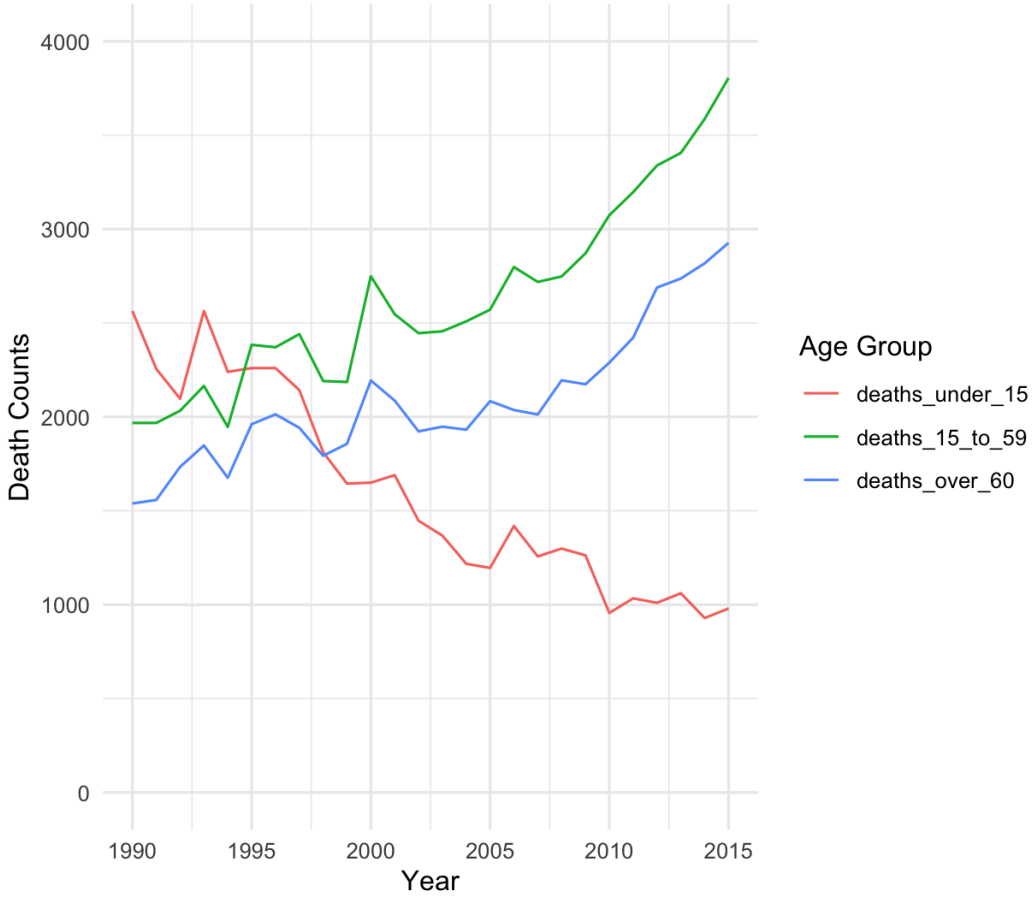
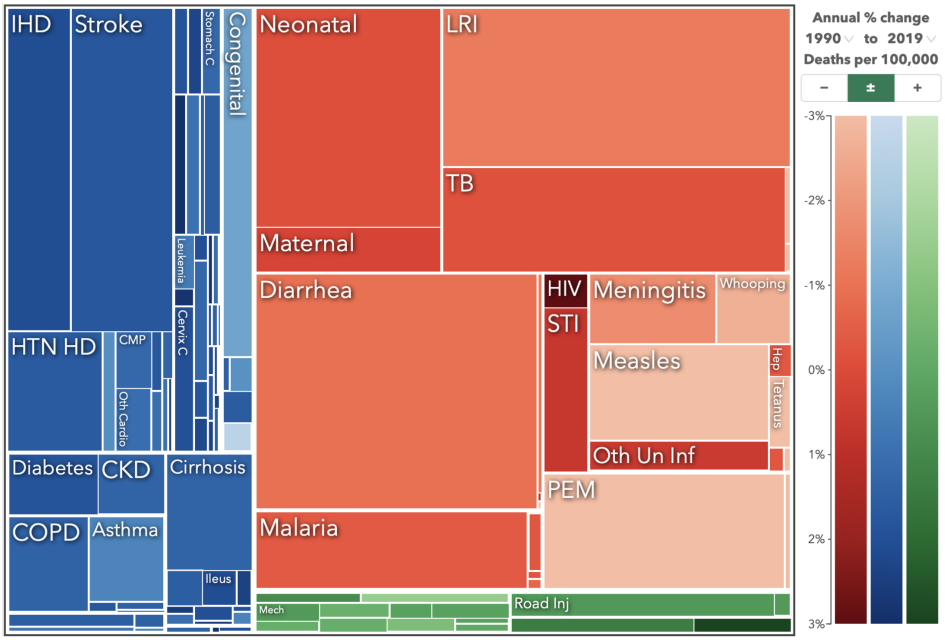
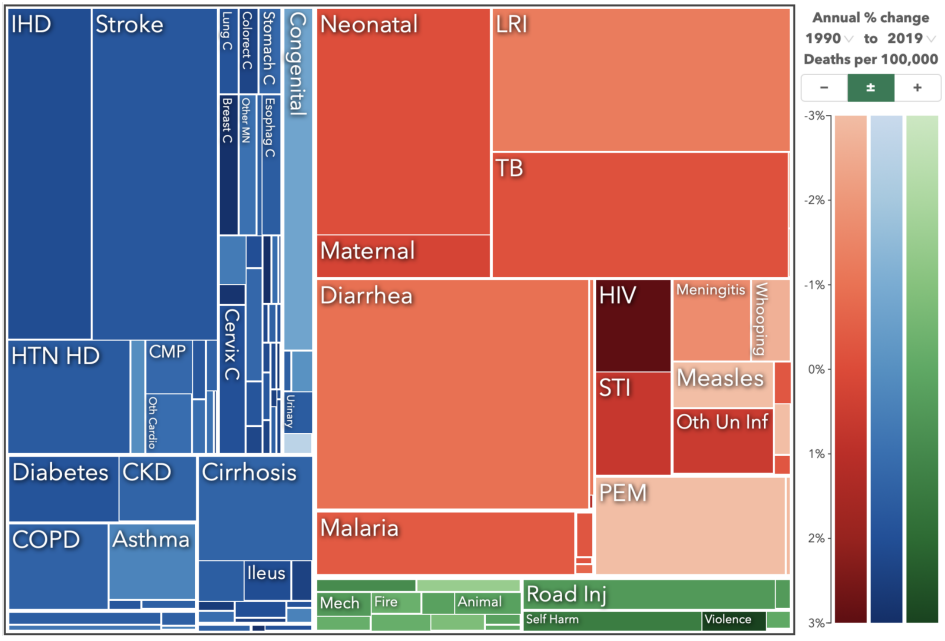


Figure 9: **Yearly death counts per age group in Antananarivo from 1990 to 2015.**
Data source: Antananarivo death records provided by the Municipal Office of Hygiene.



(a)



(b)

Figure 10: **Global Burden of Disease in Madagascar for both sexes, all ages.**
Extracted from : `https://vizhub.healthdata.org/gbd-compare/`
(a) in 2000
(b) in 2015

3 Research context : Antananarivo, Madagascar

3.1 Antananarivo, Madagascar: current climate profile

Madagascar, an island nation located off the southeastern coast of Africa, is part of the African continent. It covers an area of approximately 581,500 square kilometers and features a diverse range of altitudes, from coastal plains to highland plateaus. The country experiences diverse climatic conditions across its regions, as depicted in figure 11, reflecting a range of environmental realities. While the central plateau boasts a temperate climate, the coastal regions experience a constant warm climate throughout the year. The country is separated into six provinces : Antananarivo, Fianarantsoa, Toamasina, Mahajanga, Toliary and Antsiranana, each further subdivided into administrative sectors (Waltisperger et al., 1998). Historically, the country gained independence on the 26th of June 1960 but has since then known a rather unstable political landscape. This instability has since greatly affected other determining sectors such as the economy which relies mostly on agriculture and livestock (Waltisperger et al., 1998).

We opted to study Madagascar due to its ranking as the third most vulnerable country to climate change, as reported by the World Meteorological Organization (WMO) (Nematchoua et al., 2018). Additionally, our decision to specifically study Antananarivo stemmed from several factors. Firstly, urban areas face heightened risks from climate change, as highlighted by the Intergovernmental Panel on Climate Change (IPCC) (Field and Barros, 2014). Secondly, Antananarivo exhibits greater climate variability compared to more stable regions (Nematchoua et al., 2018). Thirdly, the availability of substantial data, which we will delve into later, played a significant role in our choice. Moreover, even though Antananarivo does not record the highest temperatures, the city stands out for its frequency of heat wave events when compared to other cities in different climates[4](see figure 12). This underscores the importance of studying temperature fluctuations in this area and their potential health implications. While other locations could have offered valuable insights, challenges in accessing timely and complete data (particularly mortality data) led us to focus on a single location for our study.

In terms of the temperature distribution in Antananarivo throughout the year, the city experiences a subtropical temperate climate (Schlüter et al., 2020) with a dry winter and a hot summer (see figure 11). Our analysis of mean temperatures for our period of observation (2000-2015) indicates warmer temperatures between November and March and cooler temper-

[4]There have been respectively 40, 33, 40 and 46 heat wave events for this period for Toamasina, Mahajanga, Toliara and Antananarivo.

atures during the months of April to October (see figure 13). The daily mean temperatures vary between 10°C and 25°C and the two main seasons are marked by visible differences with an average temperature of 17°C in the cold season and an average of around 21°C in the warmer season (see figure 13).

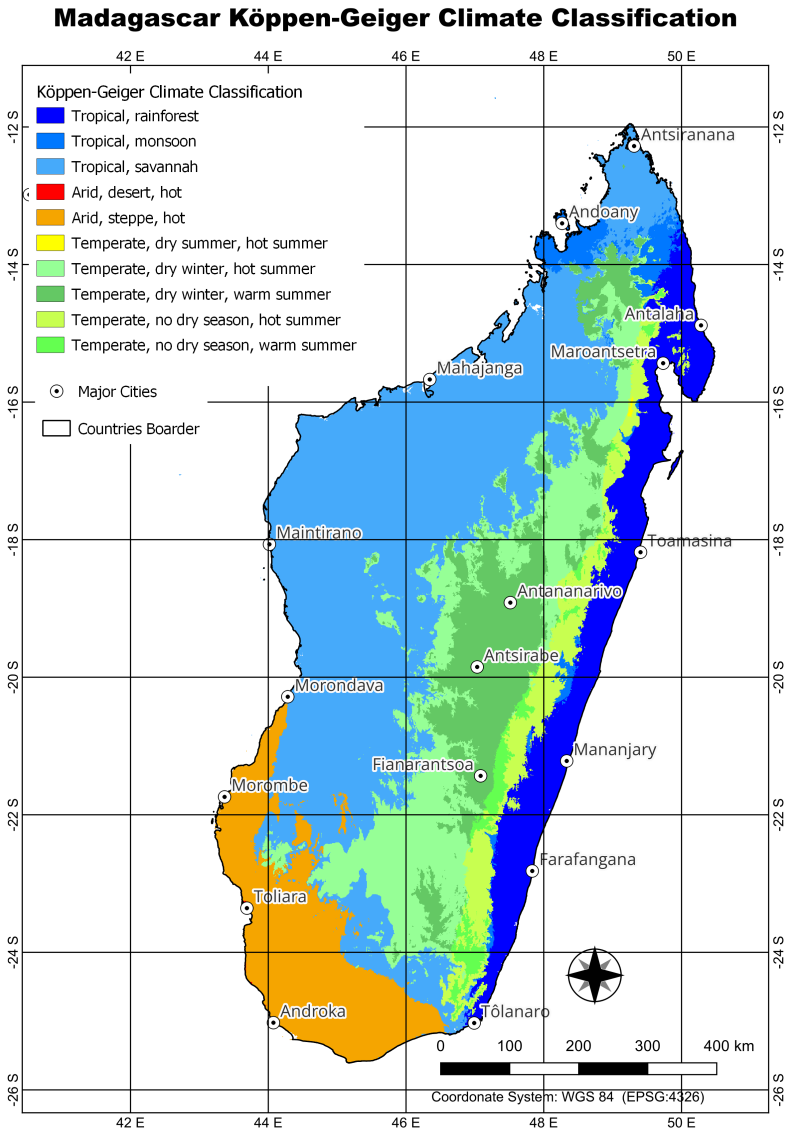


Figure 11: **Map of the different climates in Madagascar.**
Source : This map was built and shared by Emilie Castin (researcher for the Centre for Research on the Epidemiology of Disasters) using a simplified version of the Köppen-Geiger classification using ERA-5 data.

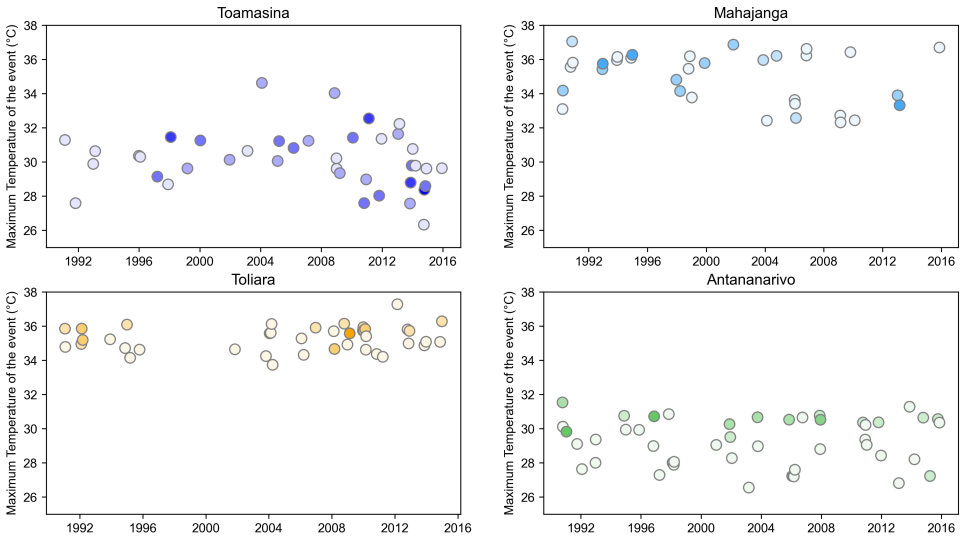


Figure 12: **Number of heat waves recorded in four Madagascan cities from 1990 to 2015.** The recorded events are when the daily maximum temperature of more than five consecutive days exceeds the average maximum temperature by 5 °C.
Source : Graphs produced and shared by Emilie Castin (researcher for the Centre for Research on the Epidemiology of Disasters) using ERA-5 data.

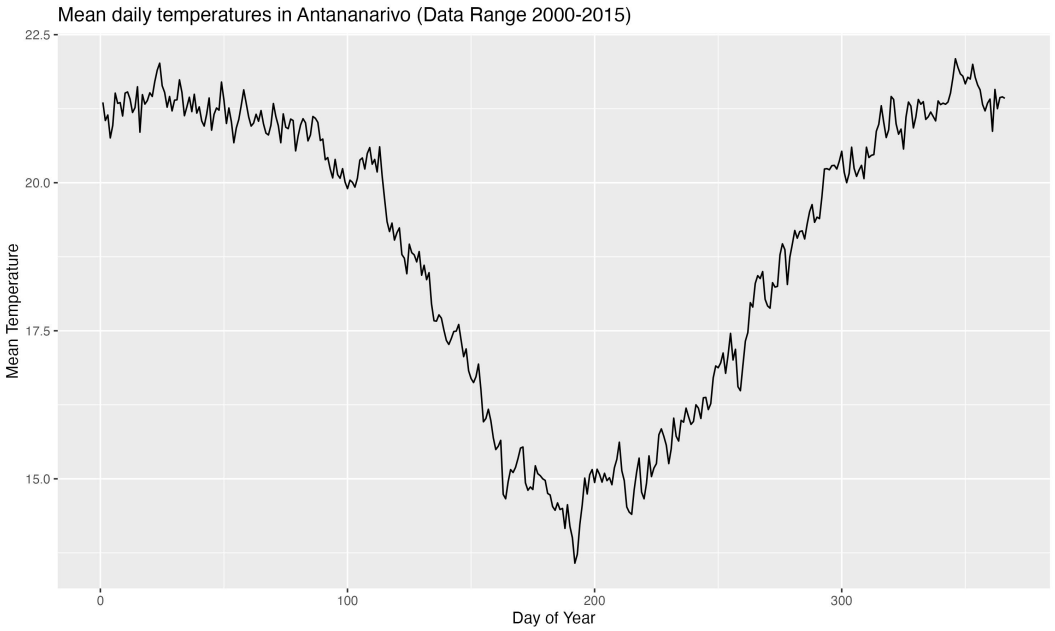


Figure 13: **Mean daily temperatures averaged for the 2000-2015 period in Antananarivo.**
Data source: NOAA.

3.2 Antananarivo, Madagascar: projected climate profile and associated health risks

As earlier mentioned, climate change implies warmer climates in Madagascar. More precisely, in Antananarivo, all Shared Socioeconomic Pathway (SSP)[5] scenarios project an increase in temperature (see figure 14). This means that whatever the course of anthropogenic emissions, temperatures are projected to rise.

Studies on the health effects of warming temperatures in the region show that the incidence of acute respiratory infections (ARI), diarrhea, malnutrition, and malaria are all projected to increase with the future temperature projections in Madagascar (Rakotoarison et al., 2018). Furthermore, studies on adaptation show that there is adaptation to warmer climate for malaria and malnutrition (in the whole country) and enteric diseases (for Antananarivo) (Rakotoarison et al., 2018; Klein and Rasoanomenjanahary, 2023). But the literature shows that the effects of adaptation will not suffice to restrict increases in mortality given the projected changes in climate (Rakotoarison et al., 2018; Klein and Rasoanomenjanahary, 2023). The analysis of rainfall reduction and increased droughts shows that there is no significant relation between climate change related droughts and food insecurity in the south of the country (Harrington et al., 2022). Finally, enteric infections are becoming less sensitive to low rainfall (Klein and Rasoanomenjanahary, 2023).

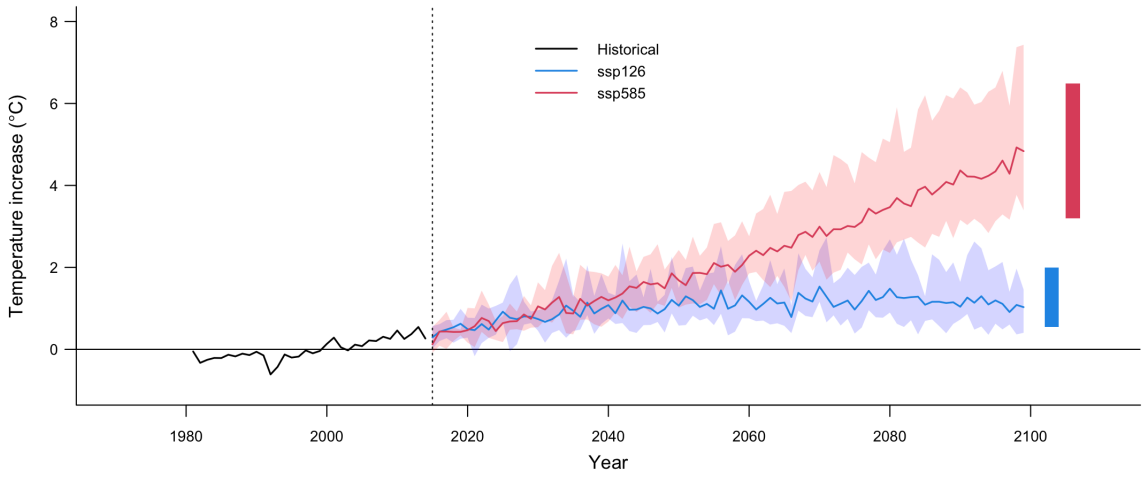


Figure 14: **Increase in °C in projected mean temperature (for ssp126 and ssp585) in Antananarivo.** *Data extracted from RNOAA and ISIMIP and processed in code 0.2.*

[5]SSPs are further explained in box 1.1.2

3.3 Antananarivo's epidemiological transition

Antananarivo is the administrative, political, economic and cultural capital of Madagascar. Located within the province of the same name, the city comprises six districts and sits at an elevation of 1000 meters above sea level. These districts housed approximately 1.28 million inhabitants in 2018 (Rousseau et al., 2023) and, as this city has been at the centre of the politics of the country, it has also been affected by these events. Despite this, the city benefits from a relatively better economic and sanitary situation compared to other regions of the country (Waltisperger et al., 2005).

During the early twentieth century until the 1940s, Antananarivo experienced a stagnation in the crude death rate, hovering around 30 deaths per 1000 live births. After that mortality rapidly declined but resurged in the 1980s. This change in mortality trends can be attributed to unstable economic conditions and the resurgence of malaria (Masquelier et al., 2014). Over the period between 1971 and 1996, the GDP per capita has known a 45% decrease which has been unmatched by any other non-war-torn country. This prolonged period of economic instability affected the health situation in the capital (Waltisperger and Meslé, 2005). Following the 1985 crisis, life expectancy at birth reached its lowest point for the 1976-2000 period, with a life expectancy reaching 45 and 53 years old for men and women respectively (see figure 15). During this period, literature documents an increase in mortality for groups which usually have lower mortality rates such as children between five and nine years old and individuals between fourteen and forty-nine years old. However, after this crisis the life expectancy grew back to reach its previous level in the 1990s and reached higher levels by the end of the century (Waltisperger et al., 2005). From this point in time, life expectancy has increased steadily even though the capital has still not reached economic stability nor has it resolved the problem of chronic malnutrition (Masquelier et al., 2014). This increase in life expectancy has also known disruptions due to COVID-19 in later years (Rabarison et al., 2023).

Presently, most of the increase in life expectancy can be attributed to a reduction of child mortality, while adult mortality has not experienced a similar decline. This result regarding adult mortality is due to a shift in the leading causes of mortality, transitioning from infectious and respiratory diseases to cardiovascular diseases, neoplasms, and other non-communicable ailments (Masquelier et al., 2014). This analysis of evolving mortality patterns underscores the concept of ET and the literature shows that Antananarivo is still in the midst of this transition. But research highlights a particular trend in the city, where instead of transitioning from one disease regime to another, Antananarivo now faces a dual burden of communicable and non-communicable diseases (Masquelier et al., 2014). To visualise this double burden of disease we present figures 16, 17 and 18 in which we represent the evolution of numbers of

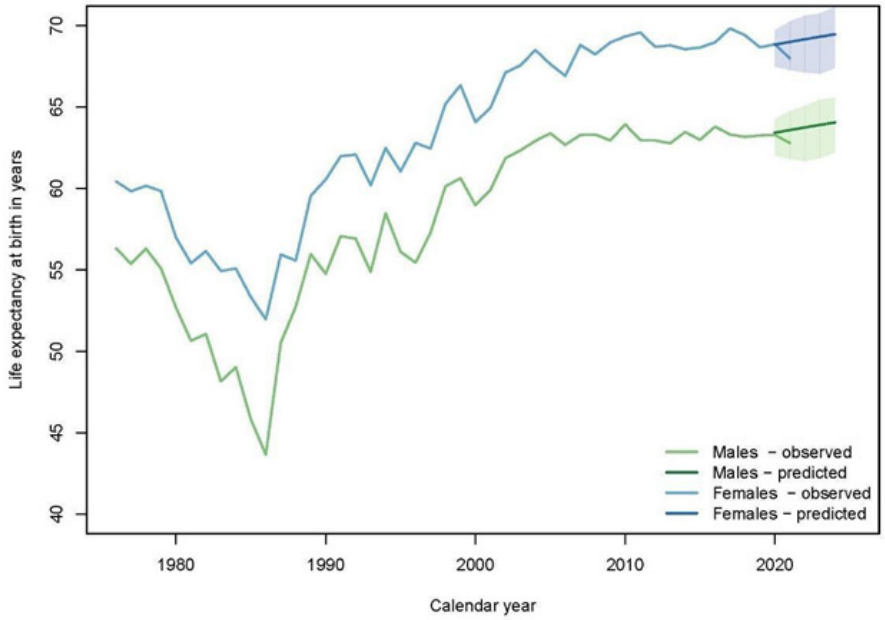


Figure 15: **Observed and predicted life expectancy at birth in Antananarivo (1976–2021).**
Source : (Rabarison et al., 2023). For males (green) and females (blue). The authors projected to 2020–24, the observed life expectancy at birth and the predicted (bold) for both sexes based on the rates measured from 1990 to 2019. This was based on a database with deaths recorded at Antananarivo by the Municipal Bureau of Hygiene and census-based population estimates.

deaths from main groups of causes of death including deaths defined by what we call "*garbage code*s", which refer to ill defined causes of deaths (Masquelier et al., 2019). On one hand, we observe a decline in mortality below 15 for all causes since 1987, with most progress being made in reduction of communicable diseases (CDs) rather than non-communicable diseases (NCDs). On the other hand, mortality for adults[6] and elderly[7] is marked by a gradual and maintained increase in mortality of NCDs (which represent most of the burden of mortality) and a stagnation in numbers of deaths from CDs. Thus, this context of the dual burden of NCDs and CDs needs to be considered when analysing the relationship between temperature variability and mortality in the region.

Finally, exploring the seasonal patterns of mortality in the city is crucial, especially considering that seasonality often diminishes during the ET. With the progress of the health transition, the shift from communicable to non-communicable diseases typically leads to a reduction in the seasonality of deaths. Communicable diseases are known to exhibit significant seasonal variations due to factors such as climate, food insecurity, and holidays (Schlüter et al., 2020; Evans et al., 2021; Rousseau et al., 2023). In the case of Antananarivo, research

[6]Even though individuals below 18 are not considered adults, we shall refer to the 15-59 age group as adults in our explanations.
[7]Elderly mortality refers to mortality from 60 years old and above.

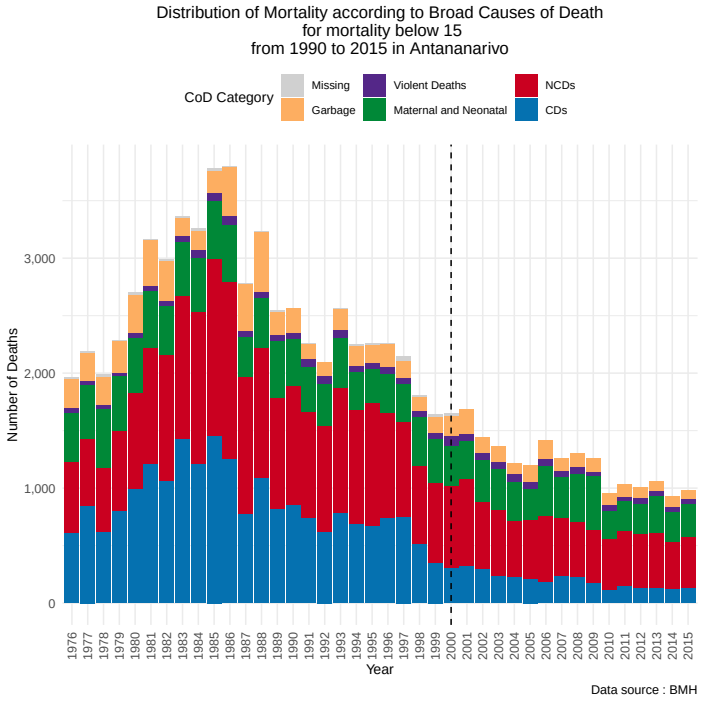


Figure 16: **Evolution in numbers of broad causes of death for deaths under 15 in Antananarivo, Madagascar**

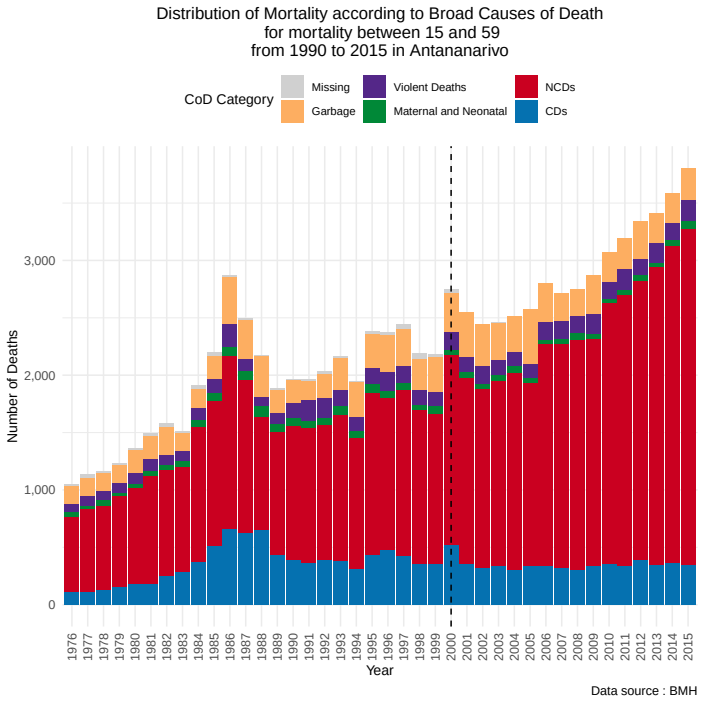


Figure 17: **Evolution in numbers of broad causes of death for deaths between 15 and 59 in Antananarivo, Madagascar**

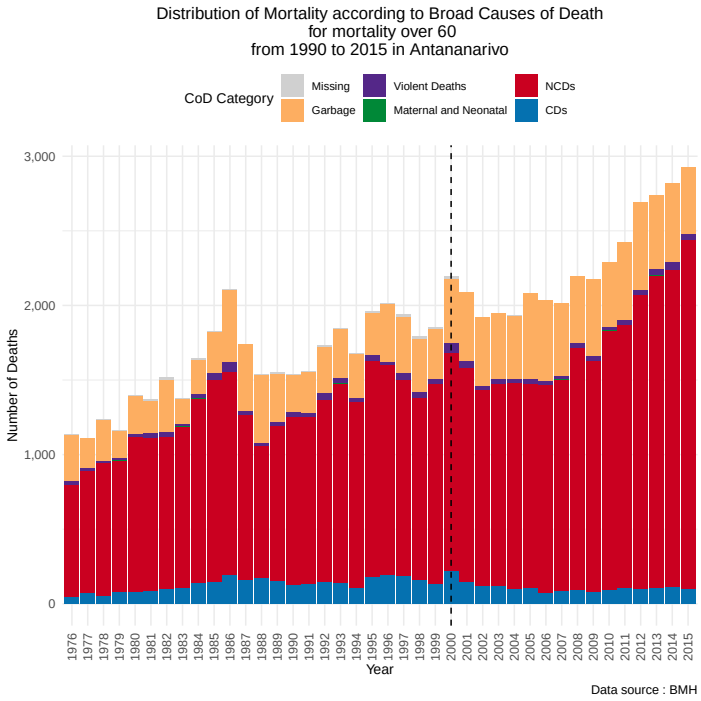


Figure 18: **Evolution in numbers of broad causes of death for deaths over 60 in Antananarivo, Madagascar**

shows changes in seasonal mortality, but these changes are mostly driven by shifts in leading causes of death rather than changes in the timing of these occurrences. When examining specific age groups, the study has shown that child mortality is highest with warmer temperatures, while mortality over 60 is more sensitive to cooler temperatures (Schlüter et al., 2020). Moreover, as the city continues to grapple with transitioning between different stages, factors such as food insecurity, tend to remain high. To illustrate how food insecurity levels fluctuate significantly in correlation with seasons, authors show that food insecurity rates are doubled before the rice harvest compared to after (Rousseau et al., 2023).

4 Research question and hypotheses

In their review of literature on the impacts of heat stress on human health across Africa, Ncongwane et al. (2021b) highligh significant gaps in existing studies. Notably, they advocate for vulnerability assessment studies focusing on specific demographic groups. Building on this recommendation and our review of the literature, this master's thesis aims to employ the dose-response measurement method developed by Gasparrini et al. (2015), incorporating demographic refinements to enhance our understanding of the context within which associations are measured. This thesis explores the efficiency of using such a method in environments

where data is limited yet available, and where the epidemiological transition deviates from the initial patterns. The primary objective is to determine the value of including demographic and methodological refinements in these contexts.

Subsequently, this thesis seeks to address the following questions: **what are the prevailing relationships between mortality and temperatures in Antananarivo today, and how might they change in the future? How effectively do DLNMs apply to LLMICs in subtropical climate contexts?** And **how does incorporating shifts in epidemiological and demographic transitions into the model improve its relevance and accuracy?** We will explore these questions using a more elaborated version of predictions based on DLNMs, which also takes into account changes in population structure and tests the effects of demographic transitions on the relationships observed. We will analyse specific relationships by cause of death to incorporate the effects of shifts in the epidemiological transition. Then, we will examine the importance of seasonality which plays a mediating role in the mortality-temperature association, and whose importance varies between age groups. Additionally, we will assess the importance of using measured data compared to modelled data.

Based on our review of the existing literature, we make several hypotheses:

- First, we hypothesise that, all things being equal, increasing temperatures will increase the attributable fraction (AF) of deaths due to heat across all age groups (Klein and Rasoanomenjanahary, 2023) (Rakotoarison et al., 2018). This exposure-response association is expected to vary between age groups (Green et al., 2019) and different causes of death (D'Amato et al., 2014; Bi et al., 2007; Huang et al., 2011; Xu et al., 2019).
- Then, through our analysis of changes in population structure, we expect to see a decrease in child mortality and an increase in mortality later in life, resulting in more deaths attributable to extreme heat for older groups compared to the constant mortality scenario. On the contrary, heat related mortality under 15 years old is hypothesised to diminish in the scenario with varying mortality.
- Additionally, we hypothesise that attributable fractions of mortality due to cold will diminish whereas heat related mortality will increase. This should be the case in all projection scenarios and for both SSPs .
- Moreover, seasonality, which significantly impacts child mortality (Schlüter et al., 2020), is hypothesised to play a greater mediating effect on mortality in under 15 years old rather than on other groups.
- Furthermore, given the differences in temperature projections between the two SSPs,

we hypothesise a greater attributable fraction of deaths due to heat in SSP5-8.5 than in the mitigation scenario.

- Finally, we hypothesise different relative risks for our model using measured versus modelled data for temperature.

Data and Methods

1 Data

Before delving into our methodological framework, it is essential to provide an overview of our data choices. As outlined in earlier sections, our focus is to assess the impact of non-optimal temperatures on mortality in Antananarivo, Madagascar. To achieve this, we have collected both exposure data (daily mean temperature) and outcome data (daily death reports).

1.1 Exposure : daily mean temperature

For the exposure data, we have selected daily mean temperatures as they best represent the general climatic conditions. In this section, we describe the data we used while also explaining the reasons for not using other potential datasets.

1.1.1 Dataset for the 2000-2015 period : NOAA data

Among the available data for Antananarivo, we referred to the datasets offered by the National Oceanic and Atmospheric Administration (NOAA), which facilitates access to a variety of climate datasets. This scientific agency, part of the United States Department of Commerce, focuses on monitoring the conditions of oceans, major waterways, and the atmosphere. The NOAA database collects weather and climate data through various methods[8]. In our case, the database allowed us to use real temperatures recorded by the Ivato International Airport in Antananarivo. Although we did not have a choice regarding the selected data for our analysis, because of the lack of other stations in the area included in the database. We

[8] https://www.noaa.gov/tools-and-resources/weather-and-climate-resources

maintain that using temperature data from Ivato airport is relevant. The airport is situated within the city, and its altitude is close to the mean altitude of the city, at 1279 meters compared to the city's average altitude of 1309 meters[9].

The code we used to access this data can be found in the code annex 0.1. To download this data, the rnoaa package in R was used, which interfaces directly with NOAA's data application programming interface.

After downloading the data, our initial step was to assess its completeness. This analysis revealed a significant number of missing values, particularly prior to the year 2000, as illustrated in graph 19. This was problematic, especially considering that the model necessitates extensive time frames of complete data. Despite this issue, we opted to proceed with using this dataset rather than resorting to modelled data from an alternative source. The justification for this decision is elaborated in the box 1.1.1 below.

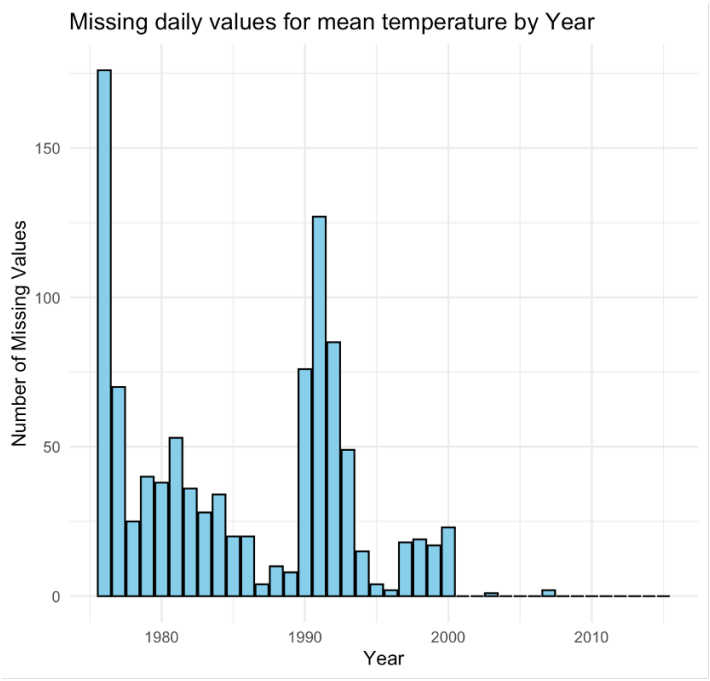


Figure 19: **Representation of all the missing values in daily temperature for each year of the NOAA dataset.**

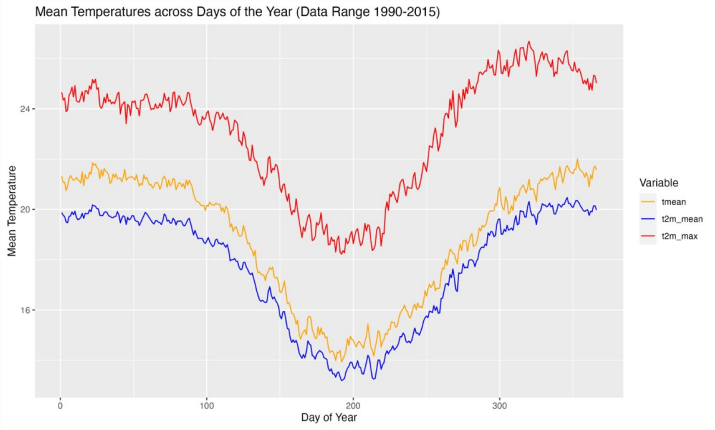
Box 1.1.1 : Choosing the exposure data

Given the number of missing values in our initial mean temperature database, we explored alternative options. Through interactions with members of Centre for Research on the Epidemiology of Disasters, we were granted access to ERA5-Land data. This dataset, sourced from the climate data store, represents

[9] `https://en-us.topographic-map.com/map-jvmcz/Antananarivo/`

gridded data. ERA5-Land is a reanalysis of the existing ERA5 dataset, combining model data with global observations to create a globally complete and consistent dataset using physical laws. Utilising data and coordinates provided by Emilie Castin (longitude: 47.422465, latitude: -18.798), which encompass most of Antananarivo city and include the airport, we extracted mean temperature data. However, it is essential to note that this temperature represents the temperature at 2 meters from the ground and is not a direct measurement[10]. ERA5-Land, being simulated data, does not have missing values. The recorded temperatures exhibit, however, marked differences when compared to our measured data. When referring to the graph below we observe the difference between the two datasets, and we can see that the NOAA data is always higher than ERA5-Land data on average (the measured average difference being 1.173°C).

Comparing exposure data: modelled vs measured.



tmean : mean temperature from NOAA, t2m mean : mean temperature from ERA5-Land, t2m max : maximum temperature from ERA5-Land.

Exploring other options

We experimented using the ERA-5 data instead of the RNOAA data as a sensitivity analysis (results found in our results section) and chose to keep the RNOAA data as the exposure. Furthermore, we experimented with various techniques to fill in missing values in the NOAA data using simulated data prior to 2000 in R. Initially, we employed a simple method by calculating the mean difference between the two datasets and adding this difference to the ERA5-Land simulated temperature to estimate missing values. Subsequently, we attempted a more intricate approach involving a loop to compute the difference between the values of the two datasets for the 15 days before and after any missing value. This loop then attributed the calculated difference to the missing value in the NOAA dataset. In cases where numerous missing values were encountered, we expanded the loop to encompass a 30-day window before and after the missing value.

Despite employing both techniques and integrating the new datasets into the model, we encountered challenges in achieving model convergence. Consequently, we decided to limit our analysis to data from 2000 onwards.

1.1.2 Dataset for the 2016-2100 period : ISIMIP data

In order to project the effects of future climate changes, it is essential to gather information on future climate scenarios. Various climate projections are available, typically based on

[10] `https://cds.climate.copernicus.eu/cdsapp#!/dataset/reanalysis-era5-land?tab=overview`

the development of Shared Socioeconomic Pathways (explained further in box 1.1.2). For our study, we sourced data from the Inter-Sectoral Impact Model Intercomparison Project (ISIMIP)[11], which provides a framework for accessing diverse datasets to understand the impacts of climate change. ISIMIP operates on the principle of open access data, requiring personal registration for access. Temperature values, initially in Kelvin, were converted to degrees celsius by subtracting 273.15. The data was shared in two files corresponding to the selected scenarios. We selected two scenarios for our analysis: SSP1-2.6 and SSP5-8.5. The choice of SSP1-2.6 aligns with the objectives of the Paris Agreement, aiming to limit global warming to 2°C (Sanderson et al., 2017). In contrast, SSP5-8.5 represents a scenario projected to induce the most significant warming. While there are other scenarios available, we opted not to include them as they would fall between these two extremes.

Finally, the two datasets included the following variables: date, year (from 1980 to 2100 which is our projection horizon), and five "*tmean*" variables, representing estimations from five different climate modelling groups. These five modelling group outputs are all incorporated into our model and use GCMs (General Circulation Models) to simulate and project earth's climate system. GCMs are complex computer-based mathematical models used to simulate the earth climate system. Under different scenarios, these GCMs present based on past earth system data a simulation of future climates. These models represent the fundamental processes which drive climate variability and change and make projections about future conditions[12]. The different models are as follows: GFDL (Geophysical Fluid Dynamics Laboratory), IPSL (Institut Pierre-Simon Laplace), MRI (Meteorological Research Institute), MPI (Max Planck Institute for Meteorology), and UKESM (UK Earth System Model).

Box 1.1.2 : Shared socioeconomic pathways

Shared Socioeconomic Pathways (SSPs), General Circulation Models (GCMs) and Representative Concentration Pathways (RCPs) are key components to research on climate changes. The intertwined but different concepts serve different aspects of climate change modelling.

SSPs are scenarios to represent different plausible trajectories of socioeconomic development over the 21st century. They capture the uncertainties in future societal, economic and technological developments that could influence green house emissions and climate change. To each SSP coincides a narrative describing assumptions about future population growth, economic development, etc. (Riahi et al., 2017).

The different SSP scenarios are the following and the developed specifics for these SSPs can be found in figure 42 in the annex.

Summarised table of different SSPs:

[11] `https://www.isimip.org`
[12] `https://celebrating200years.noaa.gov/breakthroughs/climate_model/welcome.html`

SSP1	Sustainability - Taking the green road. (Low challenges to mitigation and adaptation).
SSP2	Middle of the Road. (Medium challenges to mitigation and adaptation).
SSP3	Regional Rivalry - A rocky road. (High challenges to mitigation and adaptation).
SSP4	Inequality - A road divided. (Low challenges to mitigation. High challenges to adaptation).
SSP5	Fossil-fuelled development - Taking the Highway. (High challenges to mitigation, low challenges to adaptation).

Based on source: Riahi et al. (2017)

RCPs represent the different possible climate profiles based on different possible evolutions of the concentration of green house gases in the atmosphere and are thus coupled to SSPs to get different climatic scenarios (Intergovernmental Panel On Climate Change, 2023).

Projected climatic scenarios are represented as SSPs, with the acronym followed by the scenario number and the approximate value of radiative forcing expected to be reached by the end of the 21st century. Ultimately, an SSP encapsulates a greenhouse gas emission and global warming trajectory. The various climatic projections endorsed by the Intergovernmental Panel on Climate Change (IPCC) include the following:

SSP Scenario	RCP : associated radiative forcing	Climate projection scenarios
SSP1	RCP 2.6	SSP1-2.6
SSP2	RCP 4.5	SSP2-4.5
SSP3	Between RCP6 and RCP8.5	SSP3-7.0
SSP5	RCP 8.5	SSP5-8.5

Based on source: Intergovernmental Panel On Climate Change (2023)

The combination of these terms is summarised in figure 43 found in the annex. This figure shows how emissions, when thought of in the GCMs can result to projected changes in climate.

1.2 Outcome : daily deaths

Due to incompleteness of the death registration system of the population in Madagascar, conducting studies on all-cause and cause-specific mortality presents significant challenges (Waltisperger et al., 1998). The data accessed for this thesis originates from a research project initiated in 1993 by Unicef and Ined, providing access to data from 1976 to 2015 in Antananarivo (Waltisperger et al., 2005). These death records are maintained by the Munic-

ipal Office of Hygiene (MOH). Ratovoson et al. (2020) explain that this record system was established in 1916 to improve the healthcare system's crisis response, specifically focusing on accurately recording deaths for effective intervention. The MOH has retained this record system over time for various purposes, including assessing the accuracy of recorded home deaths (Waltisperger et al., 1998). Presently, this data is not publicly available, and access is granted upon special request. We were granted access to records from 1976 to 2015 through Bruno Masquelier. While access to the data was previously facilitated directly by the Municipal Bureau of Hygiene (BMH), it is now monitored by the Pasteur Institute of Antananarivo, and access to the more recent data from 2016 onward was not possible for this dissertation. Our access to the 1976-2015 data was contingent upon an agreement to use it exclusively for this master's thesis, with a commitment not to redistribute the data.

Before delving into the specifics of the data, it is essential to consider its quality. In Antananarivo, death declarations must be made within 12 days from the date of death, a requirement observed in 99% of cases, with over 80% of declarations occurring on the same day or the day after the death. This adherence to the 12 day delay is attributed to the long-standing tradition of death reporting in the city (Waltisperger et al., 1998). Masquelier et al. (2019) further extended this observation for data up to 2015, demonstrating that indicators measured using the database closely align with those measured based on Demographic and Health Surveys from the capital city. Regarding the precision of declarations, particularly in factors such as age, a study emphasises that age reporting has become increasingly accurate over time. By 2000, age was known to the day for more than 80% of deaths (Waltisperger et al., 2005). Furthermore, when assessing the quality of cause of death reporting, a study highlighted numerous "*garbage codes*" in the Global Burden of Disease (GBD) 2016 dataset (Masquelier et al., 2019). These codes lack precise indications of causes of death. However, for causes not classified as garbage, there was consistency between estimates from GBD 2016 for the country and data from the capital. Therefore, data from Antananarivo can be considered comprehensive and, with the removal of garbage codes, reliable for analysis of causes of death or age groups.

The mortality data provided consists of a database documenting daily deaths recorded from 1976 to 2015 in the region of Antananarivo-Renivohitra. This region comprises six districts, with the Bureau Municipal d'Hygiène (BMH) having jurisdiction over five of them. Therefore, the data covers the central parts of the city, excluding the district of Ambohimanarina. Despite spanning from 1976 to 2015, we have chosen not to use data prior to 2000. This decision is influenced by exposure data limitations and documented evidence of a severe economic crisis in Madagascar during the late 1980s, resulting in a significant decrease in life expectancy at birth (Masquelier et al., 2019; Waltisperger et al., 1998). Before our analysis, the database underwent data cleaning, including the removal of non-residents and stillbirths,

to ensure data quality and relevance. After restricting the dataset to the 2000-2015 time frame, a total of 103 068 deaths were retained (table 4 in the annex). The available variables for our analysis include the date of death, date of declaration, date of birth, sex, Cause of Death (CoD) in International Classification of Diseases - 9 (ICD-9) codes, age at death, and the year of death.

2 Methods

The objective of this thesis involves testing an established method in a distinct context. To describe our method, we start by describing the existing method in section 2.1, followed by a description of our methodological adaptations and the sequential procedures undertaken to address our research questions in section 2.2[13].

2.1 Distributed Lag Non-linear Models

2.1.1 Steps for the model

In this section, we explain the method described by Vicedo-Cabrera et al. (2019). This method is designed to assess outcomes occurring after an exposure event. The model incorporates the nonlinear and delayed effects of weather events on mortality through specific functions, with the primary objective being to define the relationship within the predictor space, to measure how changes in the predictor variable correspond to changes in the response variable (Vicedo-Cabrera et al., 2019). The different steps and graphs produced in the author's original study can be found in box 2.1.1 and figure 20.

Box 2.1.1 : Description of the DLNM according to the tutorial

Step 1 involves estimating the exposure-response associations. This entails fitting a Generalised Linear Model that links the exposure and outcomes while controlling for confounding factors such as seasonality or day of the week. This step provides the Relative Risks[14](RR) and is often accomplished using a time series quasi-Poisson regression. Moreover, DLNMs are based on the definition of a cross-basis (cb). This cb is a bi-dimensional functional space which describes the relation along the temperature range and the lag dimension. Thus, to incorporate the concepts of delay and non-linearity into the relationship, a cb term must be defined. This cross-basis includes the exposure (temperature) and natural spline functions for the maximum lag, based on three internal knots (on the 10th, 75th & 90th percentiles of the temperature distribution) (Vicedo-Cabrera et al., 2019). This function can be found at

[13]All analyses were done in R (version 2024.04.0+735).

equation 2.1.

Step 2 involves projecting the exposure and health outcome series. This entails gathering data on future climate based on GCMs and projecting future health outcomes. To project future mortality, the method assumes constant mortality rates, with seasonal variations captured based on past data.

Step 3 concerns downscaling and calibration, where different GCM data are calibrated to match recorded data using a bias correction function. This function was built to calibrate ISIMIP data.

Steps 4, 5, and 6 entail extrapolating the exposure-response curves beyond the observed range of temperatures. The impact is projected and quantified using concepts such as Attributable Numbers (ANs) and Fractions (AFs). These attributable fractions and numbers are calculated based on equation 2.2. Finally, uncertainty arises from estimation of the exposure-response function and climate projections. This uncertainty is assumed to follow a multivariate normal distribution and results are generated for each of the GCMs. The Confidence Intervals (CIs) are obtained through Monte Carlo simulation of the coefficients and are quantified in terms of empirical confidence intervals, defined as the 2.5th and 97.5th percentiles of the empirical distribution.

The following function is the mathematical representation of what was done in the DLNM code:

$$\log\left[E\left(Y_t\right)\right] = \alpha + f\left(x_t; \boldsymbol{\theta}\right) + s(t;\beta) + \sum_{p=1}^{P} h_p\left(z_{pt};\gamma_p\right) \tag{2.1}$$

Here, the outcome (Y_t) corresponds to daily death counts assumed to follow a Poisson distribution with overdispersion. The function $f(x_t;\theta)$ specifies the association with the temperature (x) at time (t), while $s(t;\beta)$ represents the baseline trend capturing the effect of confounders changing slowly over time, such as seasonal trends. Additionally, $h(z_{pt};\gamma_p)$ models the contribution of other confounders varying on a daily basis, such as the day of the week (Vicedo-Cabrera et al., 2019).
The following function represents the calculation of the attributable number of deaths due to heat and cold. The attributable numbers (D_{attr}) are calculated in reference to the minimum mortality temperature (T_{mm}), which is the temperature at which the least number of deaths are recorded. This calculation is based on the calibrated temperature series (T_{mod}).

$$D_{\text{attr}} = D \cdot \left(1 - e^{-(f^*(T^*_{\text{mod}};\theta^*_b) - s^*(T_{mm};\theta^*_b))}\right) \tag{2.2}$$

Here, f^* and θ represent the exposure-response curves calculated in step 1, and the lagged results are cumulative. To obtain results for cold and heat, the minimum mortality temperature is used as the threshold separating the two.

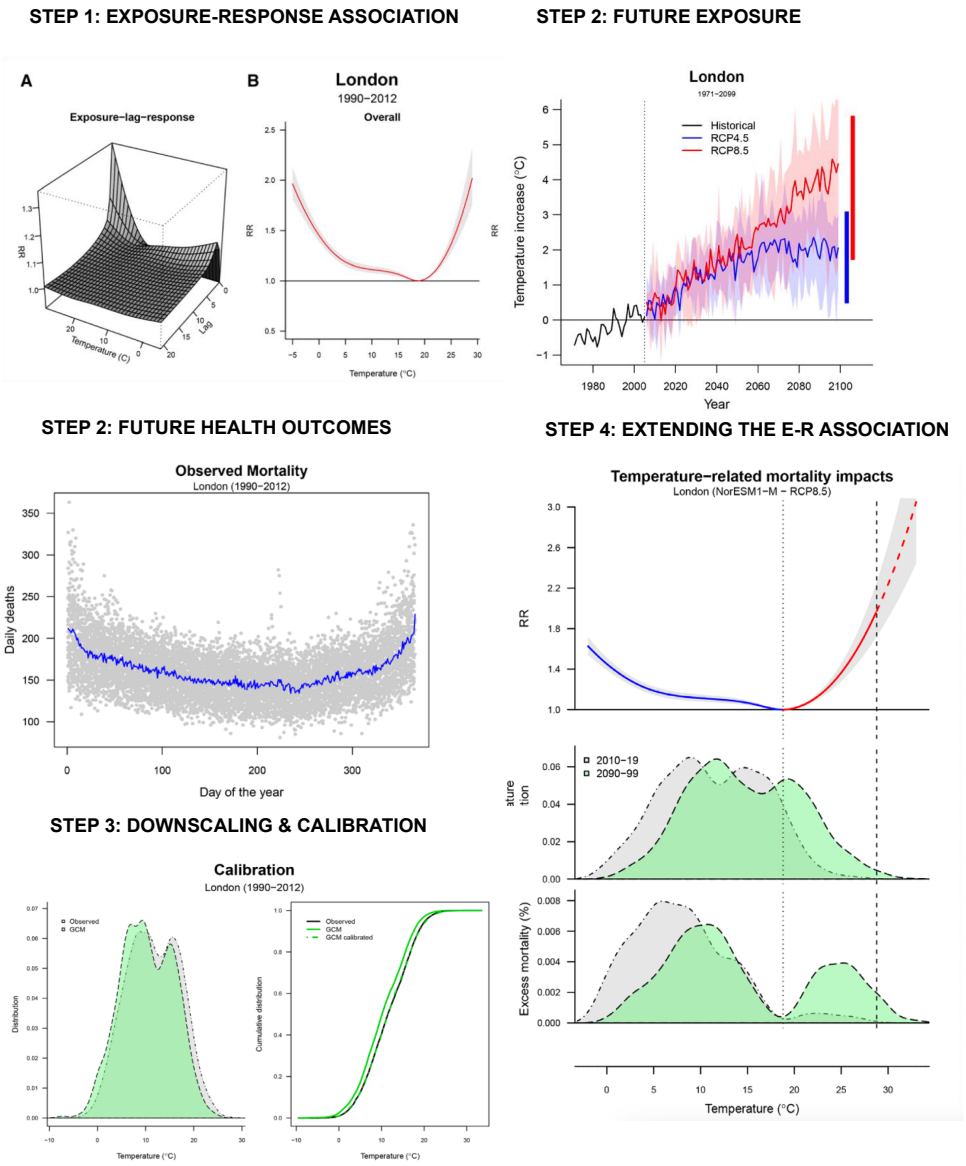


Figure 20: **Steps for applying the Vicedo-Cabrera et al. (2019) tutorial - Graphics.**

[14]Relative risks present the risks of mortality at a given temperature compared to the minimum mortality temperature (temperature at which the death counts are the smallest). These RRs could have also been analysed as rate ratios given that we used a Generalised Linear Model (GLM) with a poisson distribution.

2.1.2 Modelling choices

Before delving into the methodology used to address our research questions, it is imperative to outline the various modeling decisions made for our analysis, as these choices may significantly impact our findings. Armstrong (2006) has demonstrated the importance of modeling decisions when using DLNMs and their effects. From his analysis, we retain that choices such as the functional form assigned to the temperature-mortality curve for each lag and the specification of the form given between the coefficients across different lags induce considerable influence on the analysis outcomes. The selection of these two components' shapes can vary from linear thresholds to polynomials to natural cubic splines, which highly influence the interpretation of results (Armstrong, 2006).

Moreover, the study emphasises the significance of grounding model choices on either model fit or a priori theories regarding methodological effects. Despite not all choices leading to convergence, prioritising choices based solely on model convergence may not be ideal, as the effects of different choices are interdependent. In other words, isolating one effect at a time may not suffice.

In light of these findings, we opted to make our modelling choices based on a priori choices, ensuring model convergence while focusing decisions informed by existing literature. First, concerning the shape of temperature-mortality curves and coefficients between lags, we use natural cubic splines. This decision aligns with the findings that more flexible models are best suited in the case of exploratory, single-city studies, as natural cubic splines facilitate the analysis of temperature's systematic effects on mortality (Armstrong, 2006). Given the nature of our study, and the small numbers we work with[15], simpler models are excluded as favored for multi-city studies. Secondly, regarding the selection of knot placements and their numbers, we opt for three knots positioned at the 10th, 75th, and 90th percentiles of the temperature distribution. This choice reflects the observed linear effect of cold compared to heat. Finally, determining the maximum lag for our model, we choose 21 days to accommodate potential harvesting effects resulting from prolonged exposure to specific temperatures.

Subsequently, we conducted model runs with variations in knot placement, in maximum lag, and the functional forms of the temperature-mortality curve. The results of these tests can be found in figure and 21 where we observe that running the model with different lags, 3 knots at the 10th, 75th and 90th percentiles and natural cubic splines displays minor differences between the different models. This brought us to keep the prescribed 21 days of lag. Then in figure 22 we can see that the natural splines better explain the temperature-mortality relation for 21 days of lag compared to the Linear and Double threshold models. Finally, regarding

[15]Especially in the case of our analysis by cause of death.

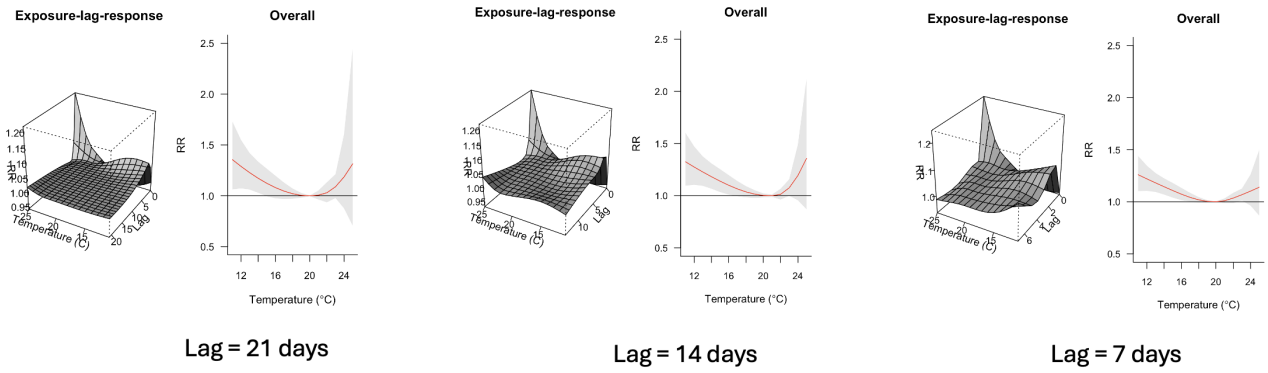


Figure 21: **Different Relative Risks for mortality (all ages) with different maximum lags.**

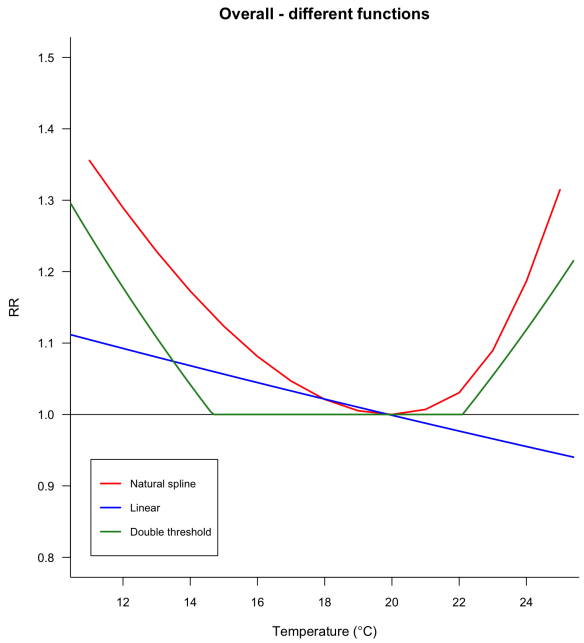


Figure 22: **The different RR curves according to the different curve form choices (based on all age mortality).**

knot placement, the prescribed placement is the only which yielded model convergence. This placement, which aligns with the tendency of cold related mortality to be more linear and than heat related mortality, was chosen for our analysis. The representation of these knots in regards to temperature distribution may be found in figure 23 where we observe one knot for cold and two for heat. Following these results, we keep our initial modeling choices, as they yielded the best model fit in our basic by-age model (further detailed in code annex 0.2).

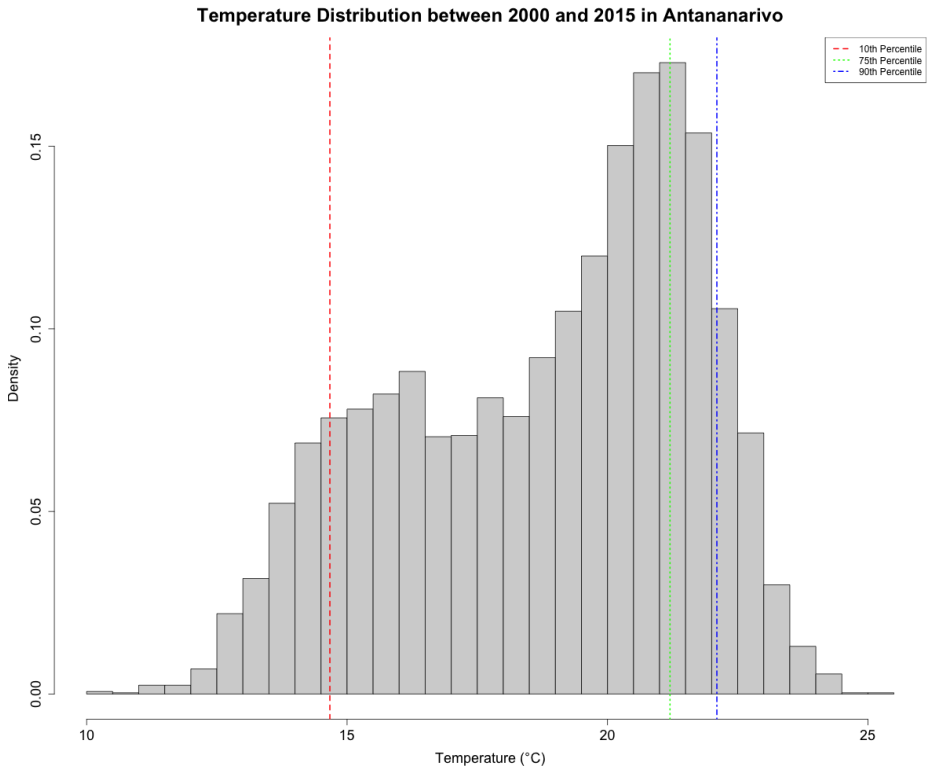


Figure 23: **Mean temperature distribution in Antananarivo for the 2000-2015 period.**
With indications for the 10th, 75th and 90th percentiles of distribution.

Finally, regarding modelling choices for the confounders, we chose to control for the effects of seasonal and long term variations using a natural cubic spline of day of the day of the year with 8 degrees of freedom (df). The confounding effect of variations in mortality between days of the week is captured by an indicator of the day of the week.

2.2 Sensitivity analyses

To address our research questions and test our hypotheses, we conducted several sensitivity tests. In this section, we detail our application of the Vicedo-Cabrera et al. (2019) method and the steps taken to explore our questions. Our code is available in annex 0.2, and we will discuss any modifications made for specific analyses within this section.

2.2.1 Sensitivity test 1: Allowing for age-specific relative risks

The initial step of our analysis focuses on implementing the Vicedo-Cabrera et al. (2019) tutorial by age groups. To achieve this, we adapt the original code to analyse multiple exposure-response curves sequentially. In this model, we maintain the assumption of constant mortality rates, implying no demographic changes. This approach allows us to investigate whether Relative Risks (RRs) vary across different age groups and facilitates comparison with models incorporating demographic changes in subsequent tests.

Given the differences between age groups impacting the heat-mortality relationship, we select groups based on several considerations: relevance for the analysis[16], adequate mortality data availability for model execution, and exploration of the existing literature for potential comparison. We choose three age groups: under 15 years old, between 15 and 59 years old, and over 60 years old. Initially, we considered four age groups, subdividing the first group into under 5 and 5-14 age brackets. However, limited data in the 5-14 age group makes this impractical. Details of the final death counts used in the analysis can be found in table 4 in the annex.

To analyse the results of this initial step, we compare the obtained RRs to assess variations between age groups. Additionally, we compare the projected Attributable Fractions (AFs) of the 2000-2010 period with those of 2050-59 and 2090-99 across different age groups under both SSP scenarios. The analysis of the RRs allows us to underline possible differences between risks for age groups. The AFs are the measure which allows us to understand which age group carries the highest burden of mortality due to non-optimal temperatures. Then, the analysis of the relative change between periods and SSPs allows us to provide preliminary information on the projected changes in climate on mortality when assumed constant. This comparative analysis allows us to discern the climate change effect on different age groups under a scenario without changes assuming constant RRs across all age groups.

Furthermore, to complete our analysis on the importance of age disaggregated models, we compare our results to an all-ages aggregated model. Strong differences in the exposure-response curves, if detected, will further confirm the importance of considering differences between age groups. This analysis is relevant given that we expect the curve to be influenced by age disaggregation.

Finally, the analysis of the minimum mortality temperature for each age group allows us to discern differences in non-optimal temperatures between age groups.

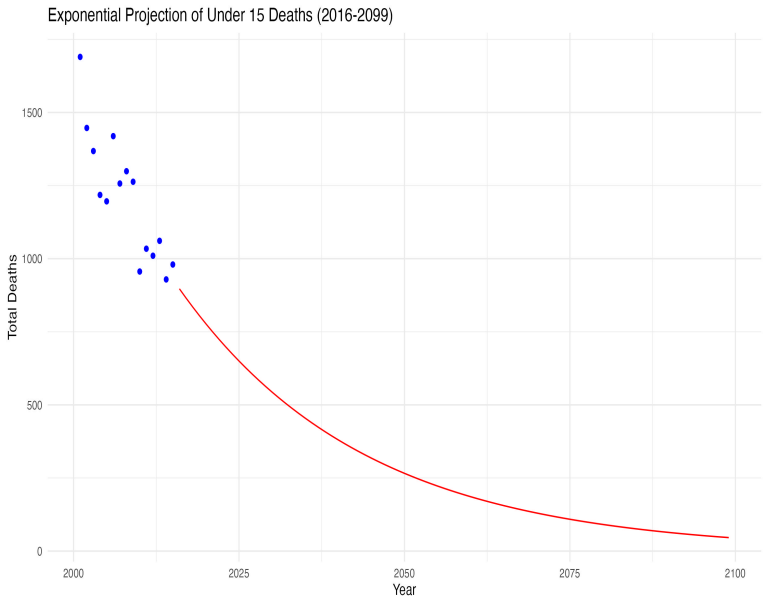
[16] we have to make sure that the groups make sense in regard to physiological responses to temperature.

2.2.2 Sensitivity test 2: Allowing for changes in the age composition of deaths in the future

To address changes in demographic transition (DT), it is necessary to discard the constant mortality assumption. DT prompts shifts in population structure, marked by an increase in the older population and a decline in the number of children. Additionally, a reduction in early-life mortality contributes to a shift of deaths to older age groups. Ideally, representing these changes involves applying varying death rates to a population of changing size, for example, through a cohort-component model. However, insufficient data on population by age limits the possibility of doing so. Consequently, we opt to represent changes in population structure and mortality patterns through exponential projections of deaths per age group.

To achieve this, we aggregate the number of deaths for each year between 2000 and 2015, minimising the noise effect of seasonal variations in projections. Then, we conduct regressions for each age group and analyse the associated R-squared values to gauge the regression's fit with past results. We then project deaths with an exponential function based on these regressions. To obtain vectors with daily death numbers for each year, we develop a seasonality function redistributing total deaths according to past seasonal patterns. We adjust this for leap and non-leap years to allocate deaths accurately across days. The code for these manipulations can be found in code annex 0.3, and projections plots and regression results can be found below in figures 24, 25, and 26. The analysis of the R-squared for all our regressions shows that most of the variance in the data is captured by the regressions (mainly for deaths under 15 and between 15 and 59). Additionally, we can see that the exponential projections for under-15 mortality are projected to decrease nine-fold between 2015 and 2099 (see figure 24). On the contrary, adult and over-60 mortality is projected to increase seven-fold and ten-fold respectively by 2099 (see figures 25 and 26).

The initial phase of this analysis involves comparing the total projected deaths for different age groups for the 2100 horizon. Subsequently, we apply the Vicedo-Cabrera et al. (2019) method by replacing the usual code, which replicates yearly mortality every year, with our vector of projected deaths. We then execute the remainder of our code in a similar manner as before, ensuring necessary adjustments when measuring ANs, as RRs remain unchanged. The objective of this phase is to quantify the effects of non-optimal temperatures on ANs when the population is projected to change. We then compare these results with the 2090-2099 ANs from the initial scenario.



(a)

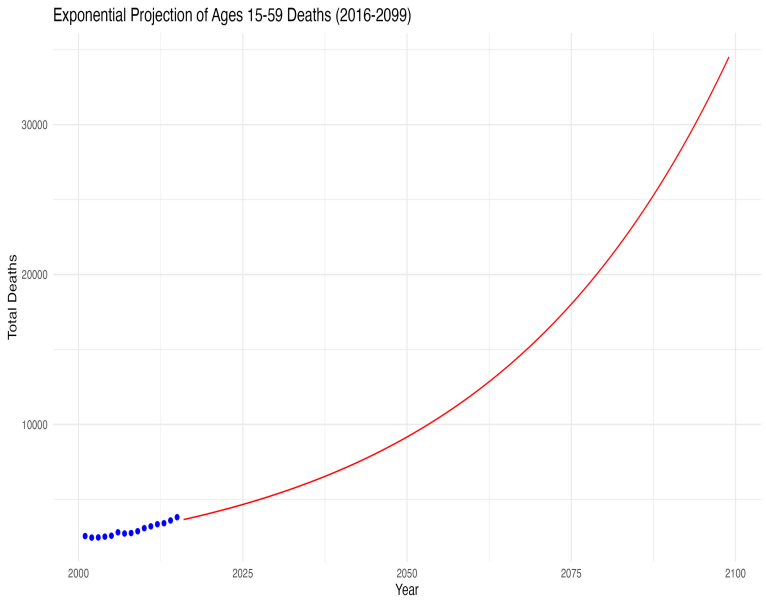
```
Residuals:
      Min        1Q    Median        3Q       Max
-0.150714 -0.038068 -0.003313  0.066680  0.101177

Coefficients:
                 Estimate Std. Error t value Pr(>|t|)
(Intercept)      78.900756   9.107258   8.664 5.35e-07 ***
as.numeric(year) -0.035765   0.004537  -7.884 1.62e-06 ***
---
Signif. codes:  0 ‘***’ 0.001 ‘**’ 0.01 ‘*’ 0.05 ‘.’ 0.1 ‘ ’ 1

Residual standard error: 0.08365 on 14 degrees of freedom
Multiple R-squared:  0.8162,    Adjusted R-squared:  0.803
F-statistic: 62.15 on 1 and 14 DF,  p-value: 1.624e-06
```

(b)

Figure 24: **Projections and Regression results for deaths under 15 years old.**
(a) Projections based on the 2000-2015 period for the 2090 horizon.
(b) Regression results for the 2000-2015 period.



(a)

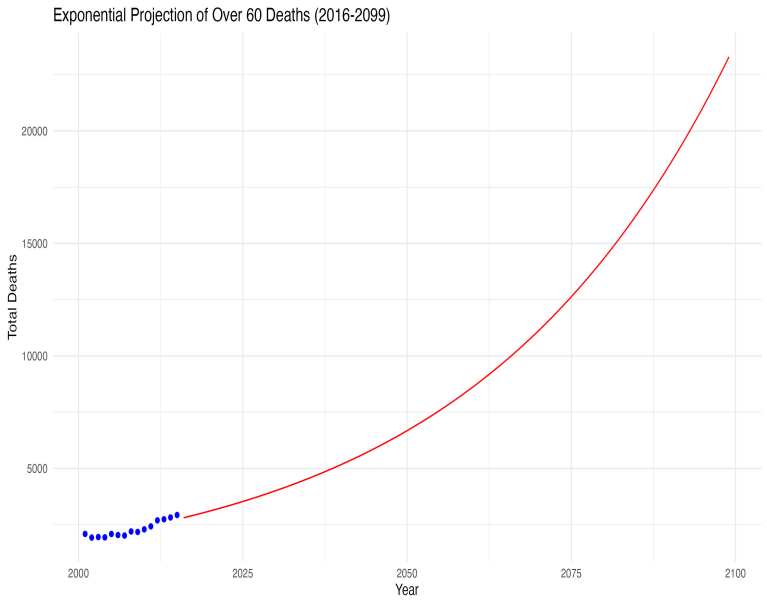
```
Residuals:
      Min        1Q    Median        3Q       Max
-0.066918 -0.049756 -0.002883  0.023953  0.150048

Coefficients:
                  Estimate Std. Error t value Pr(>|t|)
(Intercept)     -46.381489   6.413262  -7.232 4.34e-06 ***
as.numeric(year)   0.027075   0.003195   8.475 6.95e-07 ***
---
Signif. codes:  0 ‘***’ 0.001 ‘**’ 0.01 ‘*’ 0.05 ‘.’ 0.1 ‘ ’ 1

Residual standard error: 0.05891 on 14 degrees of freedom
Multiple R-squared:  0.8369,    Adjusted R-squared:  0.8252
F-statistic: 71.83 on 1 and 14 DF,  p-value: 6.952e-07
```

(b)

Figure 25: **Projections and Regression results for deaths between 15 and 59 years old.**
(a) Projections based on the 2000-2015 period for the 2090 horizon.
(b) Regression results for the 2000-2015 period.



(a)

```
Residuals:
     Min       1Q   Median       3Q      Max
-0.10185 -0.05353 -0.01948  0.05704  0.16281

Coefficients:
                  Estimate Std. Error t value Pr(>|t|)
(Intercept)     -43.48381    8.19126  -5.309  0.00011 ***
as.numeric(year)  0.02551    0.00408   6.251 2.12e-05 ***
---
Signif. codes:  0 '***' 0.001 '**' 0.01 '*' 0.05 '.' 0.1 ' ' 1

Residual standard error: 0.07524 on 14 degrees of freedom
Multiple R-squared:  0.7362,    Adjusted R-squared:  0.7174
F-statistic: 39.08 on 1 and 14 DF,  p-value: 2.122e-05
```

(b)

Figure 26: **Projections and Regression results for deaths over 60 years old.**
(a) Projections based on the 2000-2015 period for the 2090 horizon.
(b) Regression results for the 2000-2015 period.

2.2.3 Sensitivity test 3: Allowing for cause-specific relative risks

In this third part of our analysis, our aims are to document changes in epidemiological transition in Antananarivo and provide an overview of temperature-sensitive causes of death for specific age groups. To achieve this, we first re-code various ICD-9 codes into broader categories. Given that the granularity of the original codes for the causes of death in the initial database is not suitable for analysis using the DLNM method. To establish the categories, we follow the classification used by Waltisperger et al. (2005), enabling possible comparison with their analysis of the main causes of death in Antananarivo prior to 2000. The final classification can be found in figure 44 in the annex, and the code used to reclassify the causes of death in the code annex 0.4.

Then, we represent the temporal evolution of different causes of death that our review of the literature has shown to be affected by temperatures, focusing solely on relevant causes of death. We then compare these results to past trends. Finally, we divide our database by cause-of-death groups and subject them to the model to extract cause-specific relative risks (RRs) and attributable fractions (AFs) due to heat and cold when possible.

The primary focus of this section is to demonstrate if different causes of death are associated with temperatures and then see how they may respond variably to temperatures.

Therefore, our results primarily focus on the analysis of RRs, which indicate sensitivity to exposure. This choice to only analyse relative risks is explained by the fact that we may not always be able to attain model convergence. By conducting this analysis, we aim to draw conclusions on the effects of warmer temperatures on mortality by cause.

2.2.4 Sensitivity test 4: Sensitivity to control for seasonality

Based on Schlüter et al. (2020), we understand that seasonality significantly influences mortality in the study area, particularly for younger age groups. To investigate the impact of a changing epidemiological profile on the heat-mortality relationship, we run the DLNMs for different age groups without controlling for seasonality. This approach allows us to compare RRs without the confounding effect of seasonality. By comparing these results to the models where we control for seasonality, we aim to identify differences in the models for each age group with and without seasonal variations. This comparison will enable us to highlight the significance of seasonality, potentially justifying the use of a model that accounts for transitions in the analysis and further underlining the importance of distinguishing age groups. By doing so, we unveil seasonal variations in the heat-mortality relationship and, understand how it varies across different demographic profiles, to ensure that our analysis includes these seasonal patterns.

2.2.5 Sensitivity test 5 : Controlling for the effect of modelled exposure data

As detailed before, the lack of exposure (and outcome) data is a major concern in regions such as SSA. In this context, rises the question of the potential use of modelled exposure data (such as temperature) to conduct analyses. Modelled data is created based on approximations using existing recorded data and estimates from other locations. This last sensitivity test therefore aims to compare the differences in exposure-response models using ERA-5 data (modelled) and NOAA data (measured).

To do so, we first analyse the differences in data convergence with the ERA-5 data and the GCM data. This first test aims to measure whether there are differences in convergence with GCM data between modelled and measured data. If differences are observed we analyse which dataset converges best with GCM data. The next step consists in running the model for all ages aggregated, and different mortality age groups sequentially. This choice of using both aggregated and desegregated models stems from possible problems in model convergence. After having run these trials we compare the DLNM curves to the DLNM curves obtained with measured data. Running this test allows us to draw conclusions on the impact of using modelled versus measured data in our analysis.

Results

This section is structured as follows : first, we present the results of our DLNMs and the associated projected health outcomes in our scenario of constant mortality. Secondly, using these results, we analyse the differences in AN and AF when mortality rates are constant versus when they are projected to change. Thirdly, we focus on cause- and age-specific DLNM outputs. Then we will control for the effect of seasonality. Finally, we control for the effect of using modelled temperature data in our analysis.

1 Allowing for age-specific relative risks

In this first sensitivity test, we present the current temperature-mortality association in Antananarivo for different age groups. After having presented the main results of our DLNM model and having analysed and refined our choice of GCM for the exposure projection, we compare the projected health outcomes. Finally, we compare these results to the aggregated mortality model.

1.1 Main results: models disaggregated by age

As mentioned prior, the DLNM method is often used to analyse the temperature-mortality relationship across all ages (Gasparrini et al., 2015) or for mortality at older ages (Gasparrini et al., 2012). Here, we aim to find out the importance of disaggregating the analysis across age groups while also presenting the current temperature-mortality relationship in Antananarivo.

1.1.1 Age-specific relative risks and seasonality

The results of our age-specific models can be found in box 1.1.1. There, we present for our three mortality age groups the results of the DLNM and the associated seasonal trends in mortality. The graphs represent, on one hand, the relative risk of mortality for each temperature after each period of lag and, on the other hand, cumulative RRs of mortality for each temperature across all the lag period. The seasonal trend graphs represent the seasonality of mortality along the year.

The preliminary analysis of these graphs shows marked differences between our three age groups. The analysis of the cumulative mortality risk graphs (for the whole lag period) shows that there are differences in the temperature-mortality relation for the different age groups. The minimum mortality temperature (T_{mm}) of 17.8°C is the threshold defining the limit between heat and cold related excess mortality below 15 years old. This threshold is different for mortality between 15 and 59 and mortality over 60 for which the T_{mm} are respectively of 21.7°C and 19.4°C. These differences in T_{mm} are coupled with differences in the shapes of the exposure response curves as well. There is a clear negative association between the risk of dying due to cold temperatures for children and elderly (where the relative risk is the highest at 11°C for children (1.36 (95% CI= 0.77; 2.4)) and the elderly (1.92 (95% CI= 1.31; 2.81)) in comparison with the respective T_{mm}) whereas the relative risks of dying of cold temperatures for adults is fairly low and relatively constant for the whole cold temperature range (RR at 15°C= 1.13 (95% CI= 0.93; 1.38) compared to T_{mm}). Regarding heat related mortality, our middle age group exhibits a near linear positive relationship between temperature and mortality (the risk is multiplied by 1.62 (95% CI= 0.59; 4.38) at 25°C relatively to the T_{mm}). The oldest age group also presents a positive temperature-mortality curve for warm temperatures, but the difference in risks of dying associated with these temperatures is lower. The youngest age group however, does not present a linear relation as the warmest temperatures are not associated to the highest RRs for the heat related mortality (a risk multiplied by 1.23 (95% CI= 0.95; 1.59) at 23°C and multiplied by 1.19 (95% CI= 0.35; 4.04) at 25°C compared to T_{mm}). Hence, we observe that all age groups have a nonlinear temperature-mortality relationship, where there are increases in relative risk above and below the T_{mm}.

When paying attention to the shaded part of the graphs, we can see that the model yields a lot of uncertainty in the estimation of the RRs in our case study. This uncertainty tends to be higher in the estimation of RRs related to heat than in RRs related to cold.

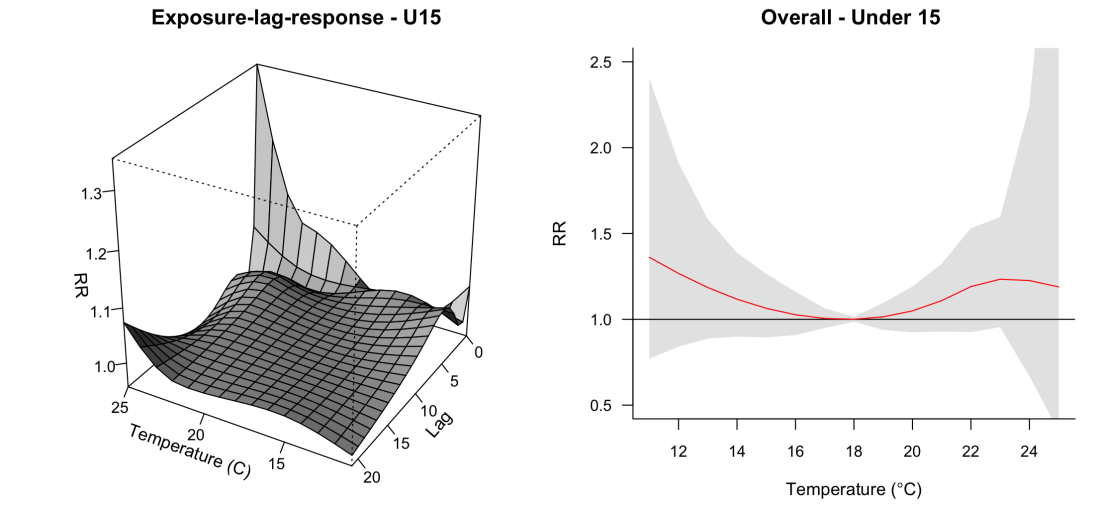
Furthermore, risks which are different for heat and cold and different age groups are also different across the lag dimension. Heat related mortality exhibits for all age groups a stronger immediate effect (mainly in the case of mortality at older ages) whereas cold related

mortality tends to occur a few days later. But paying more attention to the particularities of the different age groups, we observe that heat related mortality under 15 years old also occurs with a delayed effect. This is also true for heat related mortality between 15 and 59 which also tends to occur with a delayed effect. This observation is not applicable for mortality over 60 years old, where heat-related mortality tends to be immediate.

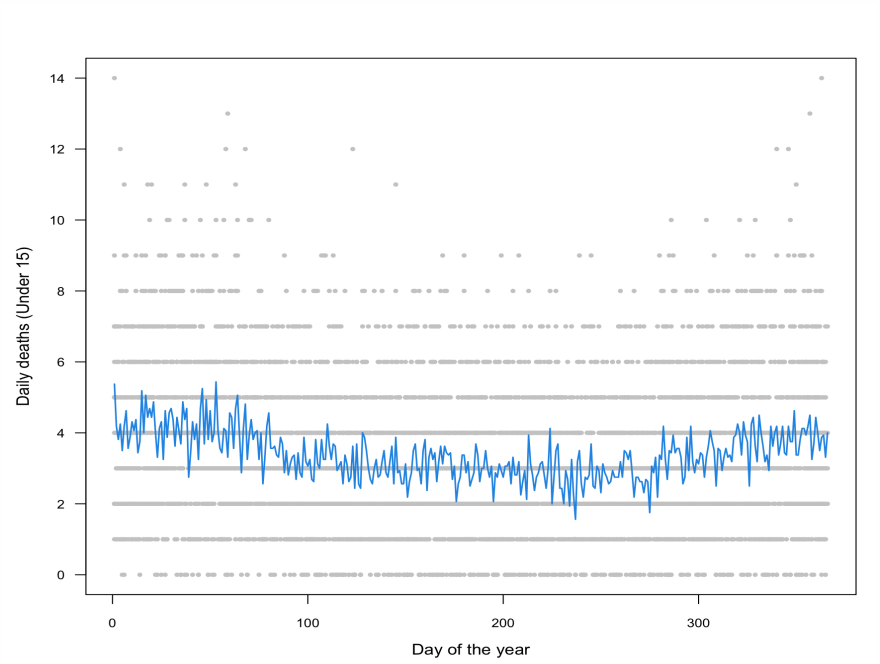
Besides, the seasonal trends of mortality also vary by age group, and, analysing the different graphs shows that all age groups present different seasonal trends in their mortality patterns. First, mortality below 15 years old seems to show the strongest seasonal trends. For this age group we can say that mortality tends to be highest in periods where temperatures are highest (November through March) with lower mortality rates during the cooler period. Then, mortality between 15 and 59 seems to be the least affected by seasonality, even though there are small marked increases in deaths during the cooler and warmer periods. Finally, mortality at later ages also shows a marked seasonal pattern with a clear increase in mortality around the cooler period. These results strongly concord with the analysis of the RRs at different temperatures and already point out a potential mediating effect of seasonality on the temperature-mortality relationship, for the youngest age group especially.

Summing our results for this first step of our analysis we emphasise the following findings: relative risks of mortality vary between different age groups, these variations are influenced by differences in sensitivity which are captured by the different minimum mortality temperatures for each age group and different relative risks. The RRs vary a lot along lag dimension between different groups and for different temperatures and the groups do not present the same seasonal patterns.

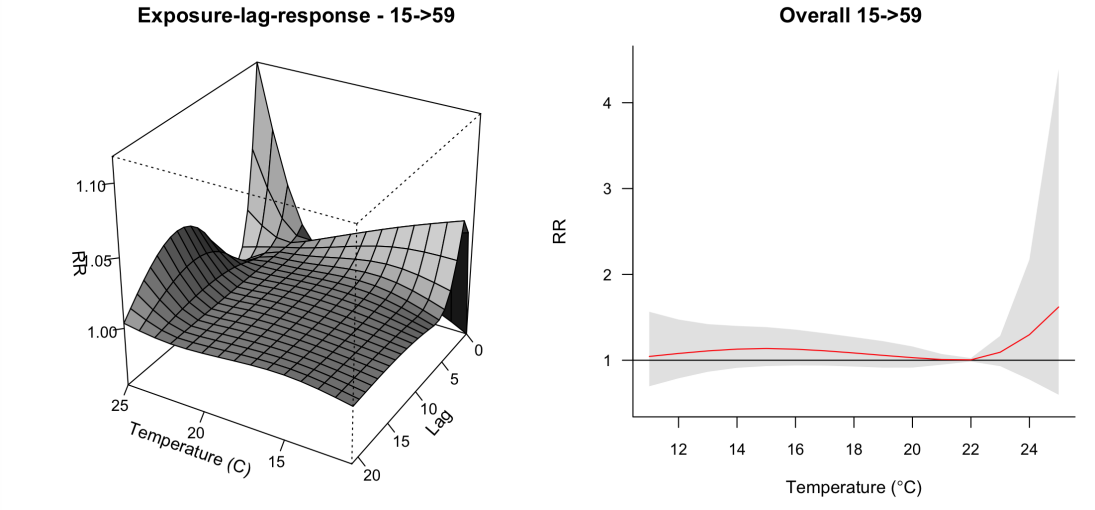
Box 1.1.1 : DLNM and seasonality by age group



Temperature-related under 15 years old mortality in Antananarivo (2000-2015).
Left: Three dimensional plot showing the estimated exposure-lag-response association between temperature and mortality.
Right: Cumulative mortality risk for all lag (RR and 95% confidence interval).

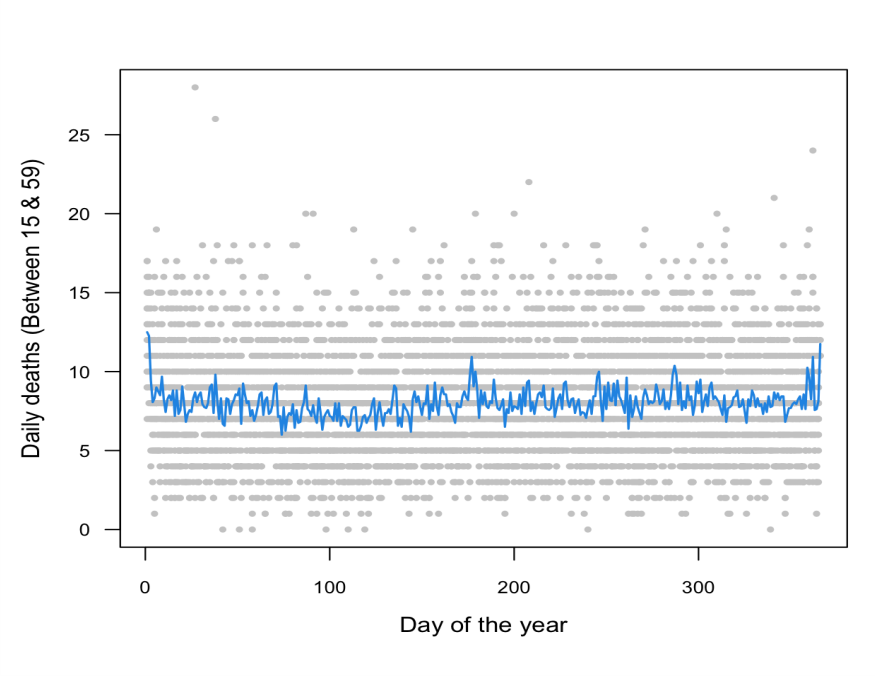


Seasonal under 15 years old mortality trends (2000-2015).
The grey dots correspond to the observed daily mortality counts registered for each day of the year for the observation period. The blue line depicts the mean number of deaths daily.

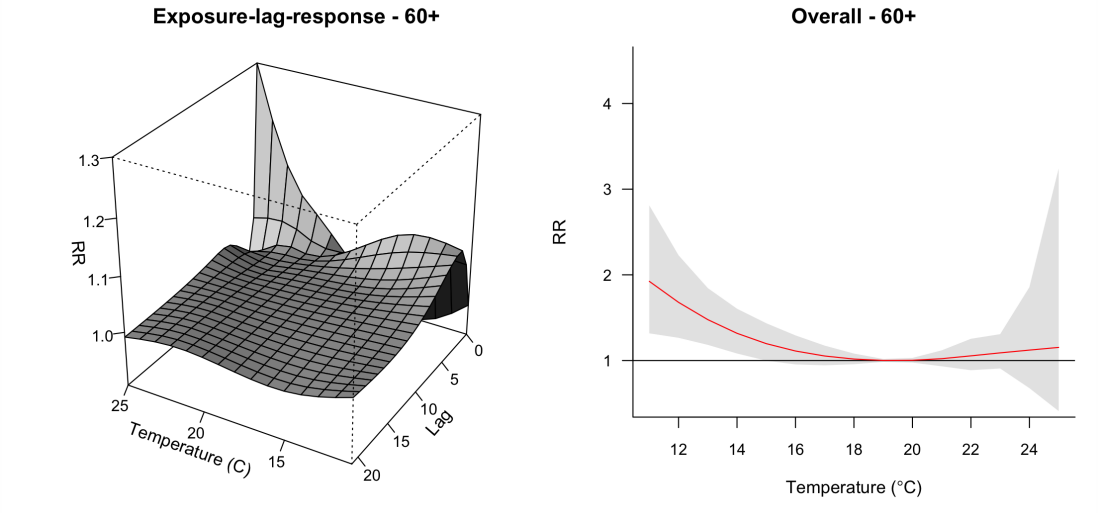


Temperature-related mortality between 15 and 59 years old in Antananarivo (2000-2015).
Left: Three dimensional plot showing the estimated exposure-lag-response association between tem-

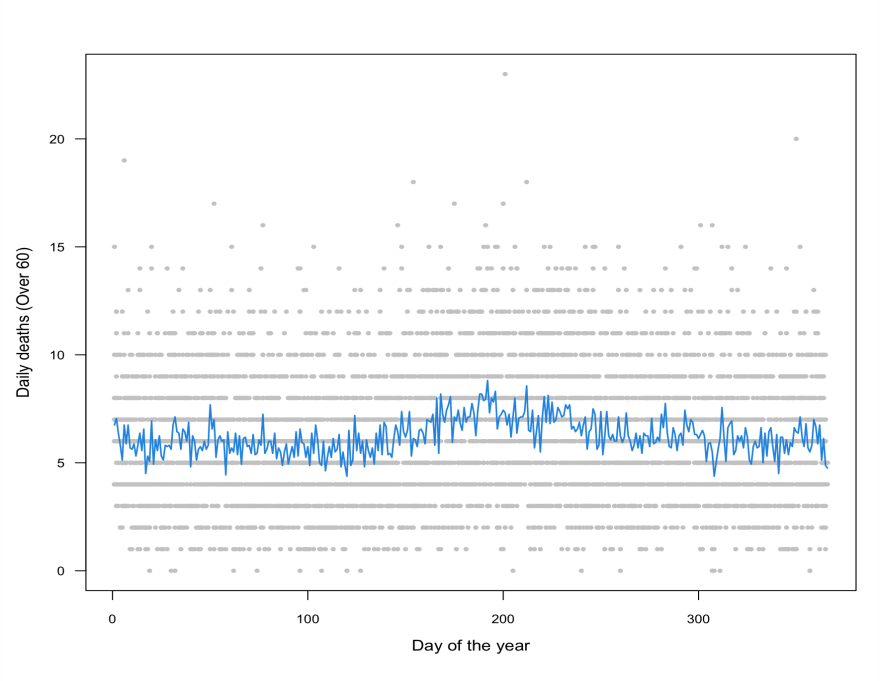
perature and mortality.
Right: Cumulative mortality risk for all lag (RR and 95% confidence interval).



Seasonal between 15 and 59 years old mortality trends (2000-2015).
The grey dots correspond to the observed daily mortality counts registered for each day of the year for the observation period. The blue line depicts the mean number of deaths daily.



Temperature-related mortality over 60 years old in Antananarivo (2000-2015).
Left: Three dimensional plot showing the estimate exposure-lag-response association between temperature and mortality.
Right: Cumulative mortality risk for all lag (RR and 95% confidence interval).



Seasonal over 60 years old mortality trends (2000-2015).
The grey dots correspond to the observed daily mortality counts registered for each day of the year for the observation period. The blue line depicts the mean number of deaths daily.

1.1.2 Projected temperature and calibration

The next step of the analysis implies projecting future temperature series and choosing the GCM which best fits the past exposure data. The different graphs for projecting mortality series and calibrating the different GCM temperatures with the past data can be found in box 1.1.2.

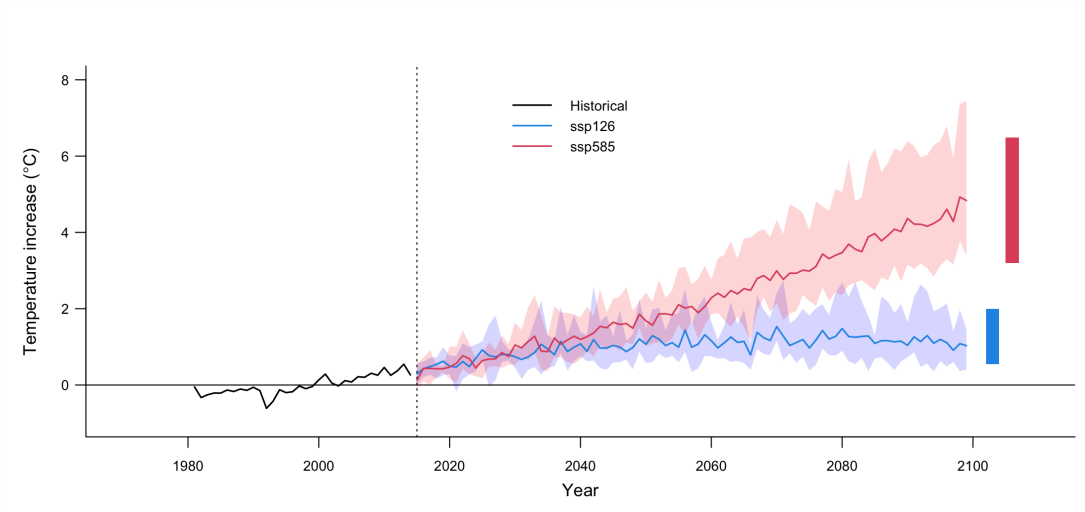
The first graph in box 1.1.2 shows the projected increase in temperatures according to each of our SSP scenarios. We notice that both SSPs project an increase in temperatures, but with big differences in the projections past 2060. Past 2060 we observe that the mitigation scenario projects a stabilised increase in temperature (1°C at most) whereas the scenario with higher radiative forcing projects an increase of around 4°C. The projected increases in temperature are nuanced by the shaded area representing the confidence interval, estimated using the range of the possible outcomes for each GCM.

The following step consists in comparing the measured past temperature distribution with the past temperature distribution estimated in the different GCMs. This step is crucial as it

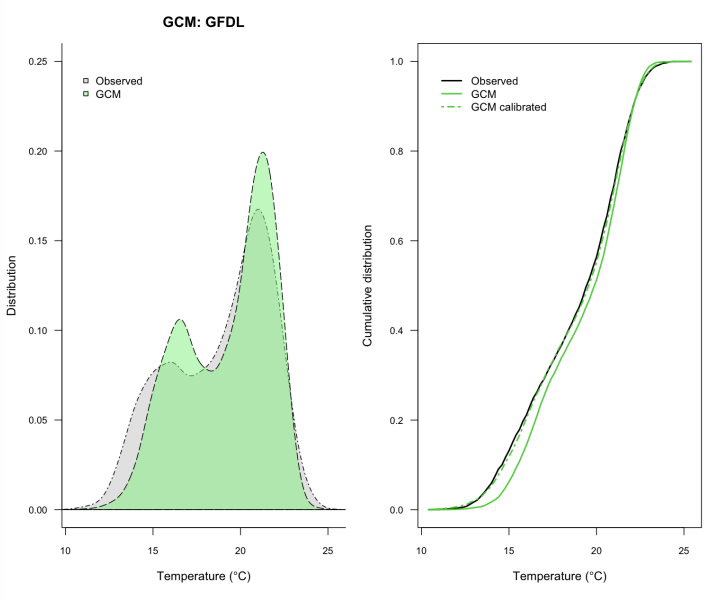
allows us to make a choice regarding the GCM used to estimate the AFs and ANs in the rest of our analysis. The comparison of the distribution which can be found in the second part of box 1.1.2 shows for each GCM the difference in temperature distribution and the necessary calibration to match distributions. The analysis of these different graphs explains our choice for the GCM from the Meteorological Research Institute (MRI) for the calculation of our attributable fractions. Though it must be said that all the GCM calibrated estimations are used in the model to project future temperature in our graphs.

Box 1.1.2 : Calibration and projected temperature series

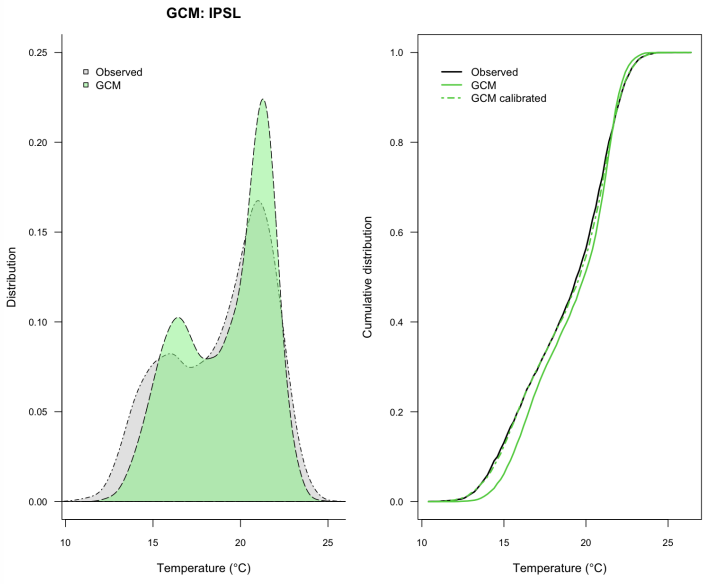
Increase in °C in projected mean temperature (for ssp126 and ssp585) in Antananarivo.
The increase in temperatures shown here are averaged across the 5 GCMs for each scenario (solid line), expressed as increase in annual mean temperature from the historical average temperature. The shaded area shows the variability in the projected temperature across GCMs.
Data extracted from RNOAA and ISIMIP and processed in code 0.2.



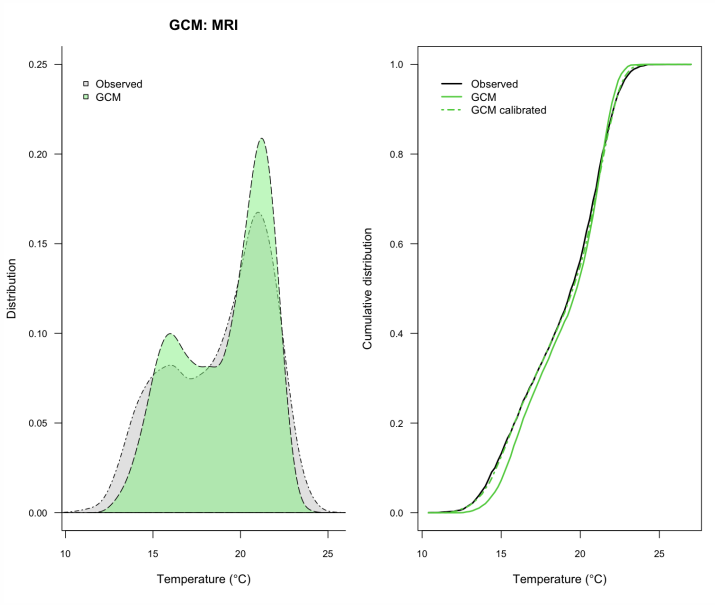
Bias correction for different GCMs
Comparison between the distribution (left) and cumulative distribution (right) of the raw bias-corrected modeled temperature (for SSP5-8.5) and the observed temperature series.



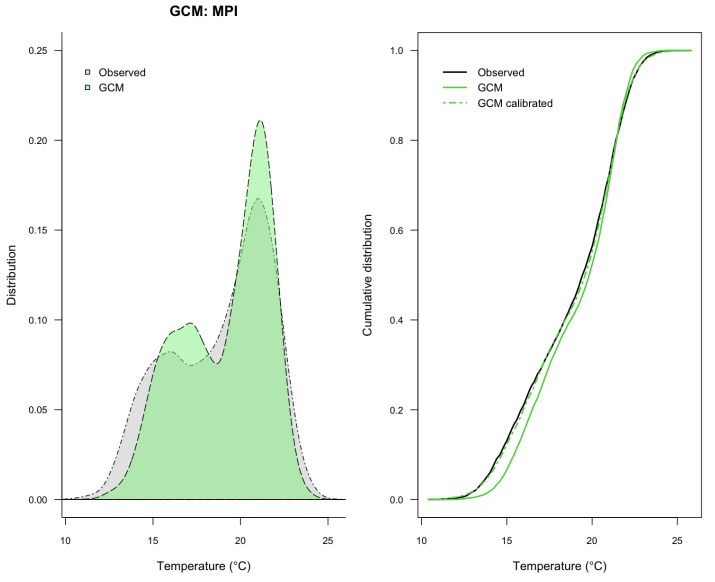
Geophysical Fluid Dynamics Laboratry



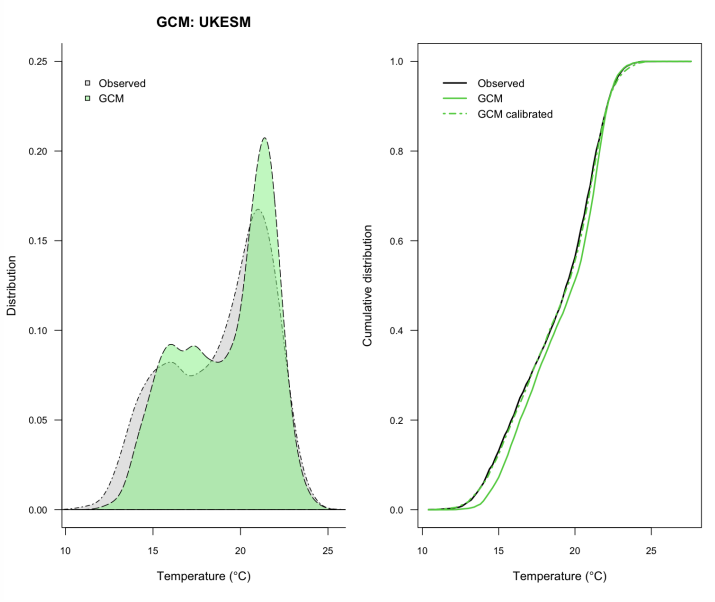
Institut Pierre-Simon Laplace



Meteorological Research Institute



Max Planck Institute for Meteorology



UK Earth System Model

1.1.3 Age-specific projected health outcomes

Now that we have estimated the risk of mortality for non-optimal temperatures (those above or below T_{mm}) for different age groups, it is time to quantify and represent which fraction of mortality can be attributed to these temperatures. In other words, this section aims to use the current knowledge on the temperature-mortality relationship to project the future attributable mortality. To summarise our results and showcase these numbers we present graphs 27 to 29 and table 1. First, in table 1, we describe the number of deaths for each decade, the absolute attributable fraction of deaths due to cold and heat (and the associated CIs[17]) for the 2000-2009 and the 2090-2099 decades for our two SSP scenarios. In this table small differences can be observed for the past AF estimates, this is due to differences in calibrated SSP scenario temperatures. Then, graphs 27 to 29 show for each age group and each SSP the extended RR curve (extended to suit the increased temperatures). To visualise AFs of deaths due to cold and heat the middle panels show the change in temperature distribution whereas the bottom panels represent the change in AF. To understand the shifts in AF we chose to represent for each SSP the difference between the current period (2000-2009) and two future periods : 2050-59 (where the differences between the two SSPs are less marked) and 2090-2099 (where the temperature projections vary more intensely).

[17]Given that a fraction of deaths due to non-optimal temperatures cannot take negative values, we have chosen to truncate the values below zero to zero. The same choice was made in the representation of ANs which cannot be negative.

Table 1: **Average deaths and attributable fractions (AF%) by age group and SSP**

Age	Average deaths per 10 years	SSP	Cold (2000-2009)			Heat (2000-2009)			Cold (2090-99)			Heat (2090-99)		
			Est	CI low	CI high	Est	CI low	CI high	Est	CI low	CI high	Est	CI low	CI high
<15	**12.350,6**	1-2.6	**1,72**	0	5,30	**6,28**	0	14,27	**1,05**	0	3,95	**8,84**	0	19,20
		5-8.5	**1,71**	0	5,29	**6,31**	0	14,30	**0,08**	0	0,72	**11,32**	0	57,93
15-59	**29.234,4**	1-2.6	**5,28**	0	14,34	**0,58**	0	1,55	**4,29**	0	11,85	**2,77**	0	10,34
		5-8.5	**5,28**	0	14,33	**0,60**	0	1,57	**1,66**	0	6,30	**23,69**	0	55,49
>60	**22.781,3**	1-2.6	**5,99**	0,24	10,97	**1,46**	0	5,27	**4,04**	0	8,73	**2,75**	0	9,04
		5-8.5	**5,95**	0,20	10,95	**1,47**	0	5,30	**0,60**	0	2,57	**8,53**	0	46,64

First, we observe for mortality below 15 years old that most of the burden attributable to non-optimal temperatures is concentrated in warmer temperatures. Indeed, even though the RRs between warm temperatures and mortality under 15 do not show a positive linear trend, the results of our analysis show that the total AF is mostly due to heat rather than cold. This is mainly due to the temperature distribution which is mostly concentrated after T_{mm} and the low RRs in temperatures between 15 and 20°C. To give numbers, we estimate the attributable fraction of deaths due to cold around 1.7% (95% CI= 0; 5.3) whereas the AF for heat is estimated higher at 6.3% (95% CI= 0; 14.3). It should be noted that both CIs include zero, due to large uncertainty. Now that the present burden of mortality attributable to non-optimal temperatures has been presented we focus on the projected changes in these estimates. First, our mitigation scenario SSP1-2.6 projects a slight shift in AF distribution which is in alignment with the small projected increase in temperature for this scenario. Hence, very small differences are observed between the AF for the 2050-2059 and the 2090-2099 decades as temperature distribution and maximum mean temperatures are very similar (see figures 27a & 27b). Then, analysing the shift in AF for SSP5-8.5 we can see that there are more differences between the two decades where the big change in temperature distribution explains a slight increase in AF (see figures 27c & 27d). Thereupon, SSP1-2.6 and SSP5-8.5 give us AFs of 1.05% (95% CI= 0; 3.95) and 0.08% (95% CI= 0; 0.72) for cold and 8.84% (95% CI= 0; 19.20) and 11.32% (95% CI= 0; 57.93) for heat. We attribute the significant but rather small differences in AF to the shape of the temperature-mortality association (which decreases and is extended to decrease). Finally, the very large confidence intervals (especially for the AFs estimated in SSP5-8.5) are explained by the existing uncertainty in future temperatures. But, these are also attributed to the already existing large uncertainty

in the association between temperature and mortality for this age group.

Secondly, we present the results obtained for the temperature-mortality association between 15 and 59 years old. In regard to the effect of temperatures on mortality for the measured period of our analysis, mortality due to non-optimal temperatures is predominantly explained by the effect of cold. Thus, while cold is estimated to be responsible for 5.28% (95% CI= 0; 14.3) of deaths for this age group, only 0.58% (95% CI= 0; 1.55) of deaths are associated to the effect of heat for the 2000-2009 decade. An analysis of the shape of the curve for the temperature-mortality association forecasts, however, much larger shifts in AF between cold and heat. Indeed, as the association between heat and mortality is nearly linear for adults in our case study, the extension of the curve for higher temperatures yields high increases in AFs. This is observed in both scenarios but at very different scales. On one hand, AF projections in the mitigation scenario yield an increase in AF due to heat and a decrease in AF due to cold (see figures 28a & 28b). But, in this case, cold still has a higher burden of mortality for both the 2050-59 and 2090-99 decades. On the other hand, our less optimistic radiative forcing scenario presents a whole new distribution of AFs (see figure 28c & 28d) where the burden of heat (23.69 % (95% CI= 0; 55.49)) is much higher on overall mortality compared to that of cold (1,66% (95% CI= 0; 6.30)). As per our analysis of mortality under 15, large confidence intervals are also measured here though they are not as large.

Thirdly, our analysis of the RRs of mortality associated with heat and cold for deaths over 60 clearly shows that cold has a greater impact than heat for this age group. Given the present distribution of temperature the AFs for the current period indicate more mortality due to cold temperatures than warmer ones. For instance, the AF associated to cold for the current period is of 5.9% (95% CI= 0.2; 10.9) whereas the AF associated to heat is of 1.4% (95% CI= 0; 5.27). This greater importance of cold-related mortality remains throughout the whole projection period for SSP1-2.6 where the mitigated increases in temperatures do not imply major shifts in AFs (see figures 29a & 29b). On the other hand, our projections of the AFs for SSP5-8.5 show a shift in patterns by the last decade of the century where the AF of deaths due to cold will decrease to 0.6% (95% CI= 0; 2.57) and where AF due to heat will increase to 8.53% (95% CI= 0; 46.64). This increase in AFs due to heat even though it is different between the two scenarios is lower than that of the previous age group given the previously very small effect of heat on mortality for these age groups.

Prior to this analysis of the AFs we had an idea of the different relative risks of mortality for a given temperature (relative to T_{mm}). There we were able to conclude that risks of dying due to non-optimal temperatures is mostly due to heat for adults, and due to cold for children and the elderly. By merging the distribution of present and future temperatures we were able to transfer the measured relative risks into proportions of deaths attributable

to non-optimal temperatures for the present and the future periods. This sheds light on significant differences between the different age groups, for the different scenarios and for different projection horizons, where, children currently bear a higher burden of mortality associated to heat than the two other age groups, which bear a higher burden due to cold temperatures.

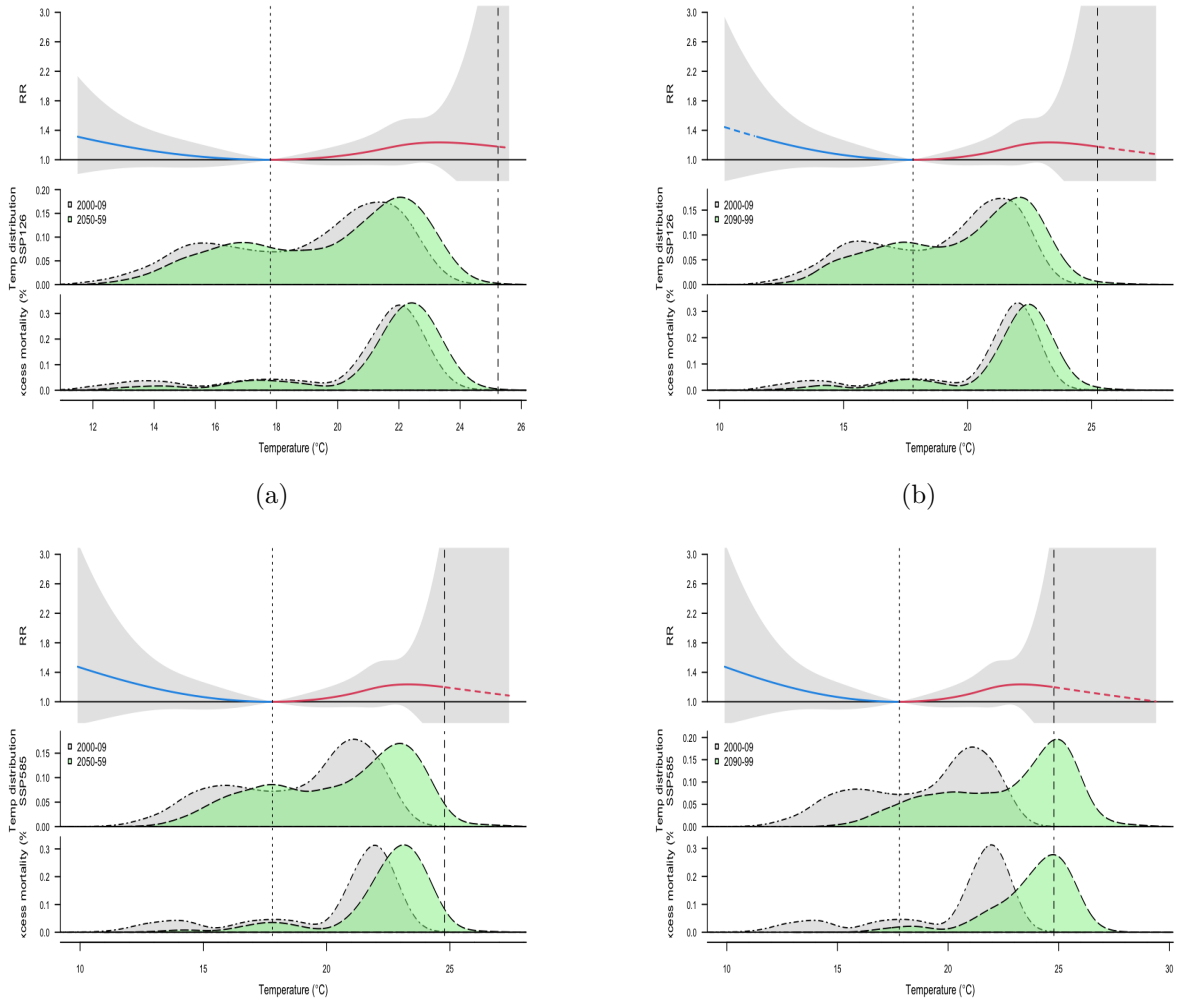


Figure 27: **Temperature and excess under 15 years old mortality for past and future periods.**
(a) SSP1-2.6 for 2000-10 and 2050-59 (b) SSP1-2.6 for 2000-10 and 2090-99 (c) SSP5-8.5 for 2000-10 and 2050-59 (d) SSP5-8.5 for 2000-10 and 2090-99.
Top panel : exposure-response curves (RRs across T°C (with 95% CI)). The dotted vertical line is the minimum mortality temperature which separates between cold (blue) and heat (red). The dashed part of the curve represents the extrapolation beyond the observed maximum temperature (2000-2015). *Mid panel*: distribution of temperature for the past (grey) and future (green) using the ensemble estimates (average impacts across GCMs) for SSP1-2.6. *Bottom panel*: the related distribution of excess mortality, expressed as the fraction of additional deaths (%) attributed to non-optimal temperature.

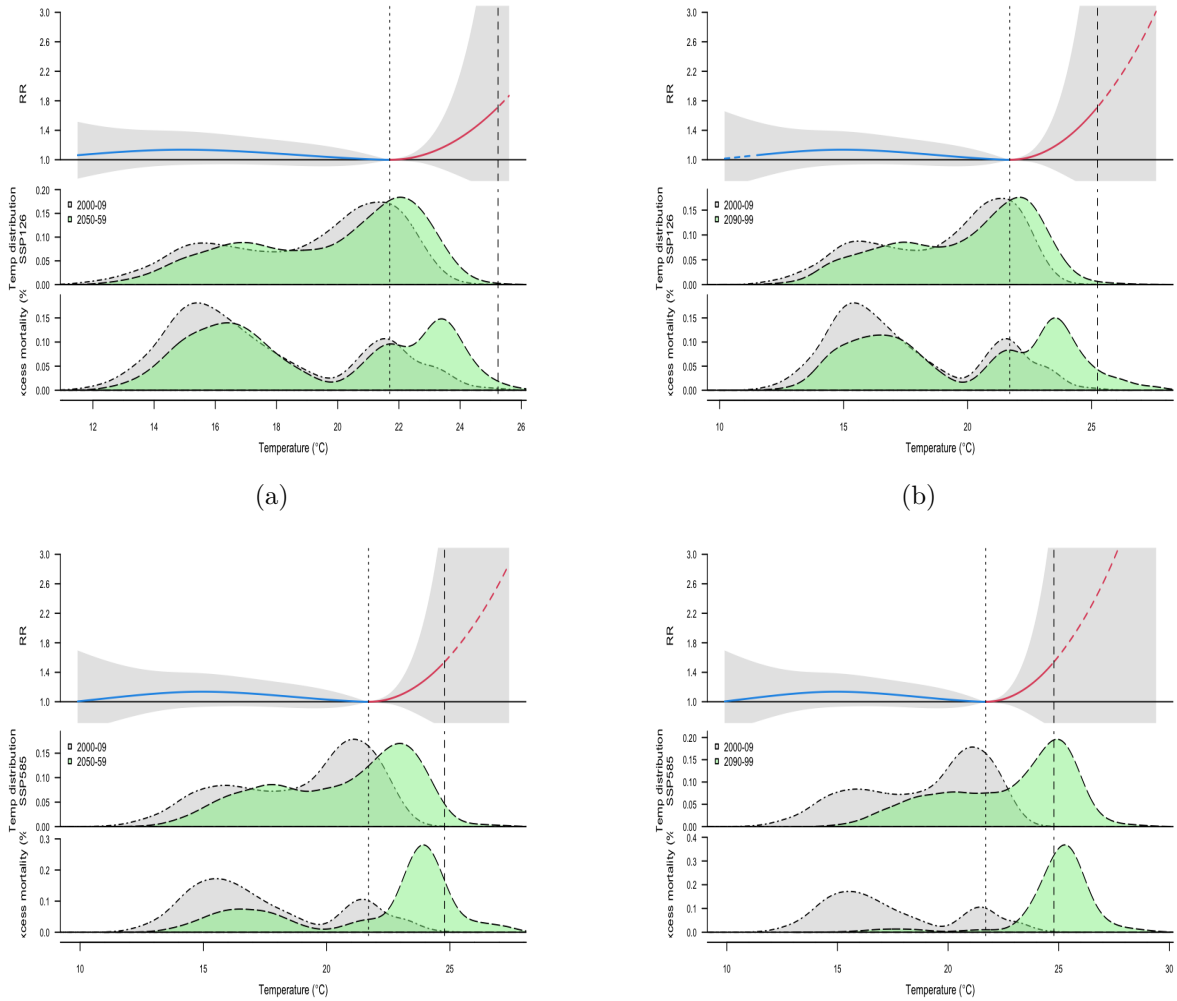


Figure 28: **Temperature and excess 15-59 years old mortality for past and future periods.**
(a) SSP1-2.6 for 2000-10 and 2050-59 (b) SSP1-2.6 for 2000-10 and 2090-99 (c) SSP5-8.5 for 2000-10 and 2050-59 (d) SSP5-8.5 for 2000-10 and 2090-99.
Top panel : exposure-response curves (RRs across T°C (with 95% CI)). The dotted vertical line is the minimum mortality temperature which separates between cold (blue) and heat (red). The dashed part of the curve represents the extrapolation beyond the observed maximum temperature (2000-2015). *Mid panel*: distribution of temperature for the past (grey) and future (green) using the ensemble estimates (average impacts across GCMs) for SSP1-2.6. *Bottom panel*: the related distribution of excess mortality, expressed as the fraction of additional deaths (%) attributed to non-optimal temperature.

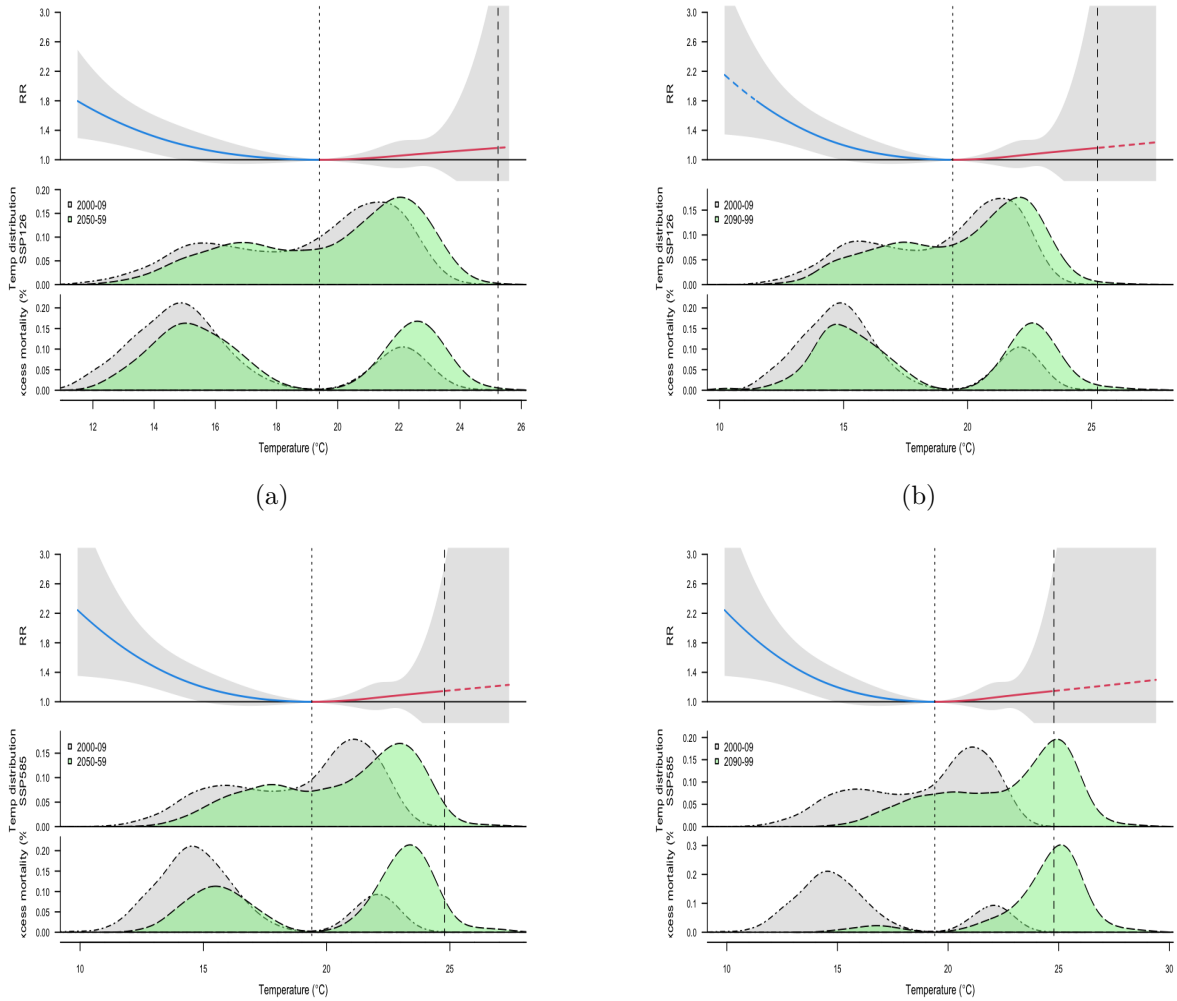


Figure 29: **Temperature and excess over 60 years old mortality for past and future periods.**
(a) SSP1-2.6 for 2000-10 and 2050-59 (b) SSP1-2.6 for 2000-10 and 2090-99 (c) SSP5-8.5 for 2000-10 and 2050-59 (d) SSP5-8.5 for 2000-10 and 2090-99.
Top panel : exposure-response curves (RRs across T°C (with 95% CI)). The dotted vertical line is the minimum mortality temperature which separates between cold (blue) and heat (red). The dashed part of the curve represents the extrapolation beyond the observed maximum temperature (2000-2015). *Mid panel*: distribution of temperature for the past (grey) and future (green) using the ensemble estimates (average impacts across GCMs) for SSP1-2.6. *Bottom panel*: the related distribution of excess mortality, expressed as the fraction of additional deaths (%) attributed to non-optimal temperature.

1.2 Comparing age-specific and overall models

The final results we describe in this section are the results of our DLNM for all age groups concurrently. We ran this model to compare it to our previous results to further underline

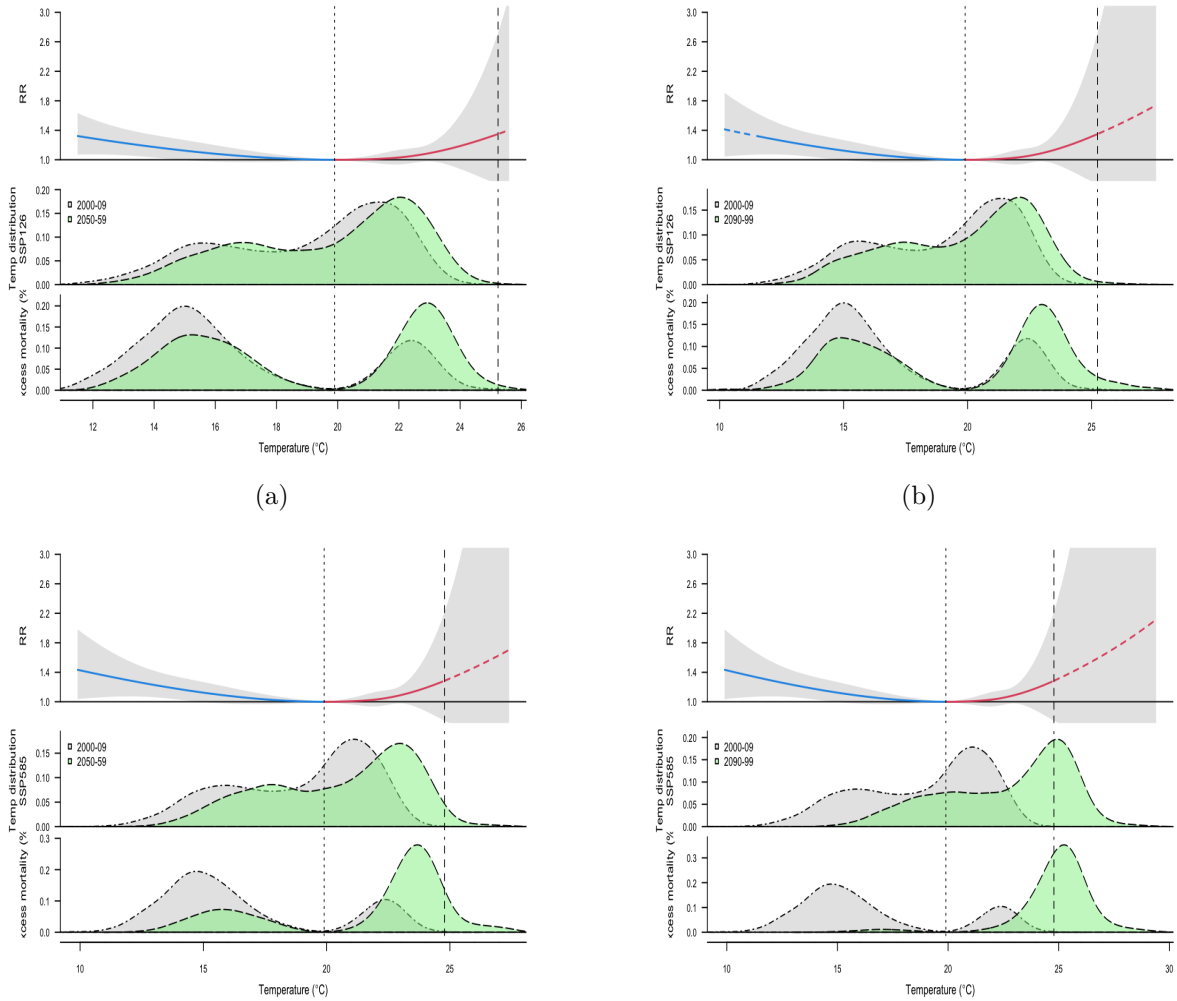


Figure 30: **Temperature and excess mortality for past and future periods - All ages.**
(a) SSP1-2.6 for 2000-10 and 2050-59 (b) SSP1-2.6 for 2000-10 and 2090-99 (c) SSP5-8.5 for 2000-10 and 2050-59 (d) SSP5-8.5 for 2000-10 and 2090-99.
Top panel : exposure-response curves (RRs across T°C (with 95% CI)). The dotted vertical line is the minimum mortality temperature which separates between cold (blue) and heat (red). The dashed part of the curve represents the extrapolation beyond the observed maximum temperature (2000-2015). *Mid panel*: distribution of temperature for the past (grey) and future (green) using the ensemble estimates (average impacts across GCMs) for SSP1-2.6. *Bottom panel*: the related distribution of excess mortality, expressed as the fraction of additional deaths (%) attributed to non-optimal temperature.

the relevance of disassociating the different groups. For this model, we observe a present situation where the AF is higher for cold than for heat (see figure 30). This AF then changes with the projections of future temperatures with a greater shift in SSP5-8.5 than in the mitigation scenario. These observations represent the temperature-mortality association for all ages combined and are expected to be highly affected by the original numbers of deaths

recorded for each age group. Indeed, there are more recorded deaths for the older age groups with 29 234 deaths for our middle group and 22 781 deaths for our older age group, compared to 12 350 deaths for the youngest age group. Hence, the observations are highly related to those of these older age groups.

2 Allowing for changes in the age composition of deaths in the future

Now that we have presented fraction of deaths attributable to non-optimal temperatures, we compare the numbers associated with these fractions to compare the burden of mortality in two scenarios : constant death counts and projected death counts. The aim of this section is to underline the importance of accounting for changes in the population structure and in death counts.

2.1 Comparing mortality due to heat and cold: constant and projected

The tutorial by Vicedo-Cabrera et al. (2019) enables the estimation of fractions of deaths attributable to non-optimal temperatures. We refer to the estimated death counts as attributable numbers (ANs). In this section, we present the projected ANs of deaths due to cold and heat, assuming constant mortality and projected mortality counts. The results of these projections can be found in figures 33 to 36, where we projected ANs for each age group and both SSP scenarios. The results are expressed for each decade. Although our confidence intervals often encompass negative values, we have chosen not to represent them in our graphs since a negative AN indicates no association between temperature and mortality, implying a null AN. ANs cannot fall below zero, as the minimum number of deaths due to non-optimal temperatures cannot be negative. Then, in table 2, we present the absolute ANs for constant and projected mortality. This table also includes the number of deaths registered for each decade. The differences in the number of deaths for the 2000-2009 decade are explained by the use of yearly mean number of deaths for the reference period replicated over time for the constant mortality assumption. And, in the case of our model with projections, the base number of deaths for the past period consists of the recorded numbers and are therefore different.

Our analysis begins with the youngest age group. By the 2090-99 horizon, deaths are projected to decrease significantly, leading to an immediate reduction in estimated ANs in both temperature scenarios. The differences between constant and projected mortality scenarios show a substantial reduction in ANs for both cold and heat. Despite an expected increase

in attributable fractions due to heat, the projected decline in mortality for the under-15 age group implies a reduction in ANs, as observed in figures 31 and 32. Mortality attributable to cold is expected to decrease, particularly in the SSP5-8.5 scenario and in the projected mortality scenarios.

Conversely, deaths for adults are projected to increase significantly, primarily due to population growth and a shift from earlier life mortality to mortality in older age groups. This substantial increase, from 29 234 to 304 440 deaths for the 2000 and 2090 decades respectively, along with the already increased projected attributable fractions, results in notable differences in ANs due to heat and cold. For instance, in the SSP1-2.6 scenario (figure 33), constant death counts implies reductions in cold-related mortality and a gradual increase in heat-related mortality. In contrast, the projection scenario shows a substantial increase in cold-related mortality, which remains higher than heat-related mortality. Conversely, the results for the higher radiative forcing scenario (see figure 34) indicate that the high increase in temperatures leads to a substantial increase in ANs due to heat for both constant and projected death counts. The differences between models are even more pronounced when considering the disparities between constant and projected death counts. For instance, the AN for the 2000-2009 decade is 156 (95% CI= 0; 408), whereas it increases to 73 932 (95% CI= 0; 172 774) in the 2090-2099 decade. To contextualise these results, the AN in the mitigation scenario is expected to increase to 8 602 (95% CI= 0; 32 026). Moreover, this divergence in death count projections suggests that the projected decrease in AN due to cold for SSP1-2.6 is counteracted by a slight but marked increase in projected death counts. Similar trends are observed in the higher radiative forcing scenario.

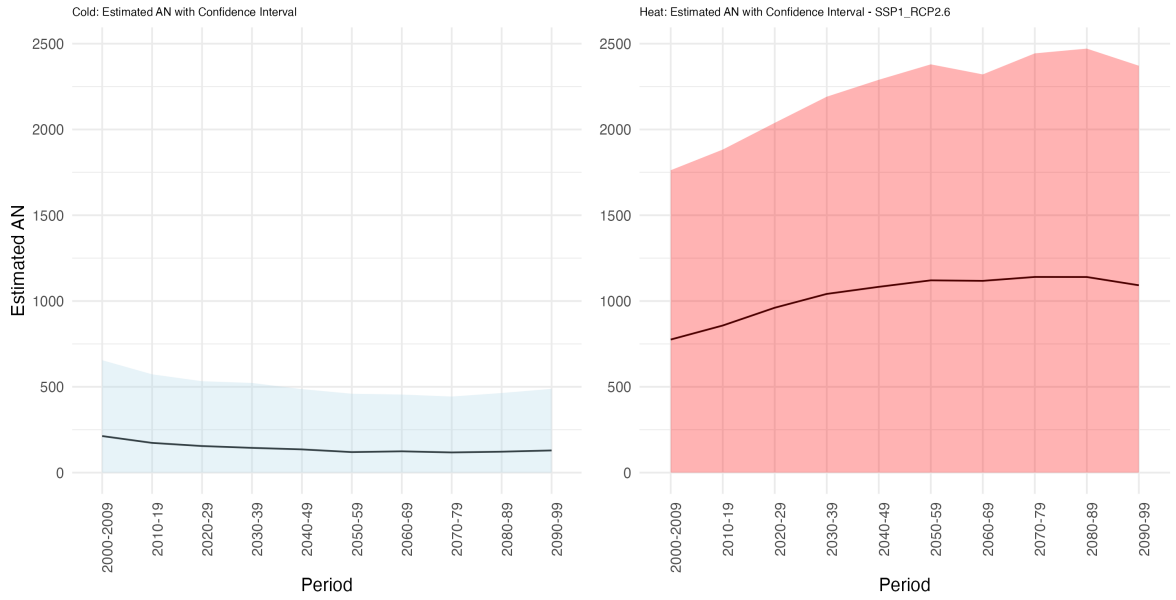
Finally, significant increases are also observed in death count projections for individuals over 60 years old. This growth can be attributed to the increasing population at risk, with more people living past 60 years old, coupled with a reduction in premature mortality, leading to a shift of deaths towards older ages. For instance, while death estimates for the 2000-2009 decade stood at 20 416, we project 206 940 deaths for the 2090-2099 decade. These increases show similar trends to those observed in the previous age group, where the most significant differences in attributable numbers stem from changes in death counts rather than the projected climate change. This is evident in both scenarios (see figures 35 and 36). To quantify these changes in the SSP5-8.5 scenario, the AN due to heat was 309 deaths (95% CI= 0; 1098) for the 2000-2009 decade and increased to 17 836 deaths (95% CI= 0; 97 445) in the 2090-2099 decade in our projections scenario. In comparison, in the mitigation scenario, the AN is anticipated to increase to 5 760 deaths (95% CI= 0; 18 910).

In conclusion, substantial differences in ANs are observed across age groups, with SSP scenarios playing a significant role in projected evolutions. However, the effect of the pro-

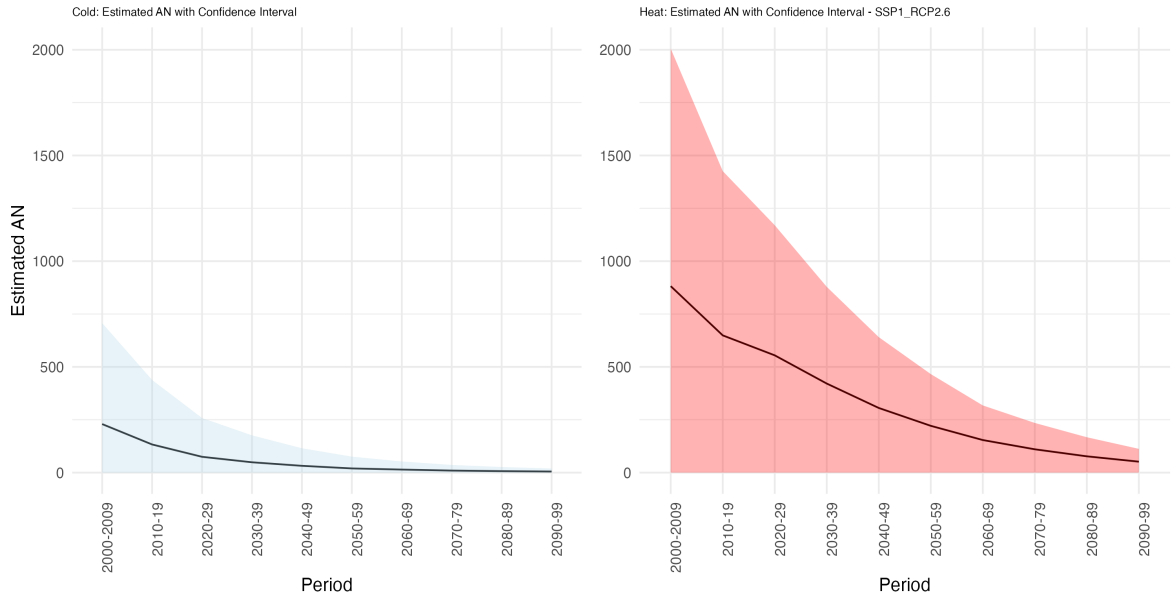
jected number of deaths is higher in comparison highlighting the importance of accounting for changes in the age distribution of deaths.

Table 2: **Estimated Attributable Numbers of deaths attributed to cold and heat for constant and projected mortality, by age group, and SSP**

Age	**Mortality assumption**	**Deaths (2000-2009)**	**SSP**	**Cold (2000-2009)**			**Heat (2000-2009)**			**Deaths (2090 -2099)**	**Cold (2090-99)**			**Heat (2090-99)**		
				Est	CI low	CI high	Est	CI low	CI high		Est	CI low	CI high	Est	CI low	CI high
<15	constant	12.351	1-2.5	**213**	0	655	**775**	0	1762	12.351	**129**	0	488	**1092**	0	2371
			5-8.4	**211**	0	653	**780**	0	1766		**10**	0	88	**1398**	0	7154
<15	exponential projection	13.694	1-2.6	**229**	0	707	**882**	0	2005	537	**5**	-9	19	**52**	0	112
			5-8.5	**227**	0	705	**887**	0	2009		**0**	0	4	**63**	0	330
15-59	constant	29.234	1-2.5	**1544**	0	4193	**170**	0	453	29.234	**1254**	0	3464	**810**	0	3022
			5-8.4	**1544**	0	4189	**174**	0	458		**486**	0	1843	**6925**	0	16221
15-59	exponential projection	26.188	1-2.6	**1390**	0	3773	**153**	0	399	304.440	**12963**	0	35820	**8602**	0	32026
			5-8.5	**1389**	0	3767	**156**	0	408		**5027**	0	18989	**73932**	0	172774
>60	constant	22.781	1-2.5	**1364**	55	2500	**332**	0	1201	22.781	**920**	0	1989	**627**	0	2060
			5-8.4	**1355**	46	2494	**335**	0	1208		**137**	0	585	**1942**	0	10626
>60	exponential projection	20.416	1-2.6	**1227**	55	2249	**306**	0	1093	206.940	**8511**	0	18291	**5760**	0	18910
			5-8.5	**1219**	50	2245	**309**	0	1098		**1268**	0	5396	**17836**	0	97445

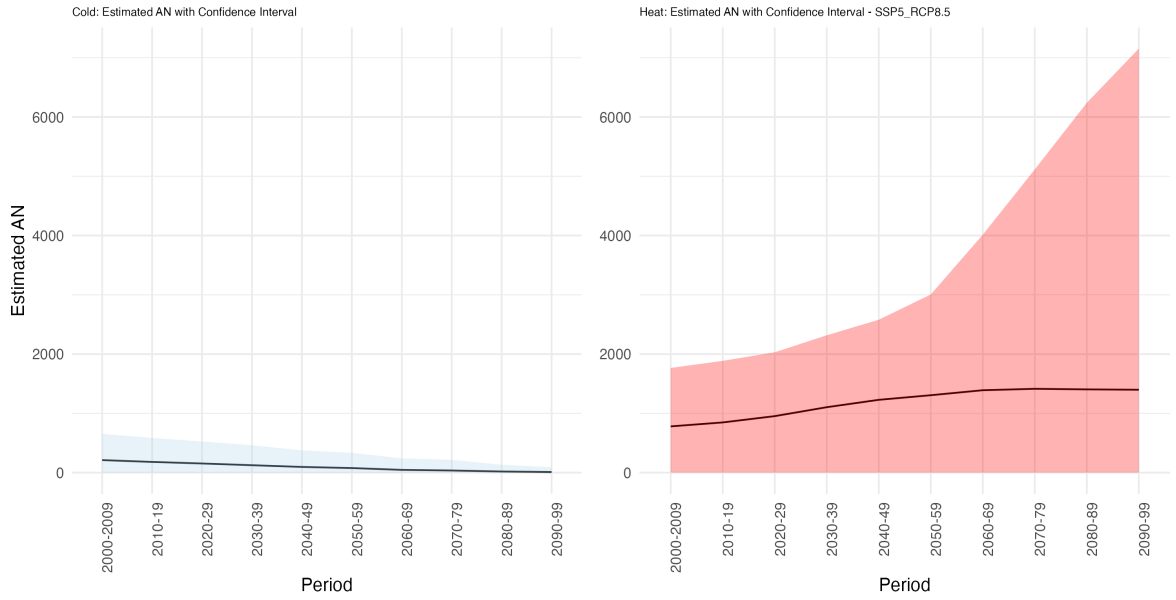


(a) constant mortality assumption

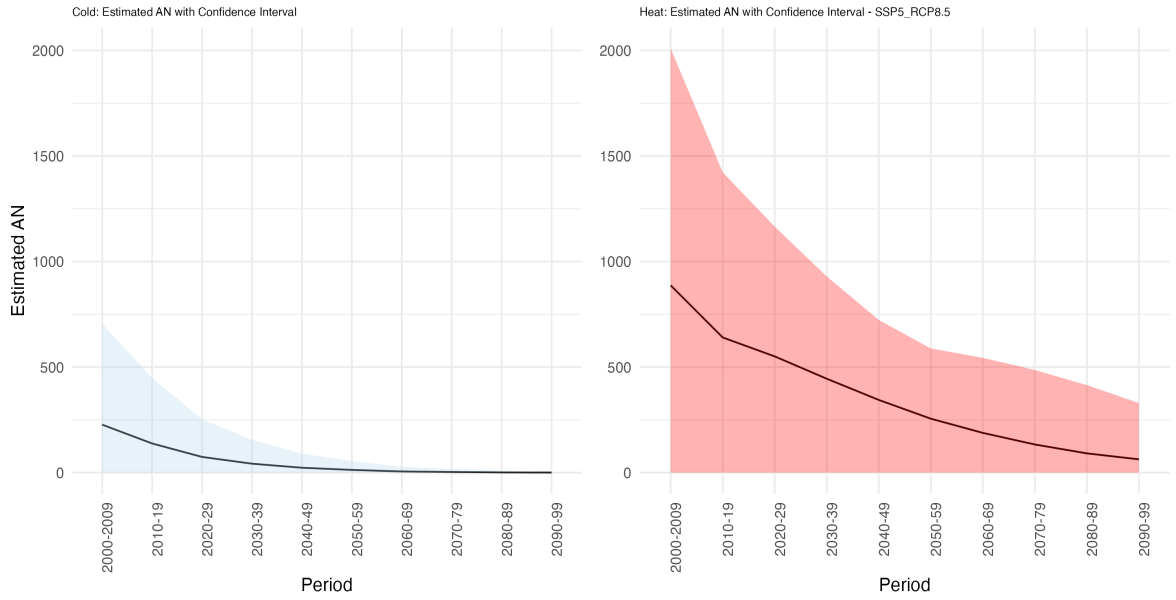


(b) projected mortality

Figure 31: **Past (2000-09) and Projected (2010-99) attributable number of deaths for under 15 years old under SSP1-2.6.**
ANs for 10 year periods. *Left panels*: in blue the deaths attributed to cold. *Right panels*: in red the deaths attributed to heat.
Note 1: The 2010-2019 period counts past (2010-15) recorded ANs and projected (2016-19) ANs.
Note 2: CIs were assumed to always be >0 as non-optimal temperature is always projected to have an effect on mortality.

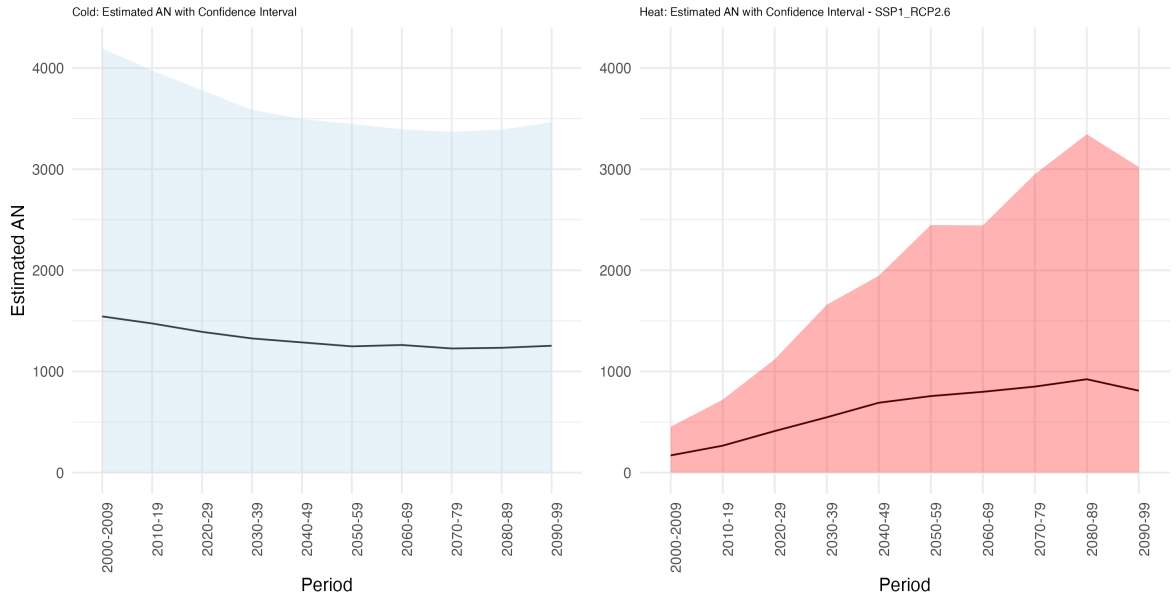


(a) constant mortality assumption

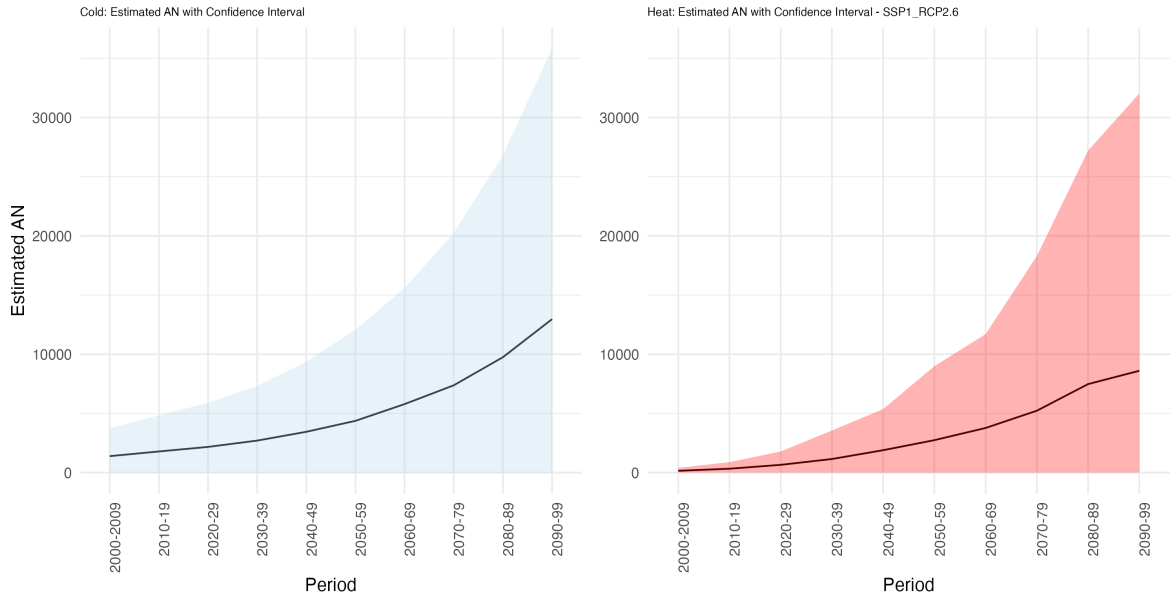


(b) projected mortality

Figure 32: **Past (2000-09) and Projected (2010-99) attributable number of deaths for under 15 years old under SSP5-8.5.**
ANs for 10 year periods.*Left panels*: in blue the deaths attributed to cold. *Right panels*: in red the deaths attributed to heat.
Note 1: The 2010-2019 period counts past (2010-15) recorded ANs and projected (2016-19) ANs.
Note 2: CIs were assumed to always be >0 as non-optimal temperature is always projected to have an effect on mortality.

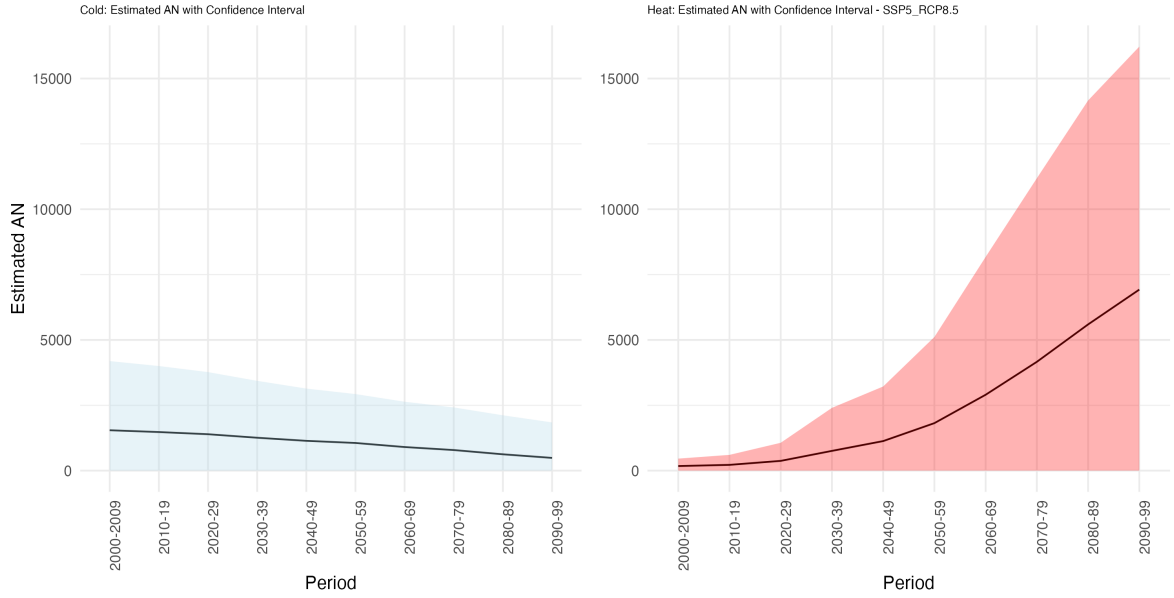


(a) constant mortality assumption

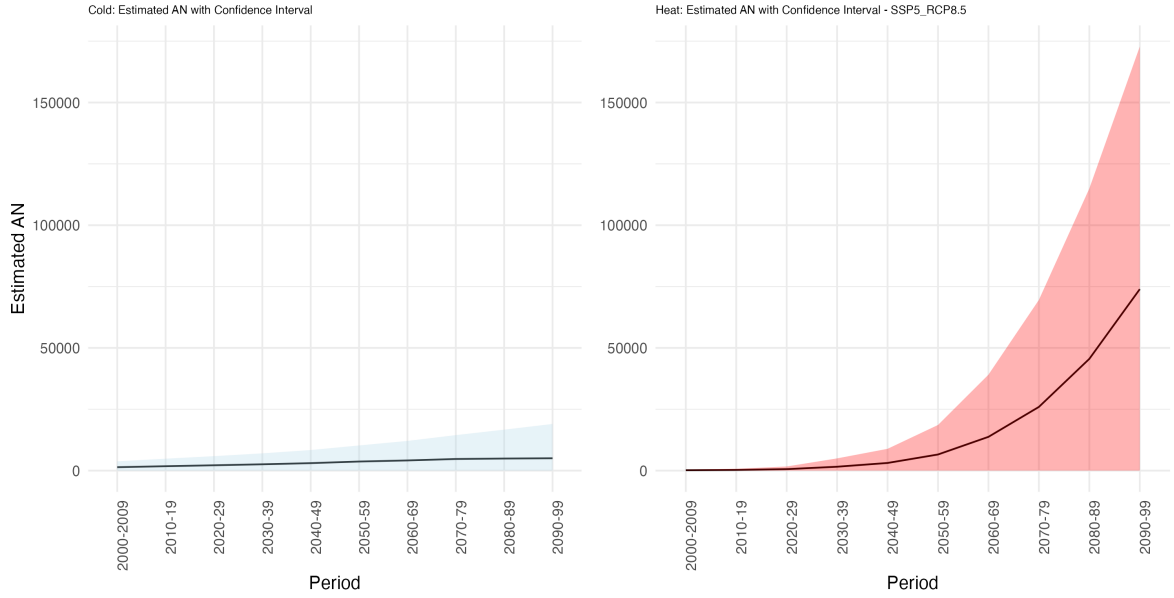


(b) projected mortality

Figure 33: **Past (2000-09) and Projected (2010-99) attributable number of deaths between 15-59 years old under SSP1-2.6.**
ANs for 10 year periods.*Left panels*: in blue the deaths attributed to cold. *Right panels*: in red the deaths attributed to heat.
Note 1: The 2010-2019 period counts past (2010-15) recorded ANs and projected (2016-19) ANs.
Note 2: CIs were assumed to always be >0 as non-optimal temperature is always projected to have an effect on mortality.

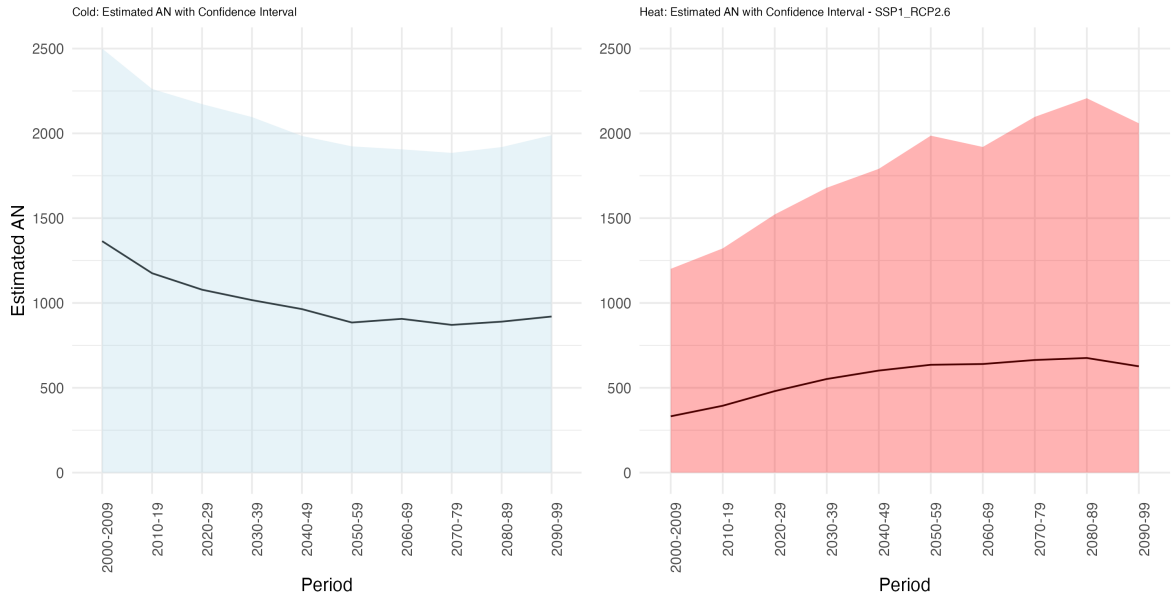


(a) constant mortality assumption

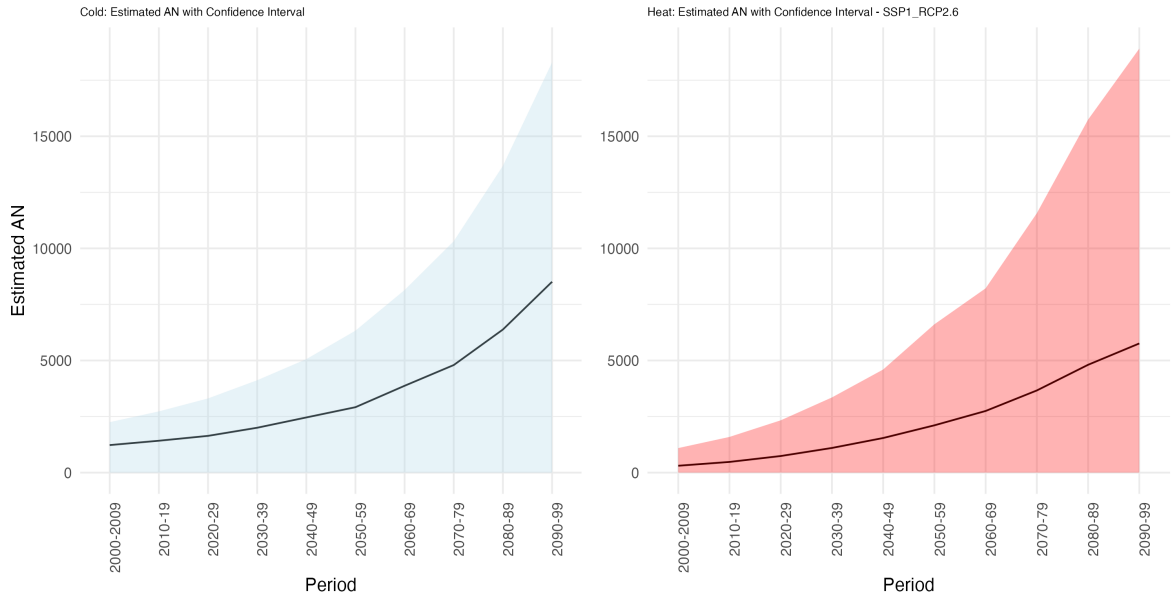


(b) projected mortality

Figure 34: **Past (2000-09) and Projected (2010-99) attributable number of deaths between 15-59 years old under SSP5-8.5.**
ANs for 10 year periods.*Left panels*: in blue the deaths attributed to cold. *Right panels*: in red the deaths attributed to heat.
Note 1: The 2010-2019 period counts past (2010-15) recorded ANs and projected (2016-19) ANs.
Note 2: CIs were assumed to always be >0 as non-optimal temperature is always projected to have an effect on mortality.

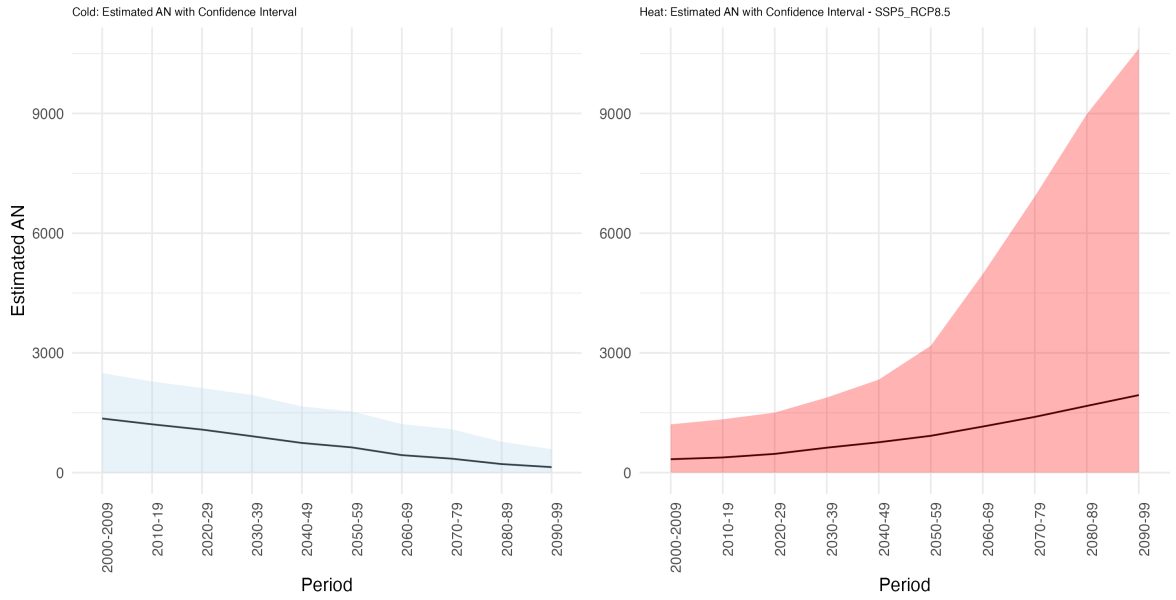


(a) constant mortality assumption

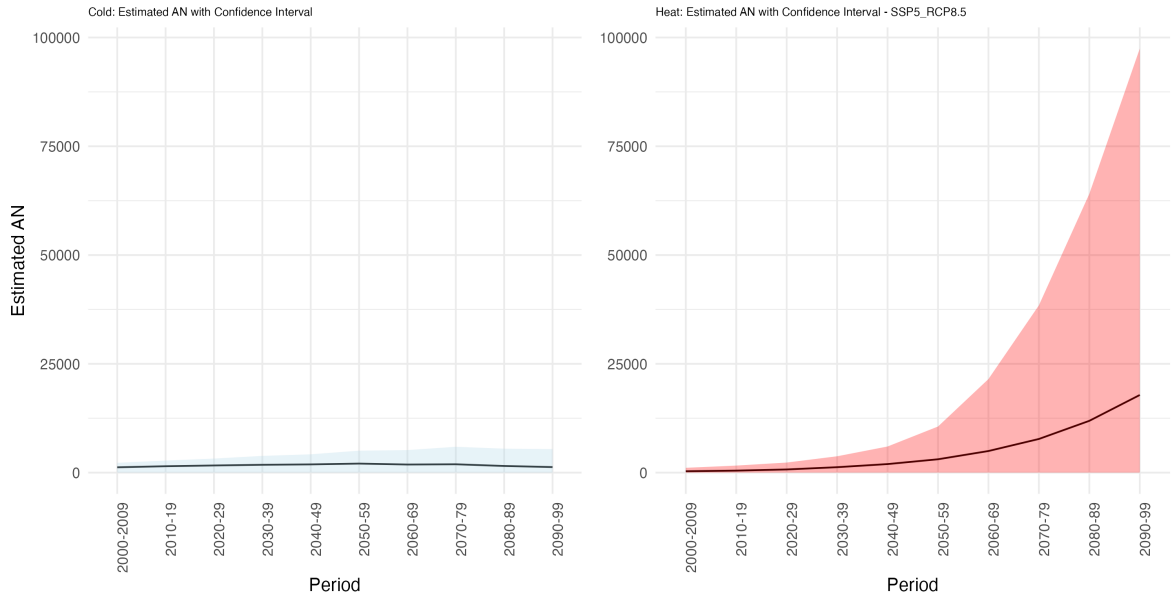


(b) projected mortality

Figure 35: **Past (2000-09) and Projected (2010-99) attributable number of deaths over 60 years old under SSP1-2.6.**
ANs for 10 year periods.*Left panels*: in blue the deaths attributed to cold. *Right panels*: in red the deaths attributed to heat.
Note 1: The 2010-2019 period counts past (2010-15) recorded ANs and projected (2016-19) ANs.
Note 2: CIs were assumed to always be >0 as non-optimal temperature is always projected to have an effect on mortality.



(a) constant mortality assumption



(b) projected mortality

Figure 36: **Past (2000-09) and Projected (2010-99) attributable number of deaths over 60 years old under SSP5-8.5.**
ANs for 10 year periods.*Left panels*: in blue the deaths attributed to cold. *Right panels*: in red the deaths attributed to heat.
Note 1: The 2010-2019 period counts past (2010-15) recorded ANs and projected (2016-19) ANs.
Note 2: CIs were assumed to always be >0 as non-optimal temperature is always projected to have an effect on mortality.

3 Allowing for cause-specific relative risks

Our next sensitivity test involves analysing the variations in the temperature-mortality relationship across different causes of death and age groups. As previously mentioned, different causes of death may exhibit different associations with temperature. This is particularly relevant in the context of Antananarivo's dual burden of disease and the variability of primary causes of death across age groups. In this sensitivity test, we first examine the historical trends of different causes of death within each age group. Subsequently, we delve into the specific temperature-mortality associations for each cause of death, concluding with an analysis of potential cause-specific health outcomes.

3.1 Trends in cause-of-death distribution

Starting with a presentation of the yearly evolution of death counts according to different causes of death, we focus on causes with established etiological, measurable, and explained relationships with temperatures. Following our literature review on temperature's effects on various causes of death, we have selected the following for analysis: cardiovascular diseases, infectious diseases, deaths related to nutritional deficiencies, and diseases of the respiratory system. The temporal variations of death counts for these causes can be found in figure 37.

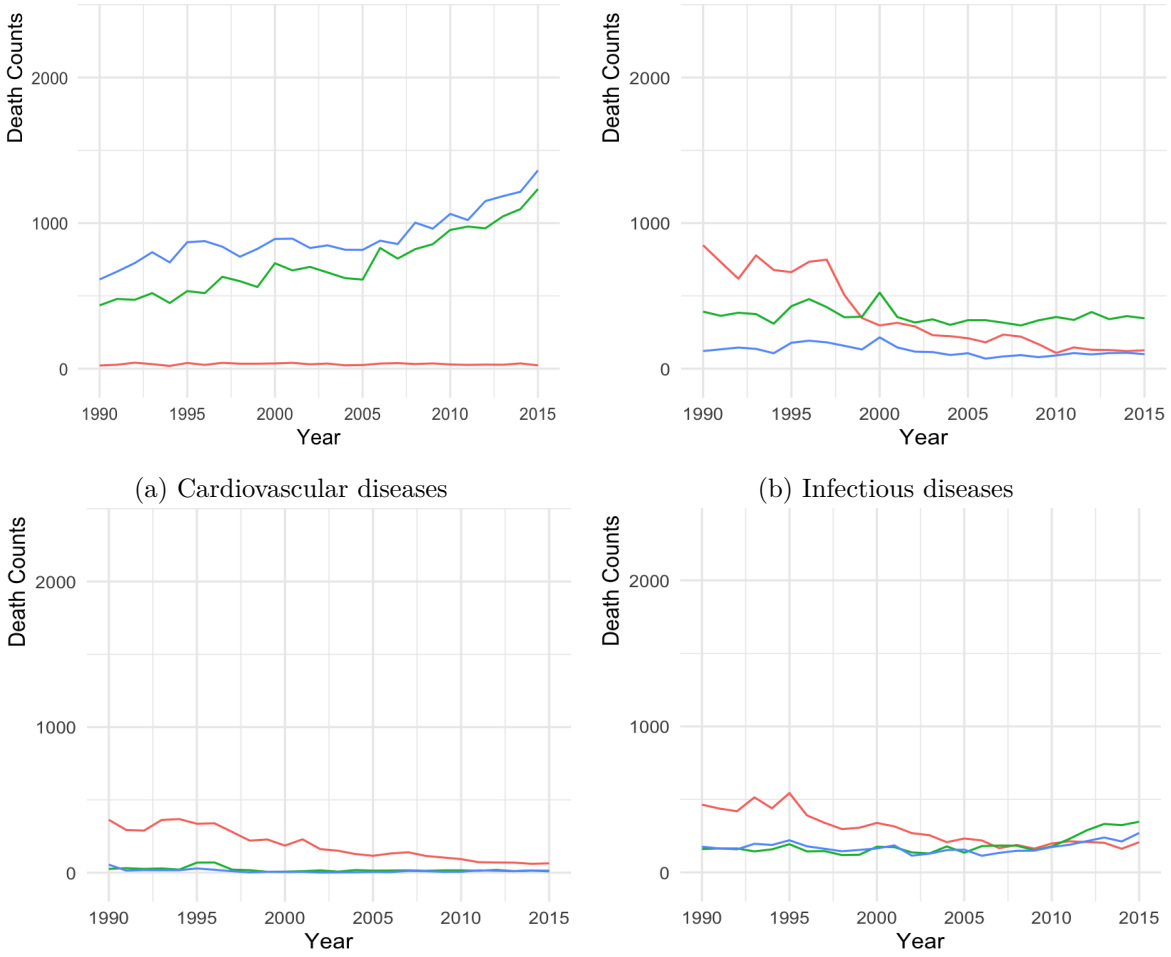
In figure 37a, we observe a significant increase in deaths from cardiovascular diseases during the 1990-2015 period. This rise is notable in the two older age groups, while mortality under 15 remains relatively stable. The increase is evident for both older age groups, with mortality between 15 and 59 nearly catching up with mortality over 60 during the observation period. Specifically, deaths from cardiovascular diseases approached 700 cases for the 15-59 age group and 850 cases for those over 60 in 2000, rising to approximately 1250 and 1400 cases respectively by 2015.

Figure 37b shows a decline in infectious mortality under 15, while infectious disease mortality remains rather stable for our two other age groups. In the 2000-2015 period, the number of deaths from infectious diseases for the under 15 age group declined from around 300 deaths to 100. Deaths in adults from infectious diseases remained around 350 a year for the reference period, while deaths in the elderly from infectious diseases remained around 100 a year.

Moving on to figure 37c, we observe a significant decrease in deaths from nutritional diseases for the under 15 age group. Deaths from this cause are very rare for our two older age groups. Apart from a small peak in the mid-1990s. These findings align with our literature review.

Finally, in figure 37d, we take a look at the evolution of death counts from diseases of the respiratory system. Deaths from this cause have gradually decreased for the under 15 age group, while increasing slowly for the two older age groups, particularly since 2005, with a more significant increase observed for mortality between 15 and 59.

Overall, the results indicate a decline in deaths among the youngest age group, while the two other age groups show an increase. Variations in mortality by cause are notably dependent on age group.



(a) Cardiovascular diseases

(b) Infectious diseases

(c) Nutritional deficiency

(d) Diseases of the respiratory system

Figure 37: **Yearly death counts per age group per cause.**
In red: deaths under 15. In green: deaths between 15 and 59. In blue: deaths over 60.

Moreover, we paid attention to the number of deaths per age group for each cause of death. These numbers are provided in the table 5 in the annex, where we present deaths per cause by age group for the 2000-2015 period. There, we note a total of 29 812 deaths from cardiovascular diseases, 10 426 from infectious diseases, 9 614 from respiratory diseases, and

2 234 from nutritional deficiencies. Considering these variations, along with differences in mortality by age, is important as they are likely to impact model convergence.

3.2 Cause-specific relative risks

In this section, we provide the results of our analysis on the temperature-mortality association for each cause, highlighting the categories where an association is observed.

3.2.1 Cardiovascular diseases

Before delving into the analysis of our results for cardiovascular disease-related mortality, it is important to note that an association was not consistently observed in our model across all age groups. This lack of model convergence resulted in graphs that did not exhibit evident minimum mortality temperatures, thereby hindering the model's ability to determine a threshold between cold and heat-related mortality. Therefore, in cases where the mortality patterns did not allow for model convergence[18], we considered that no conclusions could be drawn regarding the relationship between temperature and mortality for the given mortality group. To represent a case where there was no measured association, or, where the specifications of the model were not sufficient to depict a clear relation between cold and heat related mortality, we present figure 38 below. In this graph, which represents an attempt at measuring the temperature-mortality association for deaths of cardiovascular diseases between 15 and 59, we see that no minimum mortality temperature is defined which renders the analysis and further projection of AFs and ANs impossible.

Given that there is no measured relation between temperature and mortality of cardiovascular diseases between 15 and 59, we present in box 3.2.1 the measured association for mortality under 15 and over 60 with the measured seasonal variations of cardiovascular diseases. We observe for our youngest age group a low T_{mm} of 15.1°C with a near linear relation for cold temperatures and a curve with an "s" shape for warmer temperatures. We attribute this unexpected shape to small numbers (only 499 deaths for this cause and age group were recorded for the whole reference period) and we do not believe any conclusions on the effect of temperature on cardiovascular diseases can be made for mortality below 15 years old based on our results.

On the other hand, mortality of cardiovascular diseases for the elderly exhibits a near

[18]Not reaching model convergence here implies that given no clear delimitation between heat and cold the model was not able to distinguish cold and heat related mortality. This implies impossible conclusions given that the RRs are expressed in relation to T_{mm}.

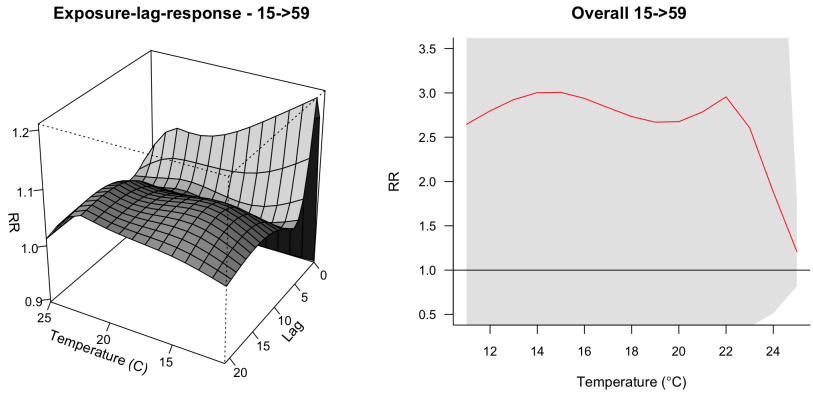
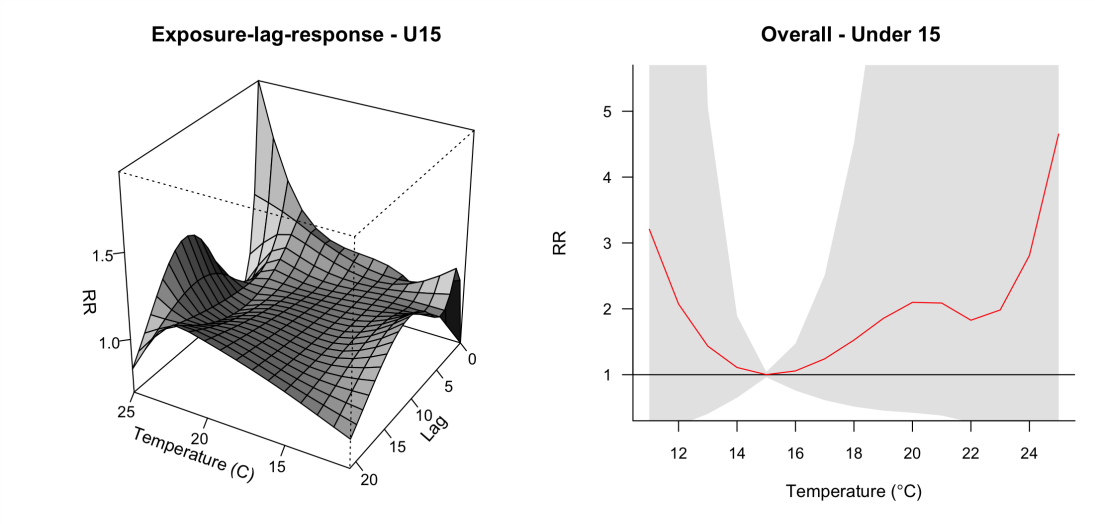


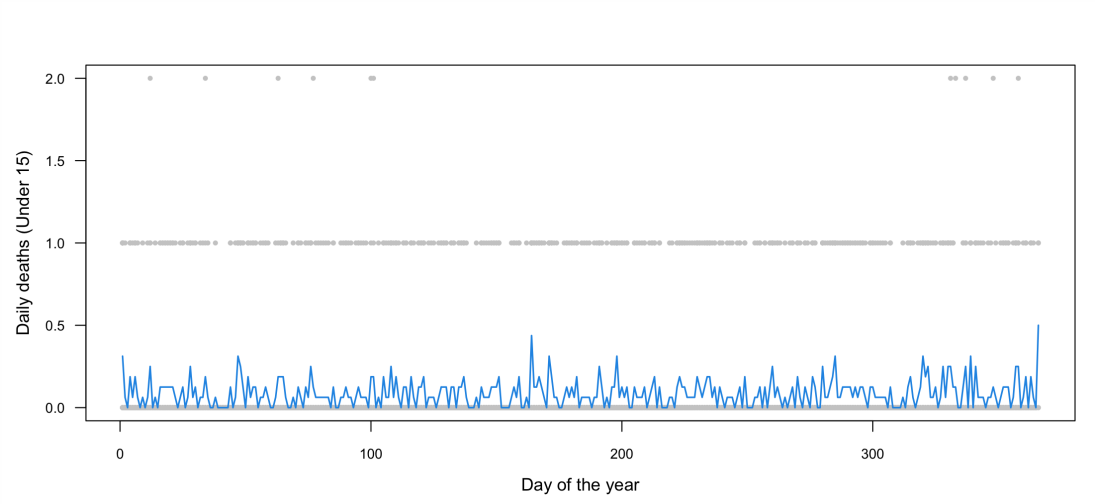
Figure 38: **Example of no measured temperature-mortality association: deaths of cardiovascular diseases between 15-59 years old.**
Left: Three dimensional plot showing the estimate exposure-lag-response association between temperature and mortality. Right: Cumulative mortality risk for all lag (RR and 95% confidence interval).

linear relation for both cold and heat. Analysing the cumulative RR graph we observe that the threshold defining the limit between cold and heat is quite high (at 21.7°C) with temperatures below 16°C and above 22°C representing higher risks of mortality for this cause and group. Specifically, the risk of mortality is multiplied by 1.44 (95% CI = 0.75; 2.78) at 11°C compared to 21.7°C and by 1.36 (95% CI= 0.24; 7.8) at 25°C compared to the T_{mm}. Next, the analysis of the lagged exposure-response association reveals a slight deviation from the traditional pattern, indicating a more immediate heat effect and a lagged cold-related effect, but with a twist: heat-related mortality also exhibits a lagged tendency. Finally, we examine seasonal variations in deaths and observe an increase in daily numbers during the coolest months of the year. This seasonality, which is controlled for in the model, implies higher mortality rates around June, July, and August.

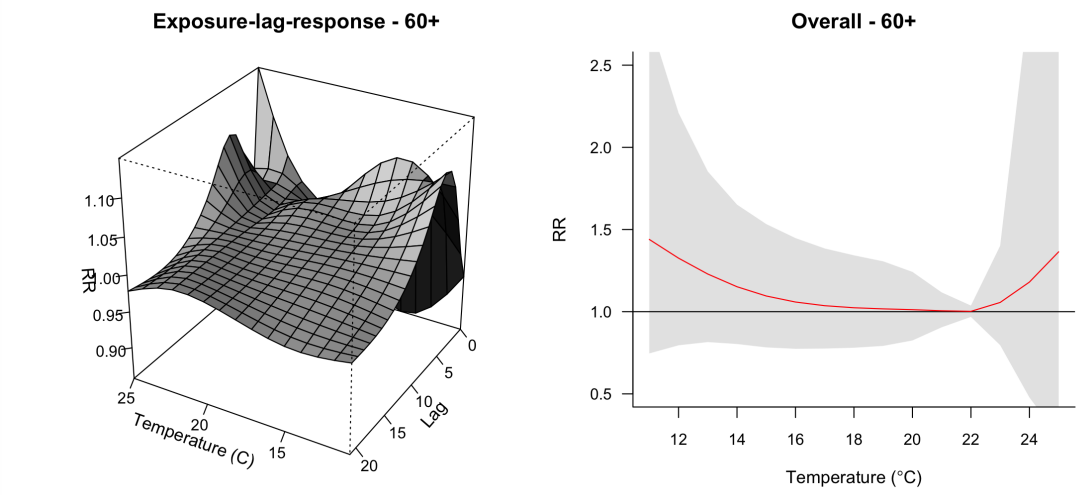
Box 3.2.1 : DLNM and seasonality for deaths of cardiovascular diseases



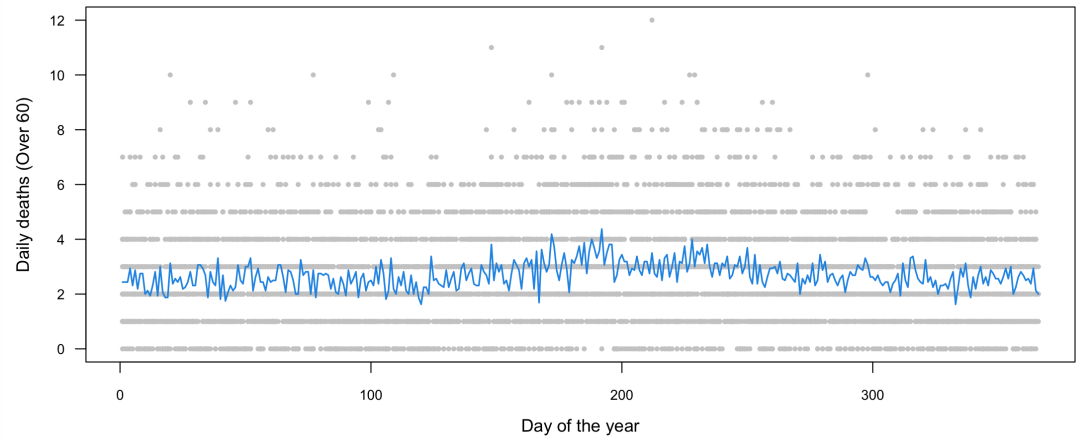
Temperature-related mortality for deaths of cardiovascular diseases below 15 years old.
Left: Three dimensional plot showing the estimate exposure-lag-response association between temperature and mortality. Right: Cumulative mortality risk for all lag (RR and 95% confidence interval).



Seasonal trends of under 15 years old cardiovascular disease mortality.
The grey dots correspond to the observed daily mortality counts registered for each day of the year for the observation period. The blue line depicts the mean number of deaths daily.



Temperature-related mortality for deaths of cardiovascular diseases over 60 years old. Left: Three dimensional plot showing the estimate exposure-lag-response association between temperature and mortality. Right: Cumulative mortality risk for all lag (RR and 95% confidence interval).



Seasonal trends of over 60 years old cardiovascular disease mortality. The grey dots correspond to the observed daily mortality counts registered for each day of the year for the observation period. The blue line depicts the mean number of deaths daily.

3.2.2 Infectious diseases

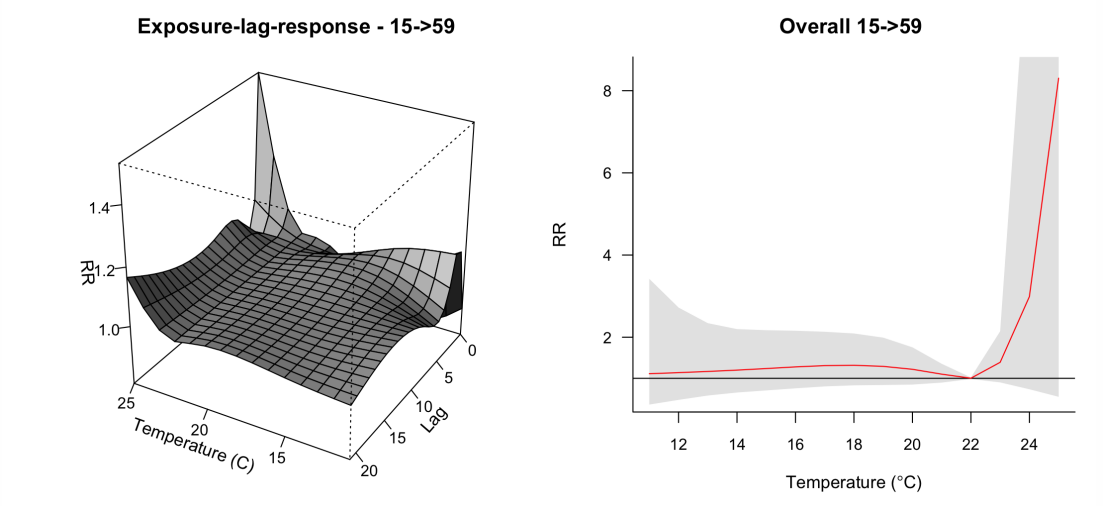
The results of our study of the effects of temperatures on deaths of infectious diseases are presented in box 3.2.2. We present the results for our two oldest age groups, as our model

did not achieve convergence for mortality below 15.

Mortality from infectious diseases in the 15-59 age group exhibits an association with temperature. This association appears to be primarily driven by warmer temperatures, despite the relatively high minimum mortality temperature at 21.9°C. While the relative risk of mortality for cold is at most 1.32 (95% CI= 0.83, 2.1) times higher than mortality at T_{mm}, this risk is multiplied to up to 8.3 (95% CI= 0.55; 125.2) times with heat. Given this strong association with heat, we observe relatively immediate mortality from infectious diseases in this age group. Furthermore, analysis of the seasonality graph reveals minimal fluctuations in deaths from infectious diseases throughout the year implying a relatively low confounding effect.

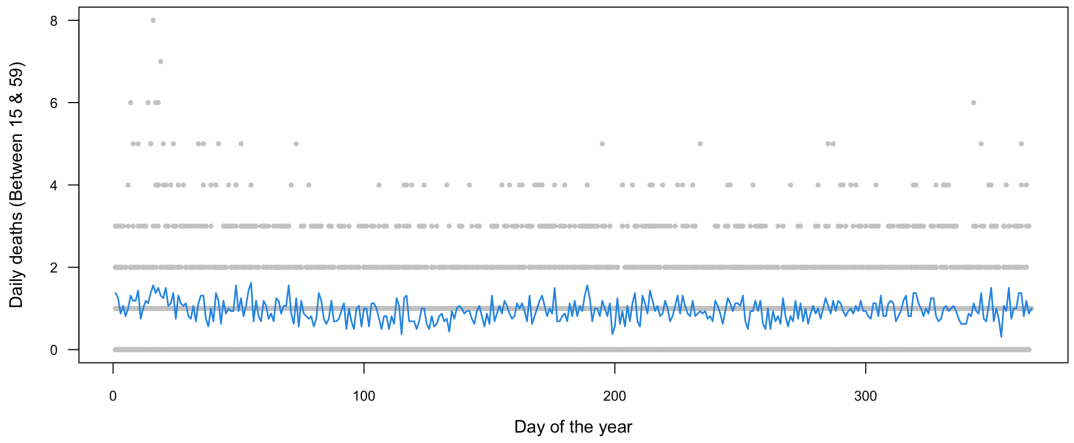
Finally, the DLNM for mortality from infectious diseases in the over 60 age group also reveals an association with temperatures. Analysing the cumulative lag graph, we observe that the minimum mortality temperature T_{mm} corresponds to 17.8°C. Mortality shows a nearly linear relationship with cold temperatures, while it is significantly associated with heat for temperatures over 18°C and below 22°C. Moreover, when temperatures exceed 23°C, the association becomes linear. Consequently, risk of mortality at 25°C is estimated to be multiplied by 4.99 (95% CI= 0.06; 417.83) compared to the risk of mortality at 18°C. Similarly, for this age group, mortality from infectious diseases occurs rather directly after exposure, with slight delayed effects observed five days after the recorded temperature. Lastly, our analysis of seasonality reveals no clear seasonal patterns for mortality in this age group.

Box 3.2.2 : DLNM and seasonality for deaths of infectious diseases

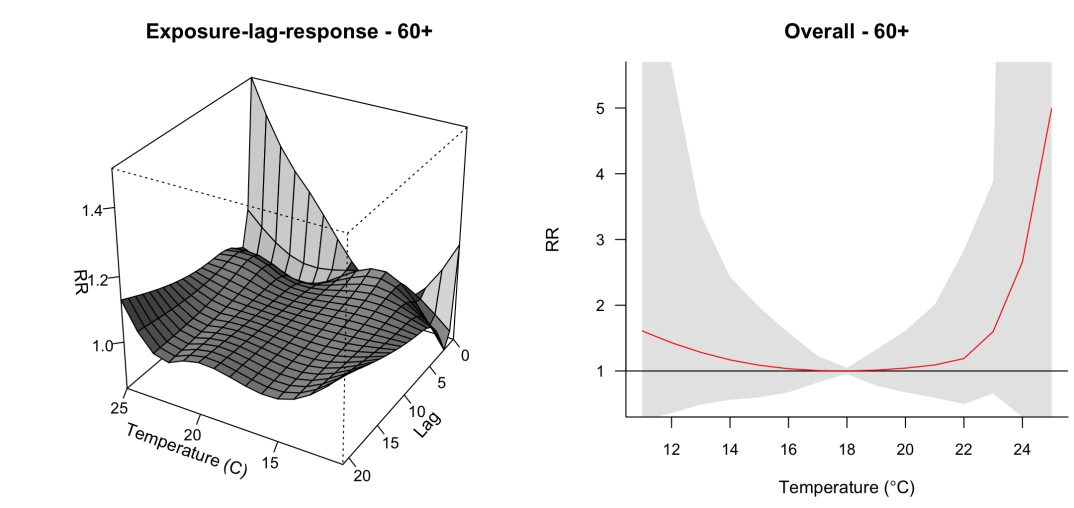


Temperature-related mortality for deaths of infectious diseases between 15-59 years old. Left: Three dimensional plot showing the estimate exposure-lag-response association between temper-

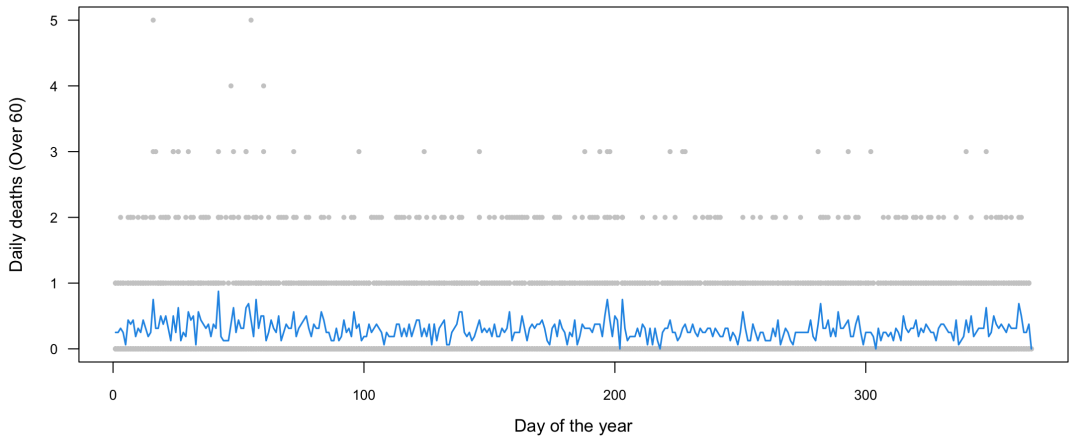
ature and mortality. Right: Cumulative mortality risk for all lag (RR and 95% confidence interval).



Seasonal trends of between 15-59 years old infectious disease mortality.
The grey dots correspond to the observed daily mortality counts registered for each day of the year for the observation period. The blue line depicts the mean number of deaths daily.



Temperature-related mortality for deaths of infectious diseases over 60 years old.
Left: Three dimensional plot showing the estimate exposure-lag-response association between temperature and mortality. Right: Cumulative mortality risk for all lag (RR and 95% confidence interval).

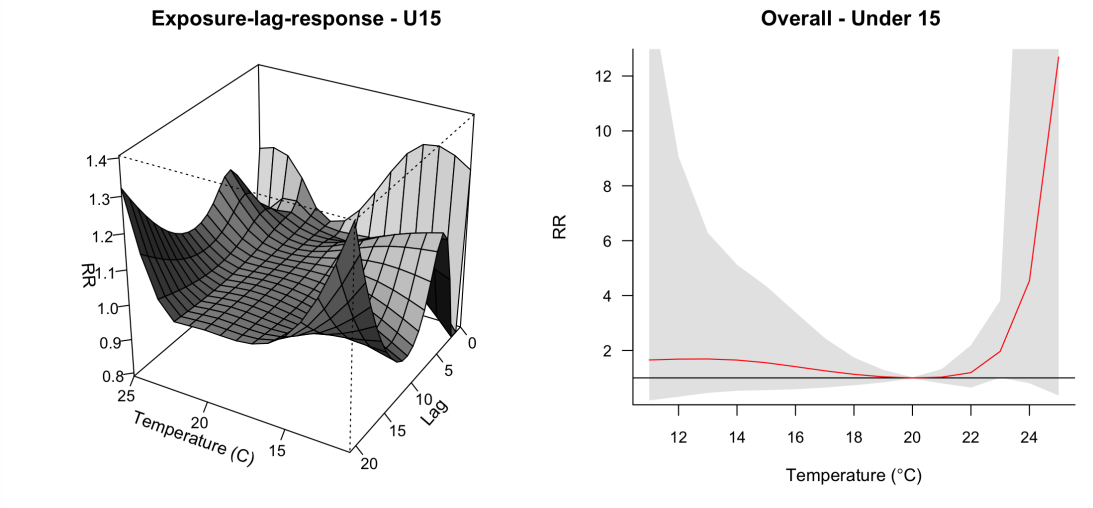


Seasonal trends of OVER 60 years old infectious disease mortality.
The grey dots correspond to the observed daily mortality counts registered for each day of the year for the observation period. The blue line depicts the mean number of deaths daily.

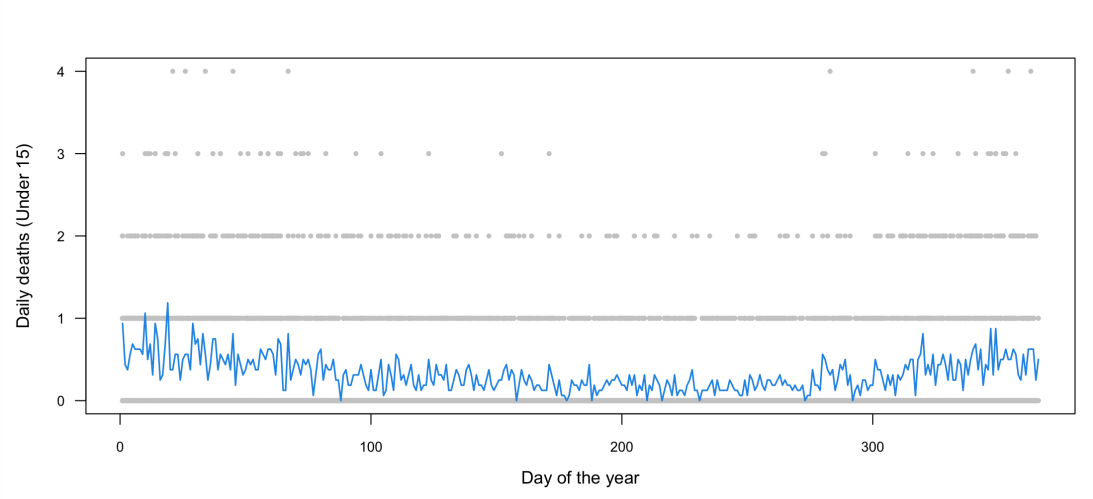
3.2.3 Nutritional deficiencies

Given the minimal occurrence of mortality due to nutritional deficiencies for adults and elderly, our analysis for this cause of death focuses on mortality below 15 years old. The results of our model are shown in box 3.2.3. We observe that nutritional deficiencies are very highly associated to warmer temperatures compared to cooler temperatures. We observe that the risk of mortality is multiplied by 12.7 (95% CI= 0.36; 445.95) at 25°C compared to the T_{mm} of 20.1°C. However, the magnitude of this relative risk is not attributed to immediate heat-related mortality in the case of nutritional deficiencies. On the contrary, it is explained by a lagged and widely distributed effect for warmer temperatures. Additionally, the analysis of seasonality reveals a pronounced seasonal pattern, with mortality from nutritional deficiencies primarily occurring during the warmer periods of the year.

Box 3.2.3 : DLNM and seasonality for deaths of nutritional deficiency



Temperature-related mortality for deaths of nutritional deficiency below 15 years old.
Left: Three dimensional plot showing the estimate exposure-lag-response association between temperature and mortality. Right: Cumulative mortality risk for all lag (RR and 95% confidence interval).



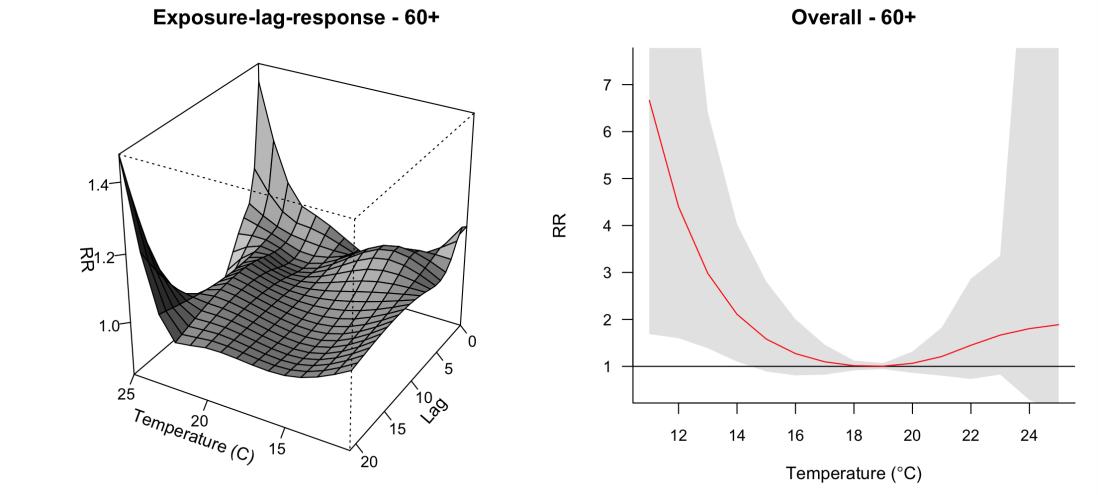
Seasonal trends of under 15 years old nutritional deficiency mortality.
The grey dots correspond to the observed daily mortality counts registered for each day of the year for the observation period. The blue line depicts the mean number of deaths daily.

3.2.4 Respiratory system diseases

Finally, the analysis of the association between deaths from respiratory system diseases and temperature yielded no clear results for the two younger age groups.

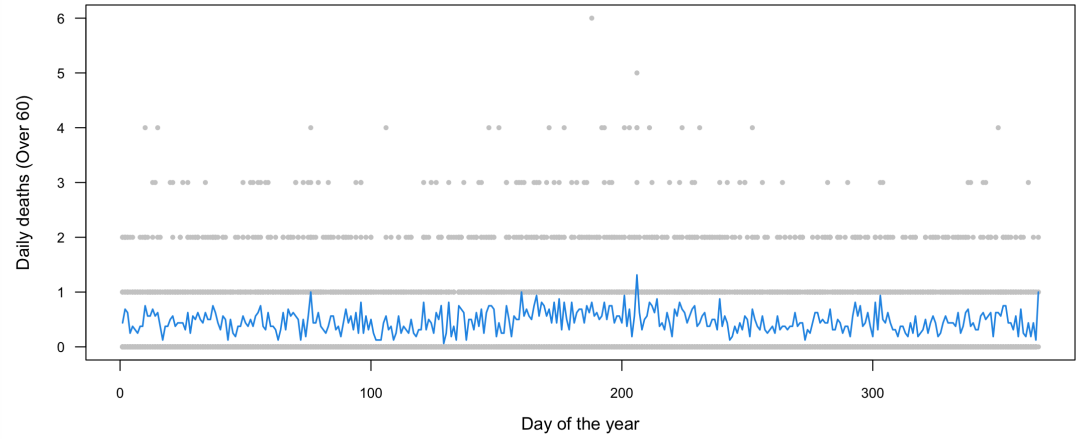
However, our model did produce results for mortality among individuals over 60 years old, where a clear association between cold and mortality was observed. The results for this association are presented in box 3.2.4, outlining a higher relative risk for the lowest temperature (11°C), where the mortality risk is 6.67 (95% CI= 1.68; 26.33) times higher than at the minimum mortality temperature (Tmm) of 18.6°C. Analysis of the lag for this association shows a more immediate effect of heat-related mortality, with lagged effects observed around 20 days after the measured temperature. Conversely, cold exhibits small immediate effects but a more extended effect along the lag dimension. Seasonal trends for this cause of death and age group are minimal, with mortality slightly higher during the middle (cooler) period of the year.

Box 3.2.4 : DLNM and seasonality for deaths of respiratory system diseases



Temperature-related mortality for deaths of diseases of the respiratory system over 60 years old.

Left: Three dimensional plot showing the estimate exposure-lag-response association between temperature and mortality. Right: Cumulative mortality risk for all lag (RR and 95% confidence interval).



Seasonal trends of mortality of respiratory system disease over 60 years old .
The grey dots correspond to the observed daily mortality counts registered for each day of the year for the observation period. The blue line depicts the mean number of deaths daily.

3.3 Cause-specific health outcomes

The results of our analysis reveal an association between temperature and some causes of death, observed within specific age groups. We now present the projection of attributable fractions of deaths due to temperature for cases where such associations have been identified. These AFs, both for the current period and projected for future periods, are summarised in table 3.

Beginning with cardiovascular diseases, we find that the AFs of deaths over 60 are associated with temperature. Presently, the AF due to cold exceeds that of heat, albeit both fractions remain relatively small. However, climate projections suggest a slight increase in AFs due to heat, especially pronounced in SSP5-8.5, where 16.2% of deaths from this cause are expected to be attributable to heat during the 2090-2099 decade.

Moving to infectious diseases, no association was observed for the youngest age group. However, this is not the case for deaths between 15 and 59, where cold currently explains a higher AF than heat. Projections indicate an increase in AFs due to heat in SSP1-2.6, yet cold remains the dominant factor. But, in SSP5-8.5, there is a shift in tendencies, with heat becoming the predominant factor. This trend is even more pronounced in the oldest age group, where infectious diseases are already heavily influenced by heat.

Table 3: **Attributable fractions (AF%) by cause of death, age group, and SSP. With the average number of deaths for the decade.**

Cause of death	Age	Average deaths per 10 years	SSP	AF (%) (2000-2009) Cold			AF (%) (2000-2009) Heat			AF (%) (2090-99) Cold			AF (%) (2090-99) Heat		
				Est	CI low	CI high	Est	CI low	CI high	Est	CI low	CI high	Est	CI low	CI high
Cardio vascular diseases	<15	310.7	1-2.6												
			5-8.5												
	15-59	8444.4	1-2.6												
			5-8.5												
	>60	9863.8	1-2.6	**3.92**	0	19.72	**0.33**	0	1.79	**2.73**	0	16	**1.68**	0	10.99
			5-8.5	**3.89**	0	19.67	**0.34**	0	1.8	**0.7**	0	8.39	**16.2**	0	56.63
Infectious diseases	<15	1950.6	1-2.6												
			5-8.5												
	15-59	3479.4	1-2.6	**14.19**	0	34.63	**1.78**	0	3.53	**11.62**	0	28.35	**8.07**	0	21.44
			5-8.5	**14.15**	0	34.49	**1.82**	0	3.61	**5.93**	0	16.36	**48.37**	0	70.18
	>60	1080.6	1-2.6	**2.59**	0	13.06	**6.78**	0	28.10	**1.51**	0	9.75	**14.10**	0	38.00
			5-8.5	**2.56**	0	13.01	**6.84**	0	28.16	**0.12**	0	2.07	**50.58**	0	76.63
Nutritional deficiency	<15	1181.3	1-2.6	**7.36**	0	18.59	**7.37**	0	20.40	**5.33**	0	14.59	**19.23**	0	39.64
			5-8.5	**7.35**	0	18.60	**7.50**	0	20.65	**1.27**	0	6.01	**66.20**	0	83.93
Diseases of the respiratory system	<15	2075.6	1-2.6												
			5-8.5												
	15-59	2213.3	1-2.6												
			5-8.5												
	>60	1712.5	1-2.6	**13.18**	0	22.93	**9.56**	0	20.87	**8.36**	0	17.84	**14.98**	0	29.19
			5-8.5	**13.10**	0	22.92	**9.63**	0	21.05	**1.06**	0	4.83	**31.20**	0	69.55

Empty AF lines = no model convergence.

Nutritional deficiencies, though rare among older age groups, exhibit an association with

temperatures for younger age groups. Presently, the burden of mortality for those under 15 due to infectious diseases is similar for both heat and cold effects. However, projected increasing temperatures imply a rise in mortality due to heat rather than cold, with variations observed across SSPs.

For respiratory diseases, no association was measured except for the over 60 age group. In this group, current AFs are slightly higher for cold. For the 2090-2099 horizon, these AFs indicate a slight increase in heat-related mortality in SSP1-2.6 and a more significant increase in SSP5-8.5.

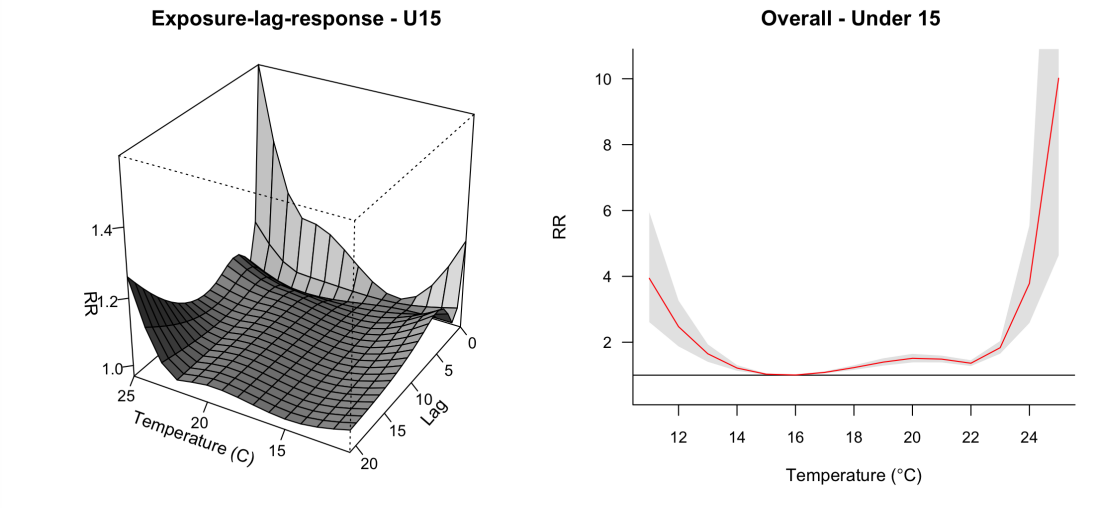
In summary, our analysis of AFs for different causes of death across various age groups indicates projected changes in the fraction of deaths due to temperature. These findings concord with our previous conclusions, underscoring variations in the temperature-related mortality patterns.

4 Sensitivity to control for seasonality

This sensitivity test aims to assess the importance of including seasonality as a confounder in the model. As outlined in our methods section, we introduced a natural spline function to capture the overall effect of seasonality on mortality in our base model. In this section, we conducted a model run without controlling for this confounder to evaluate the mediating effect of seasonality on mortality. While we attempted to run this test across all age groups, we only achieved model convergence for the youngest age group. The outcomes of this test are detailed in box 4.

Analysis of the cumulative relative risk graph in box 4 reveals a markedly different curve compared to the model where seasonality is controlled for. In this model, the confidence intervals are substantially reduced compared to the model accounting for seasonal variations in the association (refer to box 1.1.1). Additionally, we observe a more pronounced association for heat-related mortality when seasonality is not controlled for. The minimum mortality temperature also differs, decreasing from 17.8°C to 15.7°C in the model without seasonal control. These significant disparities suggest that mortality in the under 15 age group is greatly influenced by seasonal variations over time, rather than solely by temperatures. Hence, variations in mortality for different temperatures in this age group cannot be uniquely attributed to temperature effects but must also consider the impact of seasonal mortality occurring at specific temperatures.

Box 4 : DLNM by age without seasonality



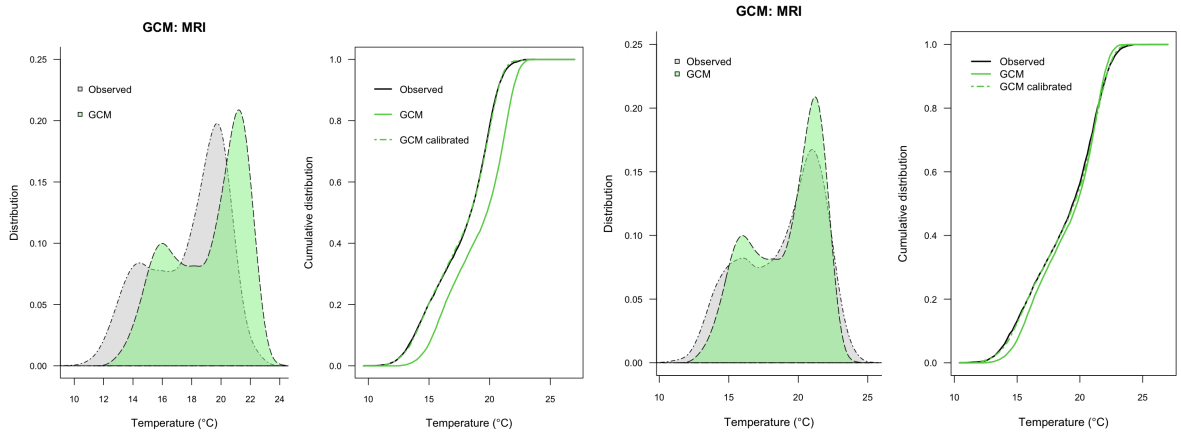
Temperature-related mortality for deaths below 15 years old with no control for seasonality. Left: Three dimensional plot showing the estimate exposure-lag-response association between temperature and mortality. Right: Cumulative mortality risk for all lag (RR and 95% confidence interval).

No definitive conclusions can be drawn regarding the effects of seasonality on the temperature-mortality association for the two other age groups, as the lack of model convergence interferes with our ability to make conclusive remarks on the subject. For the under 15 years old mortality age group, strong seasonal effects are measured meaning that this age group's temperature-mortality association is highly impacted by the time of the year.

5 Controlling for the effect of modelled exposure data

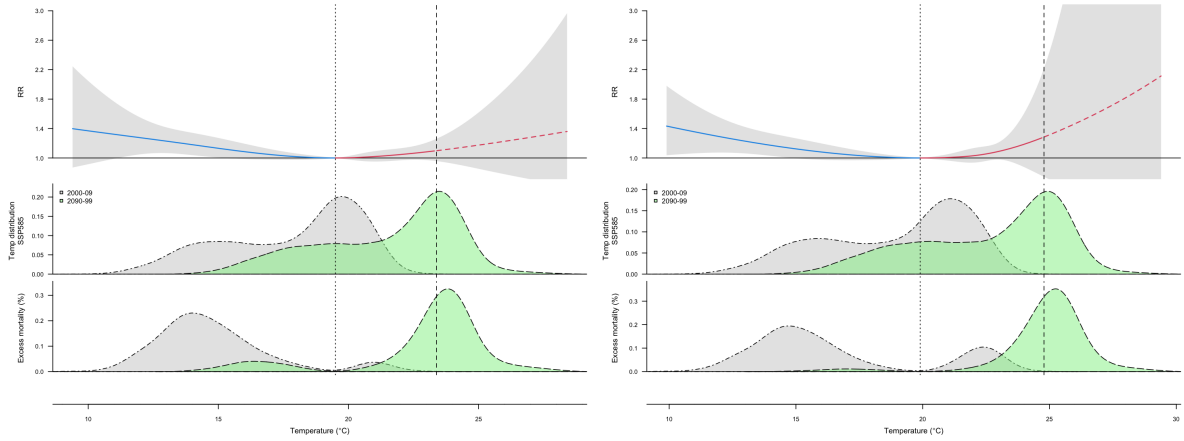
Our final sensitivity test aims to assess the impacts of using modelled temperature data on the analysis of temperature-health effects. The importance of conducting such tests is explained by the frequent absence of available meteorological data in SSA (Dinku, 2019), prompting interest in alternative datasets. Additionally, we considered using modelled data for our analysis before 2000, where numerous missing values existed in the NOAA database. Running this test is also necessary given the substantial differences between the two datasets regarding mean temperature, with ERA-5 data being consistently cooler than NOAA data (see box 1.1.1).

In this sensitivity analysis, we examined three key factors. First, we investigated the disparities between the two datasets, identifying a significant mean difference between them, this was done in box 1.1.1. Secondly, we compared the calibration between GCM data from the



(a) ERA-5 (b) NOAA

Figure 39: **Calibration between past and projected data for ERA-5 and NOAA data.**



(a) ERA-5 (b) NOAA

Figure 40: **The exposure-response curve and associated current and projected temperature distribution and AF.**

MRI for SSP5-8.5 and past temperature data, highlighting that more calibration is required when using ERA5-Land data (refer to figure 39). Thirdly, when analysing the RRs and resulting current and projected AFs using the two datasets, we consistently observed lower RRs for warmer temperatures when employing ERA5-Land data for the aggregated age model (see figure 40). Furthermore, running the model for different age groups using modelled data resulted in non-convergence for our two oldest age groups, and lower estimated RRs for heat for mortality below 15 as well. Finally, when analysing the current and projected AFs for the aggregated age model, the yielded AFs indicated significantly lower fractions using ERA-5 compared to NOAA data. These disparities in projections stem from the lower estimated association between heat and mortality, compounded by the calibration step.

Discussion

This section covers our main findings, placing them in relation to existing literature. We then discuss the limitations of our study and conclude with our recommendations.

1 Main results

The primary results of our analysis are as follows: significant differences are observed in the temperature-mortality association across different age groups. These differences range from varying minimal mortality temperatures to differing intensities in the cold and heat effects. The risks associated with cold temperatures are higher for children and the elderly compared to those associated with heat. In contrast, adults face higher risks from warm temperatures than from cold temperatures. Confidence intervals are quite large, with greater uncertainty observed for the association in warmer temperatures (>23°C), yet the shapes of the associations were sufficient to draw conclusions. Different age groups exhibit distinct seasonal patterns: mortality in those under 15 primarily occurs during the warmer months (October to March), mortality in those over 60 predominantly occurs during the cooler months (June to August), and mortality among those aged 15 to 59 shows the least pronounced seasonal trends. The confounding effect of seasonality on the temperature-mortality association was demonstrated in our analysis for child mortality, but this effect was not evident for the two other age groups in our study. Despite the differences in the risks associated with heat and cold across age groups, heat always has a more immediate effect on mortality, whereas cold tends to have a delayed effect, occurring within days or a week of the recorded temperature.

The observed differences in the temperature-mortality association were further explored in our analysis of mortality by cause. We identified associations between temperature and mortality for those over 60 due to cardiovascular diseases, mortality of adults and the elderly from infectious diseases, mortality of children due to nutritional deficiencies, and mortality of

those over 60 due to diseases of the respiratory system. This analysis revealed greater risks related to cold for cardiovascular and respiratory system-related mortality in the elderly, and a more pronounced risk of heat on mortality from infectious diseases (for adults and the elderly) and nutritional deficiencies (for children).

Risks of mortality due to non-optimal temperatures are expressed as fractions of deaths with deaths attributable to non-optimal warm and cold temperatures. The analysis of AFs shows that the effects of heat currently have a higher impact on child mortality, whereas deaths for older age groups are mostly impacted by cold. Projections for the year 2100 indicate a gradual shift, with increased temperatures leading to higher AFs due to heat. The intensity of this shift, resulting from the extension of the measured RR curve and the projected increase in temperatures, suggests a higher burden of mortality due to heat for all age groups under the SSP scenario with the highest radiative forcing (SSP5 RCP8.5). In our mitigation scenario, the AFs remain higher for cold in the older age groups. Attributable numbers determined based on AFs highlight the importance of changes in the number of deaths considered in the analysis. Our projections indicate an increase in the number of deaths for adults and the elderly, alongside a decline in child deaths. From these projections, we identified that changes in the numbers of deaths attributed to non-optimal temperatures were more significantly influenced by changes in initial death numbers than by changes in temperatures themselves.

Finally, by testing the outcomes of using modelled data for our analysis, we demonstrated that measuring the association between mortality and temperature in our context with limited data and small numbers had a major effect on the measured association. This analysis raises questions about the potential outcomes of altering other parameters and adding more variables to our model, highlighting possible limitations of our study. However, before delving into the limitations of our study, we review our results bearing in mind our initial questions and hypotheses, whilst also referring to existing literature on the subject.

1.1 Age-disaggregated models

We hypothesised that there would be variations in the temperature-mortality association among different age groups. Our results have confirmed this hypothesis. But, contrarily to past results, we show a higher sensitivity of children to cooler temperatures (where risks are higher), which goes against findings which assess higher sensitivity of children to warm temperatures (Borg et al., 2021; Song et al., 2017; Dang et al., 2016). The elderly, who are also associated with higher risks in the literature, exhibit an association in our analysis more related to the effect of cold than that of heat. This association with cold had already been assessed in studies conducted in Nairobi (Borg et al., 2021) and Vietnam (Dang et al., 2016).

Previous studies have generally acknowledged the heightened risks for these two age groups, but our analysis also reveals the existing temperature-mortality association for adults, a group rarely studied due to their presumed lower sensitivity. We also find that the existing patterns will not necessarily continue with future temperature projections. Given the shape of the curves, the extension of relative risk curves for higher temperatures implies more deaths due to non-optimal warm temperatures for adults and the elderly rather than for children. These results somewhat contradict the literature that identifies children as the most vulnerable age group to climate change (Chapman et al., 2022), but the small numbers for this age group may also explain these results.

Therefore, this analysis underscores the importance of examining temperature-mortality associations for different age groups separately, given the distinct differences between these groups and the tendency for all-age aggregated models to reflect the associations of the highest mortality groups. The tendency of past studies to discard younger age groups is understandable, given the differences in mortality structure between our case study and countries more advanced in their epidemiological and demographic transitions. From this case study, we show the necessity of examining different age groups when analysing temperature-mortality associations in LLMICs, as they respond differently.

1.2 Associations between temperature and mortality by cause

Our review of the literature highlighted the current dual burden of disease in Antananarivo, further detailed in our analysis of the evolution of mortality for different causes of death. We observed an overall decrease in mortality for children and an increase in mortality from non-communicable diseases and a near stagnation of mortality from communicable diseases for the two older age groups.

Measuring possible associations for the different age groups has shown varied results that do not always align with previous literature. We demonstrated an association between temperature and cardiovascular disease deaths for those over 60, showing more sensitivity to cold than to heat. This observation aligns with previous literature indicating a greater risk due to cold temperatures (Näyhä, 2002; Lin et al., 2013), but also suggests an unpredicted, and potentially very steep increase in risks due to heat in the future (Näyhä, 2002).

Analysing the association between infectious diseases and mortality revealed a high association between heat and infectious disease deaths in adults and the elderly, with most of the risk concentrated immediately under short lag periods. The existing literature on the association between temperature and infectious diseases is scarce, as most studies focus on possible changes in vector proliferation and survival (Van de Vuurst and Escobar, 2023). Many studies

on highly prevalent communicable diseases such as COVID-19 were measured to be affected by temperatures but did not seem pertinent for comparison with our results (Yuan et al., 2021; Zhu et al., 2021). We explain this lack of studies on the subject by the small prevalence of infectious diseases in the locations where the DLNMs have been applied in the past.

Furthermore, our analysis of the association between temperature and nutritional deficiency mortality showed heightened risks due to heat, even after 21 days of lag. Our results indicated an immediate effect of cold. In contrast, heat showed both immediate and delayed effects, which are difficult to interpret due to the lack of studies on the subject. Increased temperatures have been shown to be related to increased mortality, but this association has been analysed in the context of longer exposure periods for Sub-Saharan Africa, where increased temperatures have been shown to constrain child nutrition (Baker and Anttila-Hughes, 2020). Another factor which may further explain our results is the potential for comorbidities leading to mortality due to nutritional deficiencies, which could be positively associated with increased temperatures. However, studies on multimorbidity mainly concern adults, and a scoping review on multimorbidity in SSA has shown that research has mostly focused on adults, although children in SSA also suffer from emergent disease clusters (Obasohan et al., 2023). Furthermore, a study conducted in Uganda highlighted the high prevalence of comorbidities in children already suffering from malnutrition, with other conditions such as pneumonia, malaria, anaemia, bacteraemia, HIV, and others (Banga et al., 2020).

Finally, our analysis of the association between respiratory diseases and temperatures yielded results for the elderly, whose mortality is mostly associated with a higher risk from colder temperatures. These results align with past studies, which have highlighted that these diseases are mostly associated with cold for all ages and have been measured in different cities in China (situated in subtropical climates) and in various cities in South Africa (Zhao et al., 2019; Motlogeloa and Fitchett, 2024). The effect of heat was higher than that of cold for the elderly in Brazil, although differences are expected given the different climate (Jacobson et al., 2021). However, this contradicts the review of epidemiological evidence, which shows increased risks for the elderly at lower temperatures. Risks were also found to be higher for younger people in Lanzhou, China (Chai et al., 2020) which differs from our results given no model convergence was attained for the under 15 age group.

Our analysis, when compared to the literature, highlights the importance of analysing the temperature-mortality association for different causes of death, especially in understudied contexts such as LLMICs. The lack of comparable studies in similar settings shows no systematic convergence or difference with past literature, underscoring the need for more region-specific research.

1.3 The lagged temperature-mortality association

The differences in lag between mortality induced by heat and cold have been demonstrated numerous times in the literature, indicating an overall tendency for mortality due to heat to occur within very short lag periods, whereas the effects of cold temperatures manifest over a longer period (Ye et al., 2012; Yu et al., 2011; Bao et al., 2016; Guo et al., 2014). In our analysis across various age groups, we observed the same pattern, thereby validating our hypothesis. Furthermore, a detailed analysis of the lagged RR curves indicates a tendency for an increase in mortality following the days after a recorded heat event, particularly noticeable in the two youngest age groups. This lagged increase in relative risk is described by some researchers as a possible result of the harvesting effect, where deaths that would have occurred later are brought forward by the heat, implying reduced mortality in the days immediately following the event and an increase thereafter (Yu et al., 2011; Ferreira Braga et al., 2001).

When analysing mortality by cause, our review of existing literature suggests the necessity of considering different lag periods for analysing various causes of death. Given the unique pathways through which temperatures increase mortality risks, the lag is also varied due to differences in etiological paths. For instance, our analysis of cardiovascular diseases in the elderly highlighted a delayed occurrence of cold-related mortality, primarily between 4 to 10 days after the recorded temperature, and an immediate (1-3 days) as well as a delayed effect (up to 8 days) for heat-related mortality (which could be due to the potential harvesting effect). These results differ to some extent from existing studies, Yu et al. (2011) have investigated the lag effect from cardiovascular and respiratory diseases up to 30 days post-recorded temperature. Their study found the effect of heat to be immediate (up to 3 days) but did not record any harvesting effect for deaths due to warm temperatures. The lag was found to be quite high for respiratory diseases for the elderly, aligning with our results (Bunker et al., 2016). No studies were found using DLNMs for nutritional deficiency-related deaths, which could be due to the low prevalence of this cause of death in areas where DLNMs have been applied, and the potentially long survival period in a state of undernourishment. Moreover, we did not find any other studies using DLNMs for analysing infectious disease-related mortality, except for numerous studies on COVID-19, which were not deemed pertinent for comparison with our model (Yuan et al., 2021; Zhu et al., 2021).

From this analysis of the lagged response of mortality due to temperatures, we underscore once again the importance of using DLNMs to better understand the manifestation of mortality following a given temperature. The scarcity of studies in LLMICs requires more research on the subject where the effects of a lagged occurrence of mortality may be different.

1.4 Projecting the burden of non-optimal temperatures

We hypothesised that attributable fractions of mortality due to cold would diminish, leaving a higher AF due to heat, which our analysis confirmed. Additionally, the differences in temperature projections between the various SSPs illustrate the substantial discrepancies between the different models. These findings align with the existing literature, which greatly emphasises the necessity of mitigation efforts to reduce climate change, particularly as it is predicted to represent a higher burden in countries such as Madagascar (Amegah et al., 2016).

Our analysis also confirmed our hypothesis that the number of deaths for our younger age groups due to heat, despite the increases in AFs, is diminished due to the projected decrease in mortality based on past trends. Conversely, for adults and the elderly, the attributable numbers increase even more with the projections, implying a higher number of deaths due to heat. This increase in the number of deaths due to heat is mainly driven by changes in death counts rather than the changes in temperature. This suggests that changes in population structure could explain a higher number of deaths attributed to heat rather than the changes in climate themselves, given the possible increase in the number of deaths.

Therefore, our projections highlight the complex dynamics at play between demographic changes and climate change impacts. The increase in heat-related mortality among adults and the elderly deepens the need for targeted interventions and adaptation strategies to address the vulnerabilities of these age groups. Additionally, even though a decrease in child mortality is measured, continued efforts are necessary to ensure this trend persists with rising temperatures. The findings emphasise the importance of mitigation strategies to address the effects of climate change on mortality across different age groups.

1.5 High seasonality of deaths for children

We hypothesised that seasonality would mainly affect younger age groups. Our results confirmed this hypothesis, revealing a significant confounding effect of seasonal patterns on mortality for those under 15 years old. Given that we did not achieve model convergence for the two older age groups, we were unable to draw conclusions on the effect of seasonality for these groups. However, past literature indicates a decrease in the seasonality of mortality in Antananarivo, primarily attributed to a shift in mortality patterns (brought on by the ongoing epidemiological transition) rather than changes in the seasonal patterns of mortality by cause (Schlüter et al., 2020). These findings may explain why the model without control for seasonality did not converge, suggesting that seasonality for adults and the elderly may not be pronounced enough.

In addition, seasonal patterns in children have been shown to be significant due to socio-economic factors such as school periods, which increase contact rates and subsequently the spread of infectious diseases (Czumbel et al., 2018). The importance of focusing on this aspect in our research reinforces the necessity of including the analysis of seasonal variations in mortality when examining the temperature-mortality association, particularly for children.

To conclude, understanding seasonal variations is crucial for analysing the temperature-mortality association, especially in younger age groups. This ensures that the effects of both temperature and seasonality are accurately accounted for in the analysis. This is particularly important for children, who face higher risks at cooler temperatures. However, due to the cumulative effect of seasonal mortality during warmer periods and the risks associated with heat, the attributable fractions of mortality due to non-optimal temperatures are primarily due to heat for children.

1.6 Measured risk using modelled and measured data

Finally, our study showed the anticipated differences in the measured risks when using different exposure variables. These differences are even more salient given that we were unable to reach model convergence using ERA-5 data for our two older mortality groups. These results are potentially explained by the higher risks associated with cold in our model using NOAA data, which records higher temperatures on average compared to ERA-5. Furthermore, running the model for all age groups, these temperature differences implied lower RRs for heat than for cold. We also noted that a DLNM used in Brazil for respiratory system diseases for the elderly yielded higher risks of mortality due to heat, more than cold, when using ERA-5 data, which contrasts with our results for this cause of death (Jacobson et al., 2021). But these differences are likely attributable to variations in initial temperatures for this location and can thus not be considered a sufficient base for comparison. Hence, our sensitivity analysis highlights significant differences in results and model convergence between our model with measured data versus modelled data. No further conclusions can be made on the general use of ERA-5 data, however, it is important to note that measured data is preferred in general, and it is recommended for calibration by the authors of the tutorial (Vicedo-Cabrera et al., 2019). Finally, measured data is more easily applicable for policy making as it translates into real-life measures.

2 Study limits

The results of this thesis must be contextualised within its limitations. The complexity of associating two very different factors, each influenced by numerous contributing factors, is a limitation in itself. However, several other limitations must be highlighted.

First, our study focused on the implications of using DLNMs in LLMICs, exploring the feasibility of conducting such a study in this context. Given this angle, we did not include any potential environmental confounders in the analysis, which is recommended when examining the effects of temperatures on mortality. The most commonly associated factor is air pollution, which often interacts with temperatures (Ye et al., 2012). Although some studies have shown that controlling for air pollution may not always be necessary to capture the whole effect of temperature (Buckley et al., 2014), other factors such as socio-demographic indicators (sex, body mass index, smoking status, and drinking for example) are important confounders in this association (Bhaskaran et al., 2013). We explain the absence of control for these confounders by the lack of data on specific confounders such as socio-economic factors or further indicators. We did dispose of the sex of the deceased, but, when we attempted to run our model for men and women separately, we could not achieve model convergence, which we attribute to small death counts. Nevertheless, this remains a limitation of our study.

Another limitation is the lack of inclusion of potential adaptation in our analysis. The model allows for the integration of an increment of adaptation to heat over time, representing a decrease in risk for hot temperatures hypothesised to diminish with exposure to higher temperatures (see figure 41). Adaptation, which has been measured in past studies (Gasparrini et al., 2015), was not introduced in our model due to the absence of comparable studies in the region that might indicate the level or tendency for adaptation to heat and the lack of methods to measure adaptation (Pradyumna and Sankam, 2022). Furthermore, the only study which focuses on adaptation in Antananarivo only pertains to enteric infection related mortality, thus, no estimates on adaptation could be extracted for our analysis (Klein and Rasoanomenjanahary, 2023). Adaptation can result from physiological responses or specific strategies (Sanderson et al., 2017), which were challenging to quantify in the context of our study. We believe that an increase in studies similar to this one could enhance the measurement of adaptation in the future. Comparing this study to a similar one for the 2015-2025 period in the future could also help build more reliable estimates on adaptation.

We must also emphasise that our relative small number of deaths is not ideal for applying this method with numerous sub-categories. Previous studies typically focus on mortality groups with larger numbers of deaths or analyse all deaths together to better meet model requirements. Our decision to use the Antananarivo database from 2000 to 2015 presents a

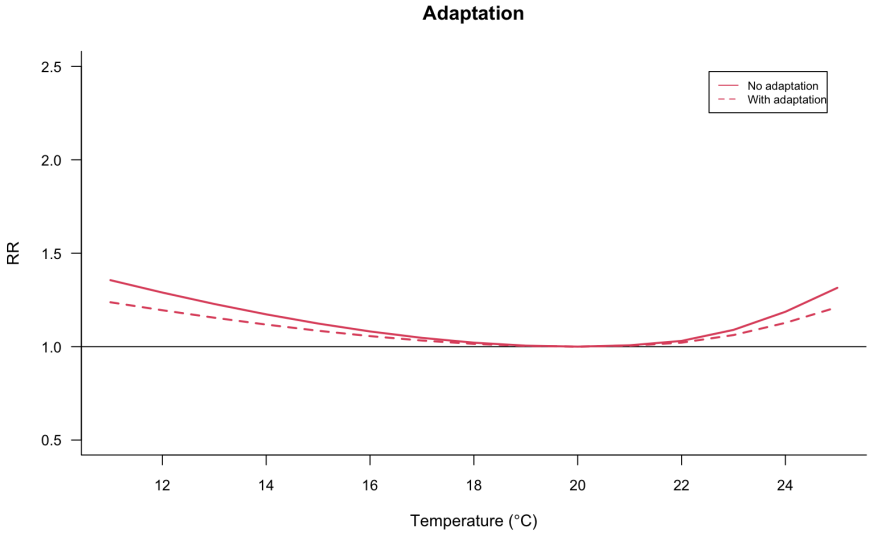


Figure 41: **Graph representing RR with and without adaptation to temperatures.** Here a 30% decrease in the risk associated to heat is assumed.

significant limitation, resulting in high confidence intervals. This level of uncertainty is further exacerbated by the unpredictability of future temperatures. To address this, we attempted to include data prior to 2000. However, the lack of reliable historical data for the exposure variable, despite our efforts to fill gaps with modelled data, prevented an increase in number of deaths included in the analysis. Additionally, using data from 1990 onwards did not achieve model convergence for all age groups. On the one hand, we attribute this to the lower mean temperatures before 2000, as mean temperatures have risen by 0.5°C between 2000 and 2015 (see figure 14), on the other hand, different age patterns and epidemiological profiles also explain lack of model convergence. Given these challenges, we were constrained to use data from 2000 to 2015. Nevertheless, we encourage future research to use data beyond 2015 to enhance the robustness of the findings in Antananarivo.

The quantification of future mortality is another major limitation of this thesis. The scarcity of data for the population at risk made the robust projection of mortality with precise estimates complicated. Factors such as evolution in mortality rates, population at risk, and quantifying migration and birth rates were not available. Hence, the lack of inclusion of potential adaptation and more precise, robust estimates on future mortality is a significant drawback, making it challenging to consider our estimated projected ANs as reliable trajectories for Antananarivo. However, this does not render the analysis futile, as it provides a good idea of the trajectory and can serve as future estimates for comparison.

While this study offers a solid foundation for future assessments of mortality risks due to non-optimal temperatures, comparing these results with other regions should be done cau-

tiously. DLNM results in the same country but different cities have shown major differences due to regional adaptation and differences in initial climate (Motlogeloa and Fitchett, 2024; Zhao et al., 2019). Thus, although comparisons with other regions of the country are necessary, the findings of this thesis must be contextualised and cannot be extended to conclusions for the entire country. They are specific to Antananarivo's unique climate and health context.

The final main limitation of this study is the lack of flexibility in modelling choices. In our methods section, we highlighted the best model choices for analysing all-cause mortality. However, comparing our results with existing literature revealed the importance of different lag periods for different causes of death. This suggests that an analysis focusing on the best methodological aspects one at a time for the specificities of different causes would have increased the accuracy of our results by cause.

3 Conclusions

In conclusion, global warming is an increasingly preoccupying phenomenon that affects human lives, compromising the physical security and overall health of populations. In this context, the increase in temperatures is one of the main concerns linked to climate change. Thus, understanding how these changes are currently affecting human populations, and how they will be in the future, is of highest importance. Equally essential is the study of the methodological implications of measuring these changes.

However, as previously mentioned there is a gap in the literature. Although climate change shows an increasing presence in scientific publishing, this trend is mainly seen in high-income countries. Conversely, research remains scarce in Low and Lower Middle Income Countries and Sub-Saharan Africa in particular. Therefore, this study has explored the methodological implications of applying exposure-response measures for temperature and mortality in Antananarivo to highlight the importance of understanding the effects on different age groups in these contexts. Specifically, we applied an existing method in a new geographical context, considering different age groups and methodological implications.

Our results are significant in several ways. We identified differences in the temperature-mortality association for different age groups in Antananarivo, where heat impacts children most, while cold affects adults and the elderly the most. This contrasts with previous literature focused mainly on older age groups due to their higher mortality rates. Our study fills this gap, particularly for SSA, where studies using DLNMs are scarce. Additionally, we found temperature-related differences in specific causes of death. This nuanced understanding highlights the need for targeted health interventions. We also quantified the significant

mortality burden due to non-optimal temperatures under both climate scenarios, emphasising changes when including shifting number of deaths. Our study offers the first estimates for Antananarivo, considering climate change and population dynamics. Our results are in line with previous observations of high seasonal patterns in younger age mortality, addressing the lack of sensitivity tests for shifts in association without controlling for seasonality. Lastly, we demonstrated that using measured temperatures is more effective than modelled temperatures, providing insights for future research and healthcare action.

Following our findings, several recommendations are drawn for future research and the scientific community. First, we find that methods such as DLNMs should be applied to different age groups (when the numbers of deaths are large enough) to identify different associations and sensitivities to temperature. Additionally, analysis of DLNMs should be done by cause of death whenever possible, especially in contexts where an epidemiological transition is ongoing. Furthermore, more studies like this one should be conducted, as we had no studies to assess for adaptation and its measurement and a very little set of studies for comparison. Moreover, studies should use measured data whenever possible, ensuring that the model is based on real-life temperatures, which can then be better translated for healthcare action.

Regarding healthcare action in the country and the international community, this study highlights that different strategies for healthcare and mitigating impacts should be developed for different population subsets. Indeed, the evolution of global warming will increase the mortality burden of some causes of death while decreasing it for others. Consequently, this means that epidemiological transition cannot be the sole basis for planning future health plans and actions, as changes in climate may induce perturbations in the epidemiological transition. Furthermore, the model without seasonality showed a high effect of seasonality for mortality due to non-optimal warm temperatures for children, which implies necessary considerations of preparing for the accumulated effect of temperatures in a given higher mortality season for children. Finally, given the measured effects of temperatures and their increase on population health, action must be taken to mitigate climate changes and support those without the necessary means to face these changes.

Our study has limits, which we discussed earlier. From these, we extract additional recommendations for others who wish to study the effects of temperatures on mortality in LLMICs. We encourage the use of DLNMs in other regions of SSA where possible, to serve as a base for comparison and to study potential adaptation. We recommend using death record datasets of larger size, as small numbers lead to high uncertainty in model outcomes, especially when working with different age groups. Model choices should suit the specificity of the local context or subgroup, particularly regarding lag. Projections of mortality should

be included in estimates to better reflect upcoming changes due to climate change, but these projections should be based on reliable estimates. Lastly, we encourage precise description of modelling choices to facilitate comparison and application for future studies.

Bibliography

Asmamaw Abera, Johan Friberg, Christina Isaxon, Michael Jerrett, Ebba Malmqvist, Cheryl Sjöström, Tahir Taj, and Ana Maria Vargas. Air Quality in Africa: Public Health Implications. *Annual Review of Public Health*, 42(1):193–210, April 2021. ISSN 0163-7525, 1545-2093. doi: 10.1146/annurev-publhealth-100119-113802. URL https://www.annualreviews.org/doi/10.1146/annurev-publhealth-100119-113802.

Samuel Agyei-Mensah and Ama de Graft Aikins. Epidemiological Transition and the Double Burden of Disease in Accra, Ghana. *Journal of Urban Health : Bulletin of the New York Academy of Medicine*, 87(5):879–897, September 2010. ISSN 1099-3460. doi: 10.1007/s11524-010-9492-y. URL https://www.ncbi.nlm.nih.gov/pmc/articles/PMC2937133/.

Zunaid Ahsan Karar, Nurul Alam, and Peter Kim Streatfield. Epidemiological transition in rural Bangladesh, 1986–2006. *Global Health Action*, 2(1):1904, November 2009. ISSN 1654-9716, 1654-9880. doi: 10.3402/gha.v2i0.1904. URL https://www.tandfonline.com/doi/full/10.3402/gha.v2i0.1904.

Hadi Allafta and Christian Opp. Climate Change Paradox: The Least Responsible for It Encounters the Most of Its Implications. *Climate*, 12(3):38, March 2024. ISSN 2225-1154. doi: 10.3390/cli12030038. URL https://www.mdpi.com/2225-1154/12/3/38. Number: 3 Publisher: Multidisciplinary Digital Publishing Institute.

A. Kofi Amegah, Giovanni Rezza, and Jouni J. K. Jaakkola. Temperature-related morbidity and mortality in Sub-Saharan Africa: A systematic review of the empirical evidence. *Environment International*, 91:133–149, May 2016. ISSN 0160-4120. doi: 10.1016/j.envint.2016.02.027. URL https://www.sciencedirect.com/science/article/pii/S0160412016300630.

Brooke G. Anderson and Michelle L. Bell. Weather-Related Mortality: How Heat, Cold, and Heat Waves Affect Mortality in the United States. *Epidemiology*, 20(2):205–213, March 2009. ISSN 1044-3983. doi: 10.1097/EDE.0b013e318190ee08. URL https://journals.lww.com/00001648-200903000-00011.

Ben Armstrong. Models for the Relationship Between Ambient Temperature and Daily Mortality. *Epidemiology*, 17(6):624, November 2006. ISSN 1044-3983. doi: 10.1097/01.ede.0000239732.50999.8f. URL https://journals.lww.com/epidem/fulltext/2006/11000/models_for_the_relationship_between_ambient.6.aspx.

Rachel E. Baker and Jesse Anttila-Hughes. Characterizing the contribution of high temperatures to child undernourishment in Sub-Saharan Africa. *Scientific Reports*, 10(1): 18796, November 2020. ISSN 2045-2322. doi: 10.1038/s41598-020-74942-9. URL https://www.nature.com/articles/s41598-020-74942-9. Publisher: Nature Publishing Group.

Desire Banga, Melvis Baren, Namale Vivian Ssonko, Franck Katembo Sikakulya, Yves Tibamwenda, Claude Banga, and Robinson Ssebuufu. Comorbidities and Factors Associated with Mortality among Children under Five Years Admitted with Severe Acute Malnutrition in the Nutritional Unit of Jinja Regional Referral Hospital, Eastern Uganda. *International Journal of Pediatrics*, 2020:e7809412, November 2020. ISSN 1687-9740. doi: 10.1155/2020/7809412. URL https://www.hindawi.com/journals/ijpedi/2020/7809412/. Publisher: Hindawi.

Junzhe Bao, Zhenkun Wang, Chuanhua Yu, and Xudong Li. The influence of temperature on mortality and its Lag effect: a study in four Chinese cities with different latitudes. *BMC Public Health*, 16(1):375, May 2016. ISSN 1471-2458. doi: 10.1186/s12889-016-3031-z. URL https://doi.org/10.1186/s12889-016-3031-z.

Alan Barreca, Karen Clay, Olivier Deschenes, Michael Greenstone, and Joseph S. Shapiro. Adapting to Climate Change: The Remarkable Decline in the US Temperature-Mortality Relationship over the Twentieth Century. *Journal of Political Economy*, 124(1):105–159, February 2016. ISSN 0022-3808, 1537-534X. doi: 10.1086/684582. URL https://www.journals.uchicago.edu/doi/10.1086/684582.

Krishnan Bhaskaran, Antonio Gasparrini, Shakoor Hajat, Liam Smeeth, and Ben Armstrong. Time series regression studies in environmental epidemiology. *International Journal of Epidemiology*, 42(4):1187–1195, August 2013. ISSN 0300-5771. doi: 10.1093/ije/dyt092. URL https://www.ncbi.nlm.nih.gov/pmc/articles/PMC3780998/.

P. Bi, J Wang, and J. E. Hiller. Weather: driving force behind the transmission of severe acute respiratory syndrome in China? *Internal Medicine Journal*, 37(8):550–554, 2007. ISSN 1445-5994. doi: 10.1111/j.1445-5994.2007.01358.x. URL https://onlinelibrary.wiley.com/doi/abs/10.1111/j.1445-5994.2007.01358.x. _eprint: https://onlinelibrary.wiley.com/doi/pdf/10.1111/j.1445-5994.2007.01358.x.

Frederikke Højgaard Borg, Johanne Greibe Andersen, Catherine Karekezi, Gerald Yonga, Peter Furu, Per Kallestrup, and Christian Kraef. Climate change and health in urban informal settlements in low- and middle-income countries – a scoping review of health impacts and adaptation strategies. *Global Health Action*, 14(1):1908064, January 2021. ISSN 1654-9716. doi: 10.1080/16549716.2021.1908064. URL https://doi.org/10.1080/16549716.2021.1908064. Publisher: Taylor & Francis _eprint: https://doi.org/10.1080/16549716.2021.1908064.

Jessie P Buckley, Jonathan Samet, and David Richardson. Commentary: Does Air Pollution Confound Studies of Temperature? *Epidemiology*, March 2014. URL https://journals.lww.com/epidem/fulltext/2014/03000/Commentary___Does_Air_Pollution_Confound_Studies.14.aspx.

Aditi Bunker, Jan Wildenhain, Alina Vandenbergh, Nicholas Henschke, Joacim Rocklöv, Shakoor Hajat, and Rainer Sauerborn. Effects of Air Temperature on Climate-Sensitive Mortality and Morbidity Outcomes in the Elderly; a Systematic Review and Meta-analysis of Epidemiological Evidence. *eBioMedicine*, 6:258–268, April 2016. ISSN 2352-3964. doi: 10.1016/j.ebiom.2016.02.034. URL https://www.thelancet.com/journals/ebiom/article/PIIS2352-3964(16)30073-1/fulltext. Publisher: Elsevier.

Lendrum Diarmid Campbell and Rosalie Woodruff. Comparative Risk Assessment of the Burden of Disease from Climate Change. *Environmental Health Perspectives*, 114(12): 1935–1941, December 2006. doi: 10.1289/ehp.8432. URL https://ehp.niehs.nih.gov/doi/full/10.1289/ehp.8432. Publisher: Environmental Health Perspectives.

Ilona Carneiro, Arantxa Roca-Feltrer, Jamie T. Griffin, Lucy Smith, Marcel Tanner, Joanna Armstrong Schellenberg, Brian Greenwood, and David Schellenberg. Age-Patterns of Malaria Vary with Severity, Transmission Intensity and Seasonality in Sub-Saharan Africa: A Systematic Review and Pooled Analysis. *PLOS ONE*, 5(2):e8988, February 2010. ISSN 1932-6203. doi: 10.1371/journal.pone.0008988. URL https://journals.plos.org/plosone/article?id=10.1371/journal.pone.0008988. Publisher: Public Library of Science.

Guorong Chai, Hua He, Yana Su, Yongzhong Sha, and Shengliang Zong. Lag effect of air temperature on the incidence of respiratory diseases in Lanzhou, China. *International Journal of Biometeorology*, 64(1):83–93, January 2020. ISSN 1432-1254. doi: 10.1007/s00484-019-01795-x. URL https://doi.org/10.1007/s00484-019-01795-x.

Sarah Chapman, Cathryn E. Birch, John H. Marsham, Chérie Part, Shakoor Hajat, Matthew F. Chersich, Kristie L. Ebi, Stanley Luchters, Britt Nakstad, and Sari Kovats. Past and projected climate change impacts on heat-related child mortality in

Africa. *Environmental Research Letters*, 17(7):074028, July 2022. ISSN 1748-9326. doi: 10.1088/1748-9326/ac7ac5. URL https://dx.doi.org/10.1088/1748-9326/ac7ac5. Publisher: IOP Publishing.

Ida Czumbel, Chantal Quinten, Pierluigi Lopalco, Jan C. Semenza, Alberto E. Tozzi, Catherine Weil-Oliver, Gordon Nichols, Hanne Nøkleby, Irina Brumboiu, Janneke Verheijen, Javier Segura del Pozo, Mira Kojouharova, Emese Szilágyi, Tiia Pertel, and The ECDC expert panel working group. Management and control of communicable diseases in schools and other child care settings: systematic review on the incubation period and period of infectiousness. *BMC Infectious Diseases*, 18(1):199, May 2018. ISSN 1471-2334. doi: 10.1186/s12879-018-3095-8. URL https://doi.org/10.1186/s12879-018-3095-8.

Shona Dalal, Juan Jose Beunza, Jimmy Volmink, Clement Adebamowo, Francis Bajunirwe, Marina Njelekela, Dariush Mozaffarian, Wafaie Fawzi, Walter Willett, Hans-Olov Adami, and Michelle D Holmes. Non-communicable diseases in sub-Saharan Africa: what we know now. *International Journal of Epidemiology*, 40(4):885–901, August 2011. ISSN 0300-5771. doi: 10.1093/ije/dyr050. URL https://doi.org/10.1093/ije/dyr050.

Tran Ngoc Dang, Xerxes T. Seposo, Nguyen Huu Chau Duc, Tran Binh Thang, Do Dang An, Lai Thi Minh Hang, Tran Thanh Long, Bui Thi Hong Loan, and Yasushi Honda. Characterizing the relationship between temperature and mortality in tropical and subtropical cities: a distributed lag non-linear model analysis in Hue, Viet Nam, 2009–2013. *Global Health Action*, 9(1):28738, December 2016. ISSN 1654-9716. doi: 10.3402/gha.v9.28738. URL https://doi.org/10.3402/gha.v9.28738. Publisher: Taylor & Francis _eprint: https://doi.org/10.3402/gha.v9.28738.

Katrien De Troeyer, Mariska Bauwelinck, Raf Aerts, Dimitrios Profer, Julie Berckmans, Andy Delcloo, Rafiq Hamdi, Bert Van Schaeybroeck, Hans Hooyberghs, Dirk Lauwaet, Claire Demoury, and An Van Nieuwenhuyse. Heat related mortality in the two largest Belgian urban areas: A time series analysis. *Environmental Research*, 188:109848, September 2020. ISSN 0013-9351. doi: 10.1016/j.envres.2020.109848. URL https://www.sciencedirect.com/science/article/pii/S001393512030743X.

Jessica Diggs. Demographic Transition Theory of Aging. In Sana JD Loue and Martha Sajatovic, editors, *Encyclopedia of Aging and Public Health*, pages 266–268. Springer US, Boston, MA, 2008. ISBN 978-0-387-33754-8. doi: 10.1007/978-0-387-33754-8_123. URL https://doi.org/10.1007/978-0-387-33754-8_123.

Tufa Dinku. Chapter 7 - Challenges with availability and quality of climate data in Africa. In Assefa M. Melesse, Wossenu Abtew, and Gabriel Senay, editors, *Extreme Hydrology and Climate Variability*, pages 71–80. Elsevier, January 2019. ISBN 978-0-12-815998-9. doi:

10.1016/B978-0-12-815998-9.00007-5. URL https://www.sciencedirect.com/science/article/pii/B9780128159989000075.

Gennaro D'Amato, Lorenzo Cecchi, Mariella D'Amato, and Isabella Annesi-Maesano. Climate change and respiratory diseases. *European Respiratory Review*, 23(132):161–169, June 2014. ISSN 0905-9180, 1600-0617. doi: 10.1183/09059180.00001714. URL https://err.ersjournals.com/content/23/132/161. Publisher: European Respiratory Society Section: European Respiratory Update.

Richard A. Easterlin. How beneficent is the market? A look at the modern history of mortality. *European Review of Economic History*, 3(3):257–294, December 1999. ISSN 1474-0044, 1361-4916. doi: 10.1017/S1361491699000131. URL https://www.cambridge.org/core/journals/european-review-of-economic-history/article/abs/how-beneficent-is-the-market-a-look-at-the-modern-history-of-mortality/6C2C61ACE1B115872F8D9CB3EFC803F6#access-block.

Kristie L Ebi, Anthony Capon, Peter Berry, Carolyn Broderick, Richard de Dear, George Havenith, Yasushi Honda, R Sari Kovats, Wei Ma, Arunima Malik, Nathan B Morris, Lars Nybo, Sonia I Seneviratne, Jennifer Vanos, and Ollie Jay. Hot weather and heat extremes: health risks. *The Lancet*, 398(10301):698–708, August 2021. ISSN 0140-6736. doi: 10.1016/S0140-6736(21)01208-3. URL https://www.sciencedirect.com/science/article/pii/S0140673621012083.

Mastawesha Misganaw Engdaw, Andrew P. Ballinger, Gabriele C. Hegerl, and Andrea K. Steiner. Changes in temperature and heat waves over Africa using observational and reanalysis data sets. *International Journal of Climatology*, 42(2):1165–1180, 2022. ISSN 1097-0088. doi: 10.1002/joc.7295. URL https://onlinelibrary.wiley.com/doi/abs/10.1002/joc.7295. _eprint: https://onlinelibrary.wiley.com/doi/pdf/10.1002/joc.7295.

Michelle V. Evans, Matthew H. Bonds, Laura F. Cordier, John M. Drake, Felana Ihantamalala, Justin Haruna, Ann C. Miller, Courtney C. Murdock, Marius Randriamanambtsoa, Estelle M. Raza-Fanomezanjanahary, Bénédicte R. Razafinjato, and Andres C. Garchitorena. Socio-demographic, not environmental, risk factors explain fine-scale spatial patterns of diarrhoeal disease in Ifanadiana, rural Madagascar. *Proceedings of the Royal Society B: Biological Sciences*, 288(1946):20202501, March 2021. doi: 10.1098/rspb.2020.2501. URL https://royalsocietypublishing.org/doi/full/10.1098/rspb.2020.2501. Publisher: Royal Society.

Alfésio Luís Ferreira Braga, Antonella Zanobetti, and Joel Schwartz. The Time Course of Weather-Related Deaths. *Epidemiology*, 12(6):662, November 2001. ISSN 1044-3983. URL https://journals.lww.com/epidem/fulltext/2001/11000/The_Time_Course_of_Weather_Related_Deaths.00014.aspx.

Christopher B. Field and Vicente R. Barros. *Climate change 2014: impacts, adaptation, and vulnerability Working Group II contribution to the fifth assessment report of the Intergovernmental panel on climate change*. Cambridge university press, New York, 2014. ISBN 978-1-107-64165-5 978-1-107-68386-0 978-1-107-05807-1 978-1-107-05816-3.

Antonio Gasparrini. Distributed Lag Linear and Non-Linear Models in R: The Package dlnm. *Journal of statistical software*, 43(8):1–20, July 2011. ISSN 1548-7660. URL `https://www.ncbi.nlm.nih.gov/pmc/articles/PMC3191524/`.

Antonio Gasparrini and Michela Leone. Attributable risk from distributed lag models. *BMC medical research methodology*, 14:55, April 2014. ISSN 1471-2288. doi: 10.1186/1471-2288-14-55.

Antonio Gasparrini, Ben Armstrong, Sari Kovats, and Paul Wilkinson. The effect of high temperatures on cause-specific mortality in England and Wales. *Occupational and Environmental Medicine*, 69(1):56–61, January 2012. ISSN 1351-0711, 1470-7926. doi: 10.1136/oem.2010.059782. URL `https://oem.bmj.com/lookup/doi/10.1136/oem.2010.059782`.

Antonio Gasparrini, Yuming Guo, Masahiro Hashizume, Eric Lavigne, Antonella Zanobetti, Joel Schwartz, Aurelio Tobias, Shilu Tong, Joacim Rocklöv, Bertil Forsberg, Michela Leone, Manuela De Sario, Michelle L Bell, Yue-Liang Leon Guo, Chang-fu Wu, Haidong Kan, Seung-Muk Yi, Micheline De Sousa Zanotti Stagliorio Coelho, Paulo Hilario Nascimento Saldiva, Yasushi Honda, Ho Kim, and Ben Armstrong. Mortality risk attributable to high and low ambient temperature: a multicountry observational study. *The Lancet*, 386 (9991):369–375, July 2015. ISSN 01406736. doi: 10.1016/S0140-6736(14)62114-0. URL `https://linkinghub.elsevier.com/retrieve/pii/S0140673614621140`.

Gaëtan Gavazzi, Francois Herrmann, and Karl-Heinz Krause. Aging and Infectious Diseases in the Developing World. *Clinical Infectious Diseases*, 39(1):83–91, July 2004. ISSN 1058-4838. doi: 10.1086/421559. URL `https://doi.org/10.1086/421559`.

Christine Giesen, Jesús Roche, Lidia Redondo-Bravo, Claudia Ruiz-Huerta, Diana Gomez-Barroso, Agustin Benito, and Zaida Herrador. The impact of climate change on mosquito-borne diseases in Africa. *Pathogens and Global Health*, 114(6):287–301, August 2020. ISSN 2047-7724. doi: 10.1080/20477724.2020.1783865. URL `https://doi.org/10.1080/20477724.2020.1783865`. Publisher: Taylor & Francis _eprint: https://doi.org/10.1080/20477724.2020.1783865.

Hunter Green, Jennifer Bailey, Lara Schwarz, Jennifer Vanos, Kristie Ebi, and Tarik Benmarhnia. Impact of heat on mortality and morbidity in low and middle income countries: A review of the epidemiological evidence and considerations for future research. *Environmen-*

tal Research, 171:80–91, April 2019. ISSN 0013-9351. doi: 10.1016/j.envres.2019.01.010. URL https://www.sciencedirect.com/science/article/pii/S0013935119300106.

Yuming Guo, Antonio Gasparrini, Ben Armstrong, Shanshan Li, Benjawan Tawatsupa, Aurelio Tobias, Eric Lavigne, Micheline de Sousa Zanotti Stagliorio Coelho, Michela Leone, Xiaochuan Pan, Shilu Tong, Linwei Tian, Ho Kim, Masahiro Hashizume, Yasushi Honda, Yue-Liang Leon Guo, Chang-Fu Wu, Kornwipa Punnasiri, Seung-Muk Yi, Paola Michelozzi, Paulo Hilario Nascimento Saldiva, and Gail Williams. Global Variation in the Effects of Ambient Temperature on Mortality: A Systematic Evaluation. *Epidemiology*, 25(6):781, November 2014. ISSN 1044-3983. doi: 10.1097/EDE.0000000000000165. URL https://journals.lww.com/epidem/FullText/2014/11000/Global_Variation_in_the_Effects_of_Ambient.1.aspx.

A Haines, Rs Kovats, D Campbell-Lendrum, and C Corvalan. Climate change and human health: impacts, vulnerability, and mitigation. *The Lancet*, 367(9528):2101–2109, June 2006. ISSN 01406736. doi: 10.1016/S0140-6736(06)68933-2. URL https://linkinghub.elsevier.com/retrieve/pii/S0140673606689332.

Luke J Harrington, Piotr Wolski, Izidine Pinto, Anzelà Mamiarisoa Ramarosandratana, Rondrotiana Barimalala, Robert Vautard, Sjoukje Philip, Sarah Kew, Roop Singh, Dorothy Heinrich, Julie Arrighi, Emmanuel Raju, Lisa Thalheimer, Thierry Razanakoto, Maarten Van Aalst, Sihan Li, Remy Bonnet, Wenchang Yang, Friederike E L Otto, and Geert Jan Van Oldenborgh. Limited role of climate change in extreme low rainfall associated with southern Madagascar food insecurity, 2019–21. *Environmental Research: Climate*, 1 (2):021003, December 2022. ISSN 2752-5295. doi: 10.1088/2752-5295/aca695. URL https://iopscience.iop.org/article/10.1088/2752-5295/aca695.

Cunrui Huang, Adrian Gerard Barnett, Xiaoming Wang, Pavla Vaneckova, Gerard FitzGerald, and Shilu Tong. Projecting future heat-related mortality under climate change scenarios: a systematic review. *Environmental Health Perspectives*, 119(12):1681–1690, December 2011. ISSN 1552-9924. doi: 10.1289/ehp.1103456.

A Huq, E B Small, P A West, M I Huq, R Rahman, and R R Colwell. Ecological relationships between Vibrio cholerae and planktonic crustacean copepods. *Applied and Environmental Microbiology*, 45(1):275–283, January 1983. doi: 10.1128/aem.45.1.275-283.1983. URL https://journals.asm.org/doi/10.1128/aem.45.1.275-283.1983. Publisher: American Society for Microbiology.

Intergovernmental Panel On Climate Change. *Climate Change 2021 – The Physical Science Basis: Working Group I Contribution to the Sixth Assessment Report of the Intergovernmental Panel on Climate Change*. Cambridge University Press, 1 edition, July 2023.

ISBN 978-1-00-915789-6. doi: 10.1017/9781009157896. URL https://www.cambridge.org/core/product/identifier/9781009157896/type/book.

Ludmilla da Silva Viana Jacobson, Beatriz Fátima Alves de Oliveira, Rochelle Schneider, Antonio Gasparrini, and Sandra de Souza Hacon. Mortality Risk from Respiratory Diseases Due to Non-Optimal Temperature among Brazilian Elderlies. *International Journal of Environmental Research and Public Health*, 18(11):5550, January 2021. ISSN 1660-4601. doi: 10.3390/ijerph18115550. URL https://www.mdpi.com/1660-4601/18/11/5550. Number: 11 Publisher: Multidisciplinary Digital Publishing Institute.

Dudley Kirk. Demographic Transition Theory. *Population Studies*, 50(3):361–387, 1996. ISSN 0032-4728. URL https://www.jstor.org/stable/2174639. Publisher: [Population Investigation Committee, Taylor & Francis, Ltd.].

Jordan D. Klein and Anjarasoa Rasoanomenjanahary. Climate Change and Health Transitions: Evidence From Antananarivo, Madagascar. *OSF Preprints*, September 2023. URL https://ideas.repec.org//p/osf/osfxxx/hk7fp.html. Number: hk7fp Publisher: Center for Open Science.

Erik W. Kolstad and Kjell Arne Johansson. Uncertainties Associated with Quantifying Climate Change Impacts on Human Health: A Case Study for Diarrhea. *Environmental Health Perspectives*, 119(3):299–305, March 2011. doi: 10.1289/ehp.1002060. URL https://ehp.niehs.nih.gov/doi/10.1289/ehp.1002060. Publisher: Environmental Health Perspectives.

R. Sari Kovats, Diarmid Campbell-Lendrum, and Franziska Matthies. Climate Change and Human Health: Estimating Avoidable Deaths and Disease. *Risk Analysis*, 25(6): 1409–1418, 2005. ISSN 1539-6924. doi: 10.1111/j.1539-6924.2005.00688.x. URL https://onlinelibrary.wiley.com/doi/abs/10.1111/j.1539-6924.2005.00688.x. _eprint: https://onlinelibrary.wiley.com/doi/pdf/10.1111/j.1539-6924.2005.00688.x.

Violaine Lepousez. Les scénarios SSP : Décryptage et recommandations d'utilisation pour une démarche d'adaptation au changement climatique, 2022.

Karen Levy, Andrew P. Woster, Rebecca S. Goldstein, and Elizabeth J. Carlton. Untangling the Impacts of Climate Change on Waterborne Diseases: a Systematic Review of Relationships between Diarrheal Diseases and Temperature, Rainfall, Flooding, and Drought. *Environmental Science & Technology*, 50(10):4905–4922, May 2016. ISSN 0013-936X. doi: 10.1021/acs.est.5b06186. URL https://doi.org/10.1021/acs.est.5b06186. Publisher: American Chemical Society.

Yu-Kai Lin, Chin-Kuo Chang, Yu-Chun Wang, and Tsung-Jung Ho. Acute and Prolonged Adverse Effects of Temperature on Mortality from Cardiovascular Diseases. *PLOS*

ONE, 8(12):e82678, December 2013. ISSN 1932-6203. doi: 10.1371/journal.pone.0082678. URL https://journals.plos.org/plosone/article?id=10.1371/journal.pone.0082678. Publisher: Public Library of Science.

Erin K. Lipp, Anwar Huq, and Rita. R Colwell. Effects of Global Climate on Infectious Disease: the Cholera Model, 2002. URL https://journals.asm.org/doi/epdf/10.1128/cmr.15.4.757-770.2002?src=getftr.

Peter J. Marcotullio, Carsten Keßler, and Balázs M. Fekete. The future urban heat-wave challenge in Africa: Exploratory analysis. *Global Environmental Change*, 66:102190, January 2021. ISSN 0959-3780. doi: 10.1016/j.gloenvcha.2020.102190. URL https://www.sciencedirect.com/science/article/pii/S0959378020307731.

Bruno Masquelier, Dominique Waltisperger, Osée Ralijaona, Gilles Pison, and Arsene Ravelo. The epidemiological transition in Antananarivo, Madagascar: an assessment based on death registers (1900–2012). *Global Health Action*, 7(1):23237, 2014. Publisher: Taylor & Francis.

Bruno Masquelier, Gilles Pison, Julio Rakotonirina, and Anjarasoa Rasoanomenjanahary. Estimating cause-specific mortality in Madagascar: an evaluation of death notification data from the capital city. *Population Health Metrics*, 17(1):8, July 2019. ISSN 1478-7954. doi: 10.1186/s12963-019-0190-z. URL https://doi.org/10.1186/s12963-019-0190-z.

Anthony J McMichael, Rosalie E Woodruff, and Simon Hales. Climate change and human health: present and future risks. *The Lancet*, 367(9513):859–869, March 2006. ISSN 01406736. doi: 10.1016/S0140-6736(06)68079-3. URL https://linkinghub.elsevier.com/retrieve/pii/S0140673606680793.

Paola Michelozzi, Gabriele Accetta, Manuela De Sario, Daniela D'Ippoliti, Claudia Marino, Michela Baccini, Annibale Biggeri, H. Ross Anderson, Klea Katsouyanni, Ferran Ballester, Luigi Bisanti, Ennio Cadum, Bertil Forsberg, Francesco Forastiere, Patrick G. Goodman, Ana Hojs, Ursula Kirchmayer, Sylvia Medina, Anna Paldy, Christian Schindler, Jordi Sunyer, Carlo A. Perucci, and PHEWE Collaborative Group. High temperature and hospitalizations for cardiovascular and respiratory causes in 12 European cities. *American Journal of Respiratory and Critical Care Medicine*, 179(5):383–389, March 2009. ISSN 1535-4970. doi: 10.1164/rccm.200802-217OC.

Mohammad Torkashvand Moradabadi, Sedigheh Hannani, and Zahra Torkashvand. Epidemilogic Study of Death Caused by Endocrine, Nutritional, and Metabolic Diseases in Iran During 2006-2018. *Iranian journal of diabetes and obesity*, September 2023. ISSN 2345-2250. doi: 10.18502/ijdo.v15i3.13737. URL https://publish.kne-publishing.com/index.php/IJDO/article/view/13737.

Ogone Motlogeloa and Jennifer M. Fitchett. Assessing the impact of climatic variability on acute respiratory diseases across diverse climatic zones in South Africa. *Science of The Total Environment*, 918:170661, March 2024. ISSN 0048-9697. doi: 10.1016/j.scitotenv.2024.170661. URL https://www.sciencedirect.com/science/article/pii/S0048969724008003.

E.N. Naumova, J.S. Jagai, B. Matyas, A. DeMaria, I.B. MacNeill, and J.K. Griffiths. Seasonality in six enterically transmitted diseases and ambient temperature. *Epidemiology and Infection*, 135(2):281–292, 2007. ISSN 1469-4409. doi: 10.1017/S0950268806006698.

Katlego P. Ncongwane, Joel O. Botai, Venkataraman Sivakumar, and Christina M. Botai. A Literature Review of the Impacts of Heat Stress on Human Health across Africa. *Sustainability*, 13(9):5312, January 2021a. ISSN 2071-1050. doi: 10.3390/su13095312. URL https://www.mdpi.com/2071-1050/13/9/5312. Number: 9 Publisher: Multidisciplinary Digital Publishing Institute.

Katlego P. Ncongwane, Joel O. Botai, Venkataraman Sivakumar, Christina M. Botai, and Abiodun M. Adeola. Characteristics and Long-Term Trends of Heat Stress for South Africa. *Sustainability*, 13(23):13249, January 2021b. ISSN 2071-1050. doi: 10.3390/su132313249. URL https://www.mdpi.com/2071-1050/13/23/13249. Number: 23 Publisher: Multidisciplinary Digital Publishing Institute.

Modeste Kameni Nematchoua, Paola Ricciardi, José A. Orosa, and Cinzia Buratti. A detailed study of climate change and some vulnerabilities in Indian Ocean: A case of Madagascar island. *Sustainable Cities and Society*, 41:886–898, August 2018. ISSN 2210-6707. doi: 10.1016/j.scs.2018.05.040. URL https://www.sciencedirect.com/science/article/pii/S2210670718300490.

Simo Näyhä. Cold and the risk of cardiovascular diseases.: A review. *International Journal of Circumpolar Health*, 61(4):373–380, December 2002. ISSN null. doi: 10.3402/ijch.v61i4.17495. URL https://doi.org/10.3402/ijch.v61i4.17495. Publisher: Taylor & Francis _eprint: https://doi.org/10.3402/ijch.v61i4.17495.

Phillips Edomwonyi Obasohan, Stephen J. Walters, Richard Jacques, and Khaled Khatab. Risk Factors Associated with Multimorbidity among Children Aged Under-Five Years in Sub-Saharan African Countries: A Scoping Review. *International Journal of Environmental Research and Public Health*, 20(2):1377, January 2023. ISSN 1660-4601. doi: 10.3390/ijerph20021377. URL https://www.mdpi.com/1660-4601/20/2/1377. Number: 2 Publisher: Multidisciplinary Digital Publishing Institute.

A. R. Omran. The epidemiologic transition. A theory of the Epidemiology of population

change. 1971. *Bulletin of the World Health Organization*, 79(2):161–170, 2001. ISSN 0042-9686. URL https://www.ncbi.nlm.nih.gov/pmc/articles/PMC2566347/.

Brian C. O'Neill, Elmar Kriegler, Keywan Riahi, Kristie L. Ebi, Stephane Hallegatte, Timothy R. Carter, Ritu Mathur, and Detlef P. van Vuuren. A new scenario framework for climate change research: the concept of shared socioeconomic pathways. *Climatic Change*, 122(3):387–400, February 2014. ISSN 1573-1480. doi: 10.1007/s10584-013-0905-2. URL https://doi.org/10.1007/s10584-013-0905-2.

R.K. Phalkey, C. Aranda-Jan, S. Marx, B. Höfle, and R. Sauerborn. Systematic review of current efforts to quantify the impacts of climate change on undernutrition. *Proceedings of the National Academy of Sciences of the United States of America*, 112(33):E4522–E4529, 2015. ISSN 0027-8424. doi: 10.1073/pnas.1409769112.

Adithya Pradyumna and Joshitha Sankam. Tools and methods for assessing health vulnerability and adaptation to climate change: A scoping review. *The Journal of Climate Change and Health*, 8:100153, October 2022. ISSN 26672782. doi: 10.1016/j.joclim.2022.100153. URL https://linkinghub.elsevier.com/retrieve/pii/S2667278222000426.

Samuel H. Preston. The Changing Relation between Mortality and level of Economic Development. *Population Studies*, 29(2):231–248, July 1975. ISSN 0032-4728. doi: 10.1080/00324728.1975.10410201. URL https://www.tandfonline.com/doi/abs/10.1080/00324728.1975.10410201. Publisher: Routledge _eprint: https://www.tandfonline.com/doi/pdf/10.1080/00324728.1975.10410201.

Joelinotahiana Hasina Rabarison, Jean Marius Rakotondramanga, Rila Ratovoson, Bruno Masquelier, Anjaraso Maharavo Rasoanomenjanahary, Anou Dreyfus, Andres Garchitorena, Fidisoa Rasambainarivo, Norosoa Harline Razanajatovo, Soa Fy Andriamandimby, C Jessica Metcalf, Vincent Lacoste, Jean-Michel Heraud, and Philippe Dussart. Excess mortality associated with the COVID-19 pandemic during the 2020 and 2021 waves in Antananarivo, Madagascar. *BMJ Global Health*, 8(7):e011801, July 2023. ISSN 2059-7908. doi: 10.1136/bmjgh-2023-011801. URL https://www.ncbi.nlm.nih.gov/pmc/articles/PMC10373673/.

Norohasina Rakotoarison, Nirivololona Raholijao, Lalao Razafindramavo, Zo Rakotomavo, Alain Rakotoarisoa, Joy Guillemot, Zazaravaka Randriamialisoa, Victor Mafilaza, Voahanginirina Ramiandrisoa, Rhino Rajaonarivony, Solonomenjanahary Andrianjafinirina, Venance Tata, Manuela Vololoniaina, Fanjasoa Rakotomanana, and Volahanta Raminosoa. Assessment of Risk, Vulnerability and Adaptation to Climate Change by the Health Sector in Madagascar. *International Journal of Environmental Research and Public Health*, 15(12):2643, November 2018. ISSN 1660-4601. doi: 10.3390/ijerph15122643. URL http://www.mdpi.com/1660-4601/15/12/2643.

Rila Ratovoson, Bruno Masquelier, Todisoa Andriatahina, Reziky Mangahasimbola, Zo Andrianirina, Gilles Pison, and Laurence Baril. Inequalities in cause-specific mortality in children and adolescents in the Moramanga health survey, Madagascar. *International Journal of Public Health*, 65(6):781–790, July 2020. ISSN 1661-8564. doi: 10.1007/s00038-020-01409-z. URL https://doi.org/10.1007/s00038-020-01409-z.

Keywan Riahi, Detlef P. van Vuuren, Elmar Kriegler, Jae Edmonds, Brian C. O'Neill, Shinichiro Fujimori, Nico Bauer, Katherine Calvin, Rob Dellink, Oliver Fricko, Wolfgang Lutz, Alexander Popp, Jesus Crespo Cuaresma, Samir Kc, Marian Leimbach, Leiwen Jiang, Tom Kram, Shilpa Rao, Johannes Emmerling, Kristie Ebi, Tomoko Hasegawa, Petr Havlik, Florian Humpenöder, Lara Aleluia Da Silva, Steve Smith, Elke Stehfest, Valentina Bosetti, Jiyong Eom, David Gernaat, Toshihiko Masui, Joeri Rogelj, Jessica Strefler, Laurent Drouet, Volker Krey, Gunnar Luderer, Mathijs Harmsen, Kiyoshi Takahashi, Lavinia Baumstark, Jonathan C. Doelman, Mikiko Kainuma, Zbigniew Klimont, Giacomo Marangoni, Hermann Lotze-Campen, Michael Obersteiner, Andrzej Tabeau, and Massimo Tavoni. The Shared Socioeconomic Pathways and their energy, land use, and greenhouse gas emissions implications: An overview. *Global Environmental Change*, 42: 153–168, January 2017. ISSN 0959-3780. doi: 10.1016/j.gloenvcha.2016.05.009. URL https://www.sciencedirect.com/science/article/pii/S0959378016300681.

Marina Romanello, Claudia Di Napoli, Carole Green, Harry Kennard, Pete Lampard, Daniel Scamman, Maria Walawender, Zakari Ali, Nadia Ameli, Sonja Ayeb-Karlsson, Paul J Beggs, Kristine Belesova, Lea Berrang Ford, Kathryn Bowen, Wenjia Cai, Max Callaghan, Diarmid Campbell-Lendrum, Jonathan Chambers, Troy J Cross, Kim R Van Daalen, Carole Dalin, Niheer Dasandi, Shouro Dasgupta, Michael Davies, Paula Dominguez-Salas, Robert Dubrow, Kristie L Ebi, Matthew Eckelman, Paul Ekins, Chris Freyberg, Olga Gasparyan, Georgiana Gordon-Strachan, Hilary Graham, Samuel H Gunther, Ian Hamilton, Yun Hang, Risto Hänninen, Stella Hartinger, Kehan He, Julian Heidecke, Jeremy J Hess, Shih-Che Hsu, Louis Jamart, Slava Jankin, Ollie Jay, Ilan Kelman, Gregor Kiesewetter, Patrick Kinney, Dominic Kniveton, Rostislav Kouznetsov, Francesca Larosa, Jason K W Lee, Bruno Lemke, Yang Liu, Zhao Liu, Melissa Lott, Martín Lotto Batista, Rachel Lowe, Maquins Odhiambo Sewe, Jaime Martinez-Urtaza, Mark Maslin, Lucy McAllister, Celia McMichael, Zhifu Mi, James Milner, Kelton Minor, Jan C Minx, Nahid Mohajeri, Natalie C Momen, Maziar Moradi-Lakeh, Karyn Morrissey, Simon Munzert, Kris A Murray, Tara Neville, Maria Nilsson, Nick Obradovich, Megan B O'Hare, Camile Oliveira, Tadj Oreszczyn, Matthias Otto, Fereidoon Owfi, Olivia Pearman, Frank Pega, Andrew Pershing, Mahnaz Rabbaniha, Jamie Rickman, Elizabeth J Z Robinson, Joacim Rocklöv, Renee N Salas, Jan C Semenza, Jodi D Sherman, Joy Shumake-Guillemot, Grant Silbert, Mikhail Sofiev, Marco Springmann, Jennifer D Stowell, Meisam Tabatabaei, Jonathon Taylor, Ross Thompson, Cathryn Tonne, Marina Treskova, Joaquin A Trinanes, Fabian Wagner, Laura Warnecke,

Hannah Whitcombe, Matthew Winning, Arthur Wyns, Marisol Yglesias-González, Shihui Zhang, Ying Zhang, Qiao Zhu, Peng Gong, Hugh Montgomery, and Anthony Costello. The 2023 report of the Lancet Countdown on health and climate change: the imperative for a health-centred response in a world facing irreversible harms. *The Lancet*, 402(10419): 2346–2394, December 2023. ISSN 01406736. doi: 10.1016/S0140-6736(23)01859-7. URL https://linkinghub.elsevier.com/retrieve/pii/S0140673623018597.

Samuel Rousseau, Jonathan Steinke, Méloé Vincent, Hanitriniavo Andriatseheno, and Julie Pontarollo. Strong seasonality in diets and alarming levels of food insecurity and child malnutrition in south-eastern Madagascar. *Frontiers in Sustainable Food Systems*, 7, June 2023. ISSN 2571-581X. doi: 10.3389/fsufs.2023.1126053. URL https://www.frontiersin.org/articles/10.3389/fsufs.2023.1126053. Publisher: Frontiers.

Sahrish Saeed, Muhammad Sohail Amjad Makhdum, Sofia Anwar, and Muhammad Rizwan Yaseen. Climate Change Vulnerability, Adaptation, and Feedback Hypothesis: A Comparison of Lower-Middle, Upper-Middle, and High-Income Countries. *Sustainability*, 15 (5):4145, January 2023. ISSN 2071-1050. doi: 10.3390/su15054145. URL https://www.mdpi.com/2071-1050/15/5/4145. Number: 5 Publisher: Multidisciplinary Digital Publishing Institute.

Michael Sanderson, Katherine Arbuthnott, Sari Kovats, Shakoor Hajat, and Pete Falloon. The use of climate information to estimate future mortality from high ambient temperature: A systematic literature review. *PloS One*, 12(7):e0180369, 2017. ISSN 1932-6203. doi: 10.1371/journal.pone.0180369.

Benjamin-Samuel Schlüter, Bruno Masquelier, C. Jessica E. Metcalf, and Anjarasoa Rasoanomenjanahary. Long-term trends in seasonality of mortality in urban Madagascar: the role of the epidemiological transition. *Global Health Action*, 13(1):1717411, December 2020. ISSN 1654-9716. doi: 10.1080/16549716.2020.1717411. URL https://doi.org/10.1080/16549716.2020.1717411. Publisher: Taylor & Francis _eprint: https://doi.org/10.1080/16549716.2020.1717411.

Olivia Serdeczny, Sophie Adams, Florent Baarsch, Dim Coumou, Alexander Robinson, William Hare, Michiel Schaeffer, Mahé Perrette, and Julia Reinhardt. Climate change impacts in Sub-Saharan Africa: from physical changes to their social repercussions. *Regional Environmental Change*, 17(6):1585–1600, August 2017. ISSN 1436-378X. doi: 10.1007/s10113-015-0910-2. URL https://doi.org/10.1007/s10113-015-0910-2.

Joyce Shirinde and Janine Wichmann. Temperature modifies the association between air pollution and respiratory disease mortality in Cape Town, South Africa. *International Journal of Environmental Health Research*, 33(11):1122–1131, November

2023. ISSN 0960-3123. doi: 10.1080/09603123.2022.2076813. URL https://doi.org/10.1080/09603123.2022.2076813. Publisher: Taylor & Francis _eprint: https://doi.org/10.1080/09603123.2022.2076813.

Lisa C. Smith and Lawrence Haddad. Reducing Child Undernutrition: Past Drivers and Priorities for the Post-MDG Era. *World Development*, 68:180–204, April 2015. ISSN 0305-750X. doi: 10.1016/j.worlddev.2014.11.014. URL https://www.sciencedirect.com/science/article/pii/S0305750X14003726.

Xuping Song, Shigong Wang, Yuling Hu, Man Yue, Tingting Zhang, Yu Liu, Jinhui Tian, and Kezheng Shang. Impact of ambient temperature on morbidity and mortality: An overview of reviews. *Science of The Total Environment*, 586:241–254, May 2017. ISSN 0048-9697. doi: 10.1016/j.scitotenv.2017.01.212. URL https://www.sciencedirect.com/science/article/pii/S0048969717302292.

Paige Van de Vuurst and Luis E. Escobar. Climate change and infectious disease: a review of evidence and research trends. *Infectious Diseases of Poverty*, 12(1):51, May 2023. ISSN 2049-9957. doi: 10.1186/s40249-023-01102-2. URL https://doi.org/10.1186/s40249-023-01102-2.

Ana M. Vicedo-Cabrera, Francesco Sera, and Antonio Gasparrini. Hands-on Tutorial on a Modeling Framework for Projections of Climate Change Impacts on Health. *Epidemiology (Cambridge, Mass.)*, 30(3):321–329, May 2019. ISSN 1044-3983. doi: 10.1097/EDE.0000000000000982. URL https://www.ncbi.nlm.nih.gov/pmc/articles/PMC6533172/.

C.L.F. Walker and R.E. Black. Diarrhoea morbidity and mortality in older children, adolescents, and adults. *Epidemiology and Infection*, 138(9):1215–1226, 2010. ISSN 1469-4409. doi: 10.1017/S0950268810000592.

Dominique Waltisperger and France Meslé. Crise économique et mortalité: Le cas d'Antananarivo 1976-2000. *Population*, 60(3):243, 2005. ISSN 0032-4663, 1957-7966. doi: 10.3917/popu.503.0243. URL http://www.cairn.info/revue-population-2005-3-page-243.htm?ref=doi.

Dominique Waltisperger, Pierre Cantrelle, and Osée Ralijaona. *La mortalité à Antananarivo de 1984 à 1995*. Number no 7 in Documents et manuels du CEPED. Centre français sur la population et le développement, Paris, 1998. ISBN 978-2-87762-110-6.

Dominique Waltisperger, France Meslé, and Jonathan Mandelbaum. Economic Crisis and Mortality: The Case of Antananarivo, 1976-2000. *Population (English Edition, 2002-)*, 60 (3):199–229, 2005. ISSN 1634-2941. doi: 10.2307/4148193. URL https://www.jstor.org/stable/4148193. Publisher: Institut National d'Études Démographiques.

WHO. Environmental health indicators: Framework and methodologies, 1999. URL https://www.who.int/publications-detail-redirect/WHO-SDE-OEH-99.10.

Rongbin Xu, Qi Zhao, Micheline S.Z.S. Coelho, Paulo H.N. Saldiva, Sophia Zoungas, Rachel R. Huxley, Michael J. Abramson, Yuming Guo, and Shanshan Li. Association between Heat Exposure and Hospitalization for Diabetes in Brazil during 2000–2015: A Nationwide Case-Crossover Study. *Environmental Health Perspectives*, 127(11):117005, November 2019. doi: 10.1289/EHP5688. URL https://ehp.niehs.nih.gov/doi/full/10.1289/EHP5688. Publisher: Environmental Health Perspectives.

Li Yang, Feng Qian, De-Xuan Song, and Ke-Jia Zheng. Research on Urban Heat-Island Effect. *Procedia Engineering*, 169:11–18, January 2016. ISSN 1877-7058. doi: 10.1016/j.proeng.2016.10.002. URL https://www.sciencedirect.com/science/article/pii/S1877705816332039.

Xiaofang Ye, Rodney Wolff, Weiwei Yu, Pavla Vaneckova, Xiaochuan Pan, and Shilu Tong. Ambient temperature and morbidity: a review of epidemiological evidence. *Environmental Health Perspectives*, 120(1):19–28, January 2012. ISSN 1552-9924. doi: 10.1289/ehp.1003198.

Weiwei Yu, Kerrie Mengersen, Wenbiao Hu, Yuming Guo, Xiaochuan Pan, and Shilu Tong. Assessing the relationship between global warming and mortality: Lag effects of temperature fluctuations by age and mortality categories. *Environmental Pollution*, 159 (7):1789–1793, July 2011. ISSN 0269-7491. doi: 10.1016/j.envpol.2011.03.039. URL https://www.sciencedirect.com/science/article/pii/S0269749111001965.

Jie Yuan, Yu Wu, Wenzhan Jing, Jue Liu, Min Du, Yaping Wang, and Min Liu. Association between meteorological factors and daily new cases of COVID-19 in 188 countries: A time series analysis. *Science of The Total Environment*, 780:146538, August 2021. ISSN 0048-9697. doi: 10.1016/j.scitotenv.2021.146538. URL https://www.sciencedirect.com/science/article/pii/S0048969721016065.

Yiju Zhao, Zhao Huang, Shengyong Wang, Jianxiong Hu, Jianpeng Xiao, Xing Li, Tao Liu, Weilin Zeng, Lingchuan Guo, Qingfeng Du, and Wenjun Ma. Morbidity burden of respiratory diseases attributable to ambient temperature: a case study in a subtropical city in China. *Environmental Health*, 18(1):89, October 2019. ISSN 1476-069X. doi: 10.1186/s12940-019-0529-8. URL https://doi.org/10.1186/s12940-019-0529-8.

Gaopei Zhu, Yuhang Zhu, Zhongli Wang, Weijing Meng, Xiaoxuan Wang, Jianing Feng, Juan Li, Yufei Xiao, Fuyan Shi, and Suzhen Wang. The association between ambient temperature and mortality of the coronavirus disease 2019 (COVID-19) in Wuhan, China:

a time-series analysis. *BMC Public Health*, 21(1):117, January 2021. ISSN 1471-2458. doi: 10.1186/s12889-020-10131-7. URL https://doi.org/10.1186/s12889-020-10131-7.

List of Figures

1 **Population pyramids for the Malagasy population in 1993 and 2018.** *The data was extracted from the INSTAT (Institut National de la Statistique) reports from the General Population and Housing Census of 1993 and 2018. The data was accessed on* `https://www.instat.mg/thematique/population`. 2

2 **The DPSEEA framework for environmental health risk assessment, applied to climate change.** *Source : Kovats et al. (2005)* 5

3 **Schematic summary of main pathways by which climate change affects population health.** *Source : McMichael et al. (2006).* 5

4 **Illustration of the physiological pathways of human heat strain.** *Source : Ebi et al. (2021).* 6

5 **Heat-related Mortality.** Percent change in annual deaths 7

6 **Per capita CO2 emissions in 2022.** *Extracted from :* `https://ourworldindata.org/co2-emissions`. 8

7 **Annual scientific production on the effects of heat on human health (globally and for Africa): research from 1968–2020.** Source: Ncongwane et al. (2021a) 14

8 **Map representing the number of studies conducted on the relation between high temperatures and health in the world.** *Source: Green et al. (2019)* 14

9 **Yearly death counts per age group in Antananarivo from 1990 to 2015.** *Data source:* Antananarivo death records provided by the Municipal Office of Hygiene. 16

10 **Global Burden of Disease in Madagascar for both sexes, all ages.** *Extracted from :* `https://vizhub.healthdata.org/gbd-compare/` (a) in 2000 (b) in 2015 17

11 **Map of the different climates in Madagascar.** *Source : This map was built and shared by Emilie Castin (researcher for the Centre for Research on the Epidemiology of Disasters) using a simplified version of the Köppen-Geiger classification using ERA-5 data.* 19

12 **Number of heat waves recorded in four Madagascan cities from 1990 to 2015.** The recorded events are when the daily maximum temperature of more than five consecutive days exceeds the average maximum temperature by 5 °C. *Source : Graphs produced and shared by Emilie Castin (researcher for the Centre for Research on the Epidemiology of Disasters) using ERA-5 data.* 20

13 **Mean daily temperatures averaged for the 2000-2015 period in Antananarivo.** *Data source: NOAA.* 20

14 **Increase in °C in projected mean temperature (for ssp126 and ssp585) in Antananarivo.** *Data extracted from RNOAA and ISIMIP and processed in code 0.2.* 21

15 **Observed and predicted life expectancy at birth in Antananarivo (1976–2021).** *Source : (Rabarison et al., 2023).* For males (green) and females (blue). The authors projected to 2020–24, the observed life expectancy at birth and the predicted (bold) for both sexes based on the rates measured from 1990 to 2019. This was based on a database with deaths recorded at Antananarivo by the Municipal Bureau of Hygiene and census-based population estimates. 23

16 **Evolution in numbers of broad causes of death for deaths under 15 in Antananarivo, Madagascar** 24

17 **Evolution in numbers of broad causes of death for deaths between 15 and 59 in Antananarivo, Madagascar** 24

18 **Evolution in numbers of broad causes of death for deaths over 60 in Antananarivo, Madagascar** 25

19 **Representation of all the missing values in daily temperature for each year of the NOAA dataset.** 30

20 **Steps for applying the Vicedo-Cabrera et al. (2019) tutorial - Graphics.** 37

21 **Different Relative Risks for mortality (all ages) with different maximum lags.** 39

22 **The different RR curves according to the different curve form choices (based on all age mortality).** 39

23 **Mean temperature distribution in Antananarivo for the 2000-2015 period.** With indications for the 10th, 75th and 90th percentiles of distribution. 40

24 **Projections and Regression results for deaths under 15 years old.** (a) Projections based on the 2000-2015 period for the 2090 horizon. (b) Regression results for the 2000-2015 period. 43

25 **Projections and Regression results for deaths between 15 and 59 years old.** (a) Projections based on the 2000-2015 period for the 2090 horizon. (b) Regression results for the 2000-2015 period. 43

26 **Projections and Regression results for deaths over 60 years old.** (a) Projections based on the 2000-2015 period for the 2090 horizon. (b) Regression results for the 2000-2015 period. 44

27 **Temperature and excess under 15 years old mortality for past and future periods.** (a) SSP1-2.6 for 2000-10 and 2050-59 (b) SSP1-2.6 for 2000-10 and 2090-99 (c) SSP5-8.5 for 2000-10 and 2050-59 (d) SSP5-8.5 for 2000-10 and 2090-99. *Top panel* : exposure-response curves (RRs across T°C (with 95% CI)). The dotted vertical line is the minimum mortality temperature which separates between cold (blue) and heat (red). The dashed part of the curve represents the extrapolation beyond the observed maximum temperature (2000-2015). *Mid panel*: distribution of temperature for the past (grey) and future (green) using the ensemble estimates (average impacts across GCMs) for SSP1-2.6. *Bottom panel*: the related distribution of excess mortality, expressed as the fraction of additional deaths (%) attributed to non-optimal temperature. 59

28 **Temperature and excess 15-59 years old mortality for past and future periods.** (a) SSP1-2.6 for 2000-10 and 2050-59 (b) SSP1-2.6 for 2000-10 and 2090-99 (c) SSP5-8.5 for 2000-10 and 2050-59 (d) SSP5-8.5 for 2000-10 and 2090-99. *Top panel* : exposure-response curves (RRs across T°C (with 95% CI)). The dotted vertical line is the minimum mortality temperature which separates between cold (blue) and heat (red). The dashed part of the curve represents the extrapolation beyond the observed maximum temperature (2000-2015). *Mid panel*: distribution of temperature for the past (grey) and future (green) using the ensemble estimates (average impacts across GCMs) for SSP1-2.6. *Bottom panel*: the related distribution of excess mortality, expressed as the fraction of additional deaths (%) attributed to non-optimal temperature. 60

29 **Temperature and excess over 60 years old mortality for past and future periods.** (a) SSP1-2.6 for 2000-10 and 2050-59 (b) SSP1-2.6 for 2000-10 and 2090-99 (c) SSP5-8.5 for 2000-10 and 2050-59 (d) SSP5-8.5 for 2000-10 and 2090-99. *Top panel* : exposure-response curves (RRs across T°C (with 95% CI)). The dotted vertical line is the minimum mortality temperature which separates between cold (blue) and heat (red). The dashed part of the curve represents the extrapolation beyond the observed maximum temperature (2000-2015). *Mid panel*: distribution of temperature for the past (grey) and future (green) using the ensemble estimates (average impacts across GCMs) for SSP1-2.6. *Bottom panel*: the related distribution of excess mortality, expressed as the fraction of additional deaths (%) attributed to non-optimal temperature. 61

30 **Temperature and excess mortality for past and future periods - All ages.** (a) SSP1-2.6 for 2000-10 and 2050-59 (b) SSP1-2.6 for 2000-10 and 2090-99 (c) SSP5-8.5 for 2000-10 and 2050-59 (d) SSP5-8.5 for 2000-10 and 2090-99. *Top panel* : exposure-response curves (RRs across T°C (with 95% CI)). The dotted vertical line is the minimum mortality temperature which separates between cold (blue) and heat (red). The dashed part of the curve represents the extrapolation beyond the observed maximum temperature (2000-2015). *Mid panel*: distribution of temperature for the past (grey) and future (green) using the ensemble estimates (average impacts across GCMs) for SSP1-2.6. *Bottom panel*: the related distribution of excess mortality, expressed as the fraction of additional deaths (%) attributed to non-optimal temperature. 62

31 **Past (2000-09) and Projected (2010-99) attributable number of deaths for under 15 years old under SSP1-2.6.** ANs for 10 year periods. *Left panels*: in blue the deaths attributed to cold. *Right panels*: in red the deaths attributed to heat. *Note 1*: The 2010-2019 period counts past (2010-15) recorded ANs and projected (2016-19) ANs. *Note 2*: CIs were assumed to always be >0 as non-optimal temperature is always projected to have an effect on mortality. 66

32 **Past (2000-09) and Projected (2010-99) attributable number of deaths for under 15 years old under SSP5-8.5.** ANs for 10 year periods.*Left panels*: in blue the deaths attributed to cold. *Right panels*: in red the deaths attributed to heat. *Note 1*: The 2010-2019 period counts past (2010-15) recorded ANs and projected (2016-19) ANs. *Note 2*: CIs were assumed to always be >0 as non-optimal temperature is always projected to have an effect on mortality. 67

33 **Past (2000-09) and Projected (2010-99) attributable number of deaths between 15-59 years old under SSP1-2.6.** ANs for 10 year periods.*Left panels*: in blue the deaths attributed to cold. *Right panels*: in red the deaths attributed to heat. *Note 1*: The 2010-2019 period counts past (2010-15) recorded ANs and projected (2016-19) ANs. *Note 2*: CIs were assumed to always be >0 as non-optimal temperature is always projected to have an effect on mortality. 68

34 **Past (2000-09) and Projected (2010-99) attributable number of deaths between 15-59 years old under SSP5-8.5.** ANs for 10 year periods.*Left panels*: in blue the deaths attributed to cold. *Right panels*: in red the deaths attributed to heat. *Note 1*: The 2010-2019 period counts past (2010-15) recorded ANs and projected (2016-19) ANs. *Note 2*: CIs were assumed to always be >0 as non-optimal temperature is always projected to have an effect on mortality. 69

35 **Past (2000-09) and Projected (2010-99) attributable number of deaths over 60 years old under SSP1-2.6.** ANs for 10 year periods.*Left panels*: in blue the deaths attributed to cold. *Right panels*: in red the deaths attributed to heat. *Note 1*: The 2010-2019 period counts past (2010-15) recorded ANs and projected (2016-19) ANs. *Note 2*: CIs were assumed to always be >0 as non-optimal temperature is always projected to have an effect on mortality. 70

36 **Past (2000-09) and Projected (2010-99) attributable number of deaths over 60 years old under SSP5-8.5.** ANs for 10 year periods.*Left panels*: in blue the deaths attributed to cold. *Right panels*: in red the deaths attributed to heat. *Note 1*: The 2010-2019 period counts past (2010-15) recorded ANs and projected (2016-19) ANs. *Note 2*: CIs were assumed to always be >0 as non-optimal temperature is always projected to have an effect on mortality. 71

37 **Yearly death counts per age group per cause.** In red: deaths under 15. In green: deaths between 15 and 59. In blue: deaths over 60. 73

38 **Example of no measured temperature-mortality association: deaths of cardiovascular diseases between 15-59 years old.** Left: Three dimensional plot showing the estimate exposure-lag-response association between temperature and mortality. Right: Cumulative mortality risk for all lag (RR and 95% confidence interval). . 75

39 **Calibration between past and projected data for ERA-5 and NOAA data.** 87

40 **The exposure-response curve and associated current and projected temperature distribution and AF.** 87

41 **Graph representing RR with and without adaptation to temperatures.** Here a 30% decrease in the risk associated to heat is assumed. 97

42 **Different SSP scenarios as per described in literature.** Source : Riahi et al. (2017) 123

43 **Representation of how Green house gas emissions are computed into climate profiles**. Source : Lepousez (2022) using IPCC representations and IPSL numeric model 124

44 **Groups created to reclassify mortality by Waltisperger and colleagues.** *Source :*Waltisperger et al. (2005) 125

List of Tables

1 **Average deaths and attributable fractions (AF%) by age group and SSP** 57

2 **Estimated Attributable Numbers of deaths attributed to cold and heat for constant and projected mortality, by age group, and SSP** . 65

3 **Attributable fractions (AF%) by cause of death, age group, and SSP. With the average number of deaths for the decade.** 84

4 **Number of recorded deaths in Antananarivo by Age at death (2000-2015)** 127

5 **Number of recorded deaths in Antananarivo by cause of death and age at death (2000-2015)** 128

Figure appendix

Table 2
Summary of SSP narratives.

SSP1	Sustainability – Taking the Green Road (Low challenges to mitigation and adaptation) *The world shifts gradually, but pervasively, toward a more sustainable path, emphasizing more inclusive development that respects perceived environmental boundaries. Management of the global commons slowly improves, educational and health investments accelerate the demographic transition, and the emphasis on economic growth shifts toward a broader emphasis on human well-being. Driven by an increasing commitment to achieving development goals, inequality is reduced both across and within countries. Consumption is oriented toward low material growth and lower resource and energy intensity.*
SSP2	Middle of the Road (Medium challenges to mitigation and adaptation) *The world follows a path in which social, economic, and technological trends do not shift markedly from historical patterns. Development and income growth proceeds unevenly, with some countries making relatively good progress while others fall short of expectations. Global and national institutions work toward but make slow progress in achieving sustainable development goals. Environmental systems experience degradation, although there are some improvements and overall the intensity of resource and energy use declines. Global population growth is moderate and levels off in the second half of the century. Income inequality persists or improves only slowly and challenges to reducing vulnerability to societal and environmental changes remain.*
SSP3	Regional Rivalry – A Rocky Road (High challenges to mitigation and adaptation) *A resurgent nationalism, concerns about competitiveness and security, and regional conflicts push countries to increasingly focus on domestic or, at most, regional issues. Policies shift over time to become increasingly oriented toward national and regional security issues. Countries focus on achieving energy and food security goals within their own regions at the expense of broader-based development. Investments in education and technological development decline. Economic development is slow, consumption is material-intensive, and inequalities persist or worsen over time. Population growth is low in industrialized and high in developing countries. A low international priority for addressing environmental concerns leads to strong environmental degradation in some regions.*
SSP4	Inequality – A Road Divided (Low challenges to mitigation, high challenges to adaptation) *Highly unequal investments in human capital, combined with increasing disparities in economic opportunity and political power, lead to increasing inequalities and stratification both across and within countries. Over time, a gap widens between an internationally-connected society that contributes to knowledge- and capital-intensive sectors of the global economy, and a fragmented collection of lower-income, poorly educated societies that work in a labor intensive, low-tech economy. Social cohesion degrades and conflict and unrest become increasingly common. Technology development is high in the high-tech economy and sectors. The globally connected energy sector diversifies, with investments in both carbon-intensive fuels like coal and unconventional oil, but also low-carbon energy sources. Environmental policies focus on local issues around middle and high income areas.*
SSP5	Fossil-fueled Development – Taking the Highway (High challenges to mitigation, low challenges to adaptation) *This world places increasing faith in competitive markets, innovation and participatory societies to produce rapid technological progress and development of human capital as the path to sustainable development. Global markets are increasingly integrated. There are also strong investments in health, education, and institutions to enhance human and social capital. At the same time, the push for economic and social development is coupled with the exploitation of abundant fossil fuel resources and the adoption of resource and energy intensive lifestyles around the world. All these factors lead to rapid growth of the global economy, while global population peaks and declines in the 21st century. Local environmental problems like air pollution are successfully managed. There is faith in the ability to effectively manage social and ecological systems, including by geo-engineering if necessary.*

Figure 42: **Different SSP scenarios as per described in literature.**
Source : Riahi et al. (2017)

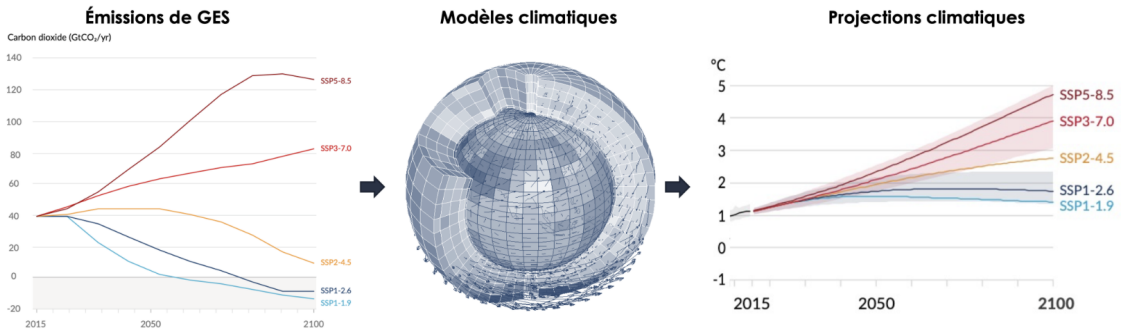


Figure 43: **Representation of how Green house gas emissions are computed into climate profiles**.
Source : Lepousez (2022) using IPCC representations and IPSL numeric model

Groups of causes of death used and correspondence with detailed list of 9th Revision of International Classification of Diseases (ICD9)

Causes of death	Items of detailed ICD9 list
Infectious diseases	
Diarrhoea	009
Other intestinal infections	001 to 008
Tuberculosis	010 to 018
Plague	020
Diphtheria	032
Whooping cough	033
Tetanus	037
Poliomyelitis	045
Measles	055
Viral hepatitis	070
Malaria	084
Other infectious and parasitic diseases	021 to 139 (except 032, 033, 037, 045, 055, 070, 084)
Neoplasms	140 to 239
Nutritional deficiency	260 to 269
Cardiovascular diseases	
Hypertensive diseases	401 to 409
Ischemic heart disease	410 to 414
Heart failure	428
Cerebrovascular diseases	430 to 438
Other diseases of circulatory system	390 to 459 (except 401 to 414, 428, 430 to 438)
Diseases of respiratory system	
Pneumonia, bronchopneumonia, influenza, acute respiratory infections	480 to 487
Other diseases of respiratory system	460 to 519 (except 480 to 487)
Other diseases	
Endocrine diseases and diabetes	240 to 259
Metabolic diseases	270 to 279
Blood diseases	280 to 289
Mental disorders (including alcoholism)	290 to 319
Diseases of nervous system	320 to 379
Diseases of the ear (including otitis)	380 to 389
Diseases of digestive system	520 to 579
Diseases of genito-urinary organs	580 to 629
Pregnancies with abortive outcome	630 to 639
Complications related to pregnancy	640 to 648
Complications related to labour and delivery	650 to 669
Complications of the puerperium	670 to 679
Diseases of the skin and muscles	680 to 739
Disorders relating to short gestation and unspecified low birthweight	765
Hypoxia	768
Tetanus neonatorum	771.3
Congenital anomalies and other perinatal conditions	740 to 779 (except 765,768,771.3)
Injury and accidents	800 to 999
Unknown and ill-defined causes (including senility)	780 to 799

Figure 44: **Groups created to reclassify mortality by Waltisperger and colleagues.**
*Source :*Waltisperger et al. (2005)

Table appendix

Table 4: **Number of recorded deaths in Antananarivo by Age at death (2000-2015)**

Age group	**Number of deaths**
Under 15	19777
Between 15-59	46822
Over 60	36469
All ages	103068

Table 5: **Number of recorded deaths in Antananarivo by cause of death and age at death (2000-2015)**

Age group	**Number of deaths**
Deaths of Infectious diseases	
< 15	3126
15 - 59	5571
> 60	1729
All	10426
Deaths of Cardiovascular diseases	
< 15	499
15 - 59	13523
> 60	15790
All	29812
Deaths of Nutritional deficiencies	
< 15	1892
15 - 59	215
> 60	127
All	9614
Deaths of Respiratory system related diseases	
< 15	3544
15 - 59	3326
> 60	2744
All	9614

Code appendix

0.1 Retrieving data

Code : Retrieving mean temperature from NOAA in R
All the available information on how to extract the data can also be found at :
https://www.rdocumentation.org/packages/rnoaa/versions/0.9.0

```
tmean = ghcnd_search("MA000067083", var = "DD", date_min
    = "1976-01-01", date_max = "2015-12-31") # DD for
    degree days all the necessary
```

0.2 DLNM and Projections - The Vicedo-Cabrera et al. (2019) method

The following code is our adaptation of the Gasparrini method (Gasparrini and Leone, 2014). This is an example of the adapted code which was duplicated many times to suit the needs of our analysis. In this code we show our adaptation of the code using constant mortality, in the case of our model with projections we included the population projections directly.

```
#START ###############################################
# DESCRIPTION OF THE METHOD AND AUTHOR RIGHTS:

#######################################################
# Requirements:
#  - R version 3.5.1
```

```
#  - 'dlnm' package version 2.3.5
#  - 'splines' package version  3.5.1
#  - 'MASS' package version 7.3-50
#

# HERE WE HAVE USED THE GASPARRINI METHOD AND HAVE ADAPTED IT FOR THE NEEDS OF
    THE ANALYSIS (BASED ON SECTION 7 : ADAPTATION AND POPULATION CHANGES)

#THE FOLLOWING DATABASES HAVE BEEN CREATED BASED ON THE INITIAL EXTRACT
    DATABASE.

# LOAD THE DATABASES AND PACKAGES

rm(list=ls(all=TRUE))
library(dlnm) ; library(splines) ; library(MASS) ; library(tsModel)
setwd("/Users/EmmaKuijt/Desktop/M moire")

load("~/Desktop/M moire/by_age_4GASP.Rda")
load("~/Desktop/M moire/infect_by_age_4GASP.Rda")
load("~/Desktop/M moire/cardio_dis_by_age_4GASP.Rda")
load("~/Desktop/M moire/resp_sys_by_age_4GASP.Rda")
load("~/Desktop/M moire/Nut_dis_by_age_4GASP.Rda")


#01ESTIMATION OF THE EXPOSURE-RESPONSE ASSOCIATIONS##############################

#For each of our sensitivity tests we ran the model for all causes and
    different sub-causes:

#DEFINING THE OBSERVATION
  obs = by_age_4GASP
  #obs = infect_by_age_4GASP
  #obs = cardio_dis_by_age_4GASP
  #obs = resp_sys_by_age_4GASP
  #obs = Nut_dis_by_age_4GASP

#DEFINING OBSERVATION DATE RANGE
  obs = obs[obs$date <= '2015-12-31',]
  obs = obs[obs$date >= '2000-01-01',]

#Finding out the number of observations for each age group
  sum(obs$all_u_15)
  sum(obs$all_15_59)
  sum(obs$all_060)
  sum(obs$all_all)

  #
  # #|Age_Group | ALL Deaths|
  #    #|:----------|-------:|
  #    #|Under 15   |   19777|
  #    #|15-59      |   46822|
  #    #|60+        |   36469|
  #    #|All        |  103068|
```

```
# #|Age_Group | Deaths INFECT DIS
#   #|:---------|------:|
#   #|Under 15  |   3126|
#   #|15-59     |   5571|
#   #|60+       |   1729|
#   #|All       |  10426|

# #|Age_Group | Deaths CARDIO DIS
#   #|:---------|------:|
#   #|Under 15  |    499|
#   #|15-59     |  13523|
#   #|60+       |  15790|
#   #|All       |  29812|

# #|Age_Group | Deaths RESP DIS
#   #|:---------|------:|
#   #|Under 15  |   3544|
#   #|15-59     |   3326|
#   #|60+       |   2744|
#   #|All       |   9614|

# #|Age_Group | Deaths NUT DIS
#   #|:---------|------:|
#   #|Under 15  |   1892|
#   #|15-59     |    215|
#   #|60+       |    127|
#   #|All       |   2234|


# DEFINITION OF THE CROSS-BASIS FOR TEMPERATURE
# - SPECIFICATION PARAMETERS OF THE EXPOSURE-RESPONSE DIMENSION OF THE
    CROSS-BASIS

# argvar: main model, cubic natural spline with three internal knots in the
    10th, 75th, 90th percentiles of the temperature distribution

argvar <- list(fun="ns", knots = quantile(obs$t2m_mean,c(10,75,90)/100,
    na.rm=T),
                Bound=range(obs$t2m_mean,na.rm=T))
maxlag <- 21
arglag <- list(fun="ns",knots=logknots(maxlag,nk=3))

cb <-crossbasis(obs$t2m_mean,maxlag,argvar,arglag)

# FIT THE MODEL
# Apply the same model defined in the script 01 to the age-specific counts:

m <- glm(all_all ~ cb + dow + ns(date,df=round(8*length(date)/365.25)),
         data=obs, family=quasipoisson)
m_U_15 <- glm(all_u_15 ~ cb + dow + ns(date,df=round(8*length(date)/365.25)),
              data=obs, family=quasipoisson)
m_15_59 <- glm(all_15_59 ~ cb + dow +
```

```
    ns(date,df=round(8*length(date)/365.25)),
                data=obs, family=quasipoisson)
m_O_60 <- glm(all_060 ~ cb + dow + ns(date,df=round(8*length(date)/365.25)),
                data=obs, family=quasipoisson)

# GET PREDICTIONS & PLOT
# - DEFINE PROVVISIONAL CENTERING POINT TO HAVE THE INITIAL PREDICTION
varcen <- 19

# - ESTIMATE MMT FROM THE PREDICTED EXPOSURE-RESPONSE ASSOCIATION
#     FOR EACH AGE CATEGORY

cp <- crosspred(cb, m, cen=varcen, by=0.1)
cen <- cp$predvar[which.min(cp$allRRfit)]

cpU_15 <- crosspred(cb,m_U_15,cen=varcen,by=0.1)
cenU_15 <- cpU_15$predvar[which.min(cpU_15$allRRfit)]

cp15_59 <- crosspred(cb,m_15_59,cen=varcen,by=0.1)
cen15_59 <- cp15_59$predvar[which.min(cp15_59$allRRfit)]

cpO_60 <- crosspred(cb,m_O_60,cen=varcen,by=0.1)
cenO_60 <- cpO_60$predvar[which.min(cpO_60$allRRfit)]

# - RE-CENTER & GET PREDICTIONS FOR EACH MODEL CENTERING ON THE MMT
pred <- crosspred(cb, m, cen=cen, by=1)

predU_15 <- crosspred(cb, m_U_15, cen=cenU_15, by=1)
pred15_59 <- crosspred(cb, m_15_59, cen=cen15_59, by=1)
predO_60 <- crosspred(cb, m_O_60, cen=cenO_60, by=1)

#GRAPHS (REPLICATED FOR ALL DEATHS AND EACH AGE GROUP)

#GRAPH - UNDER 15

xlab <- expression(paste("Temperature (",degree,"C)"))

#pdf("Figure 1.pdf",height=4.5,width=10)
layout(matrix(c(1,2),ncol=2,byrow=T))

# PLOT - 3D
par(mar=c(2,3,3,1),mgp=c(3,1,0),las=1,cex.axis=0.9,cex.lab=1)
plot(predU_15,"3d",ltheta=150,xlab="Temperature (C)",ylab="Lag",zlab="RR",
     col=gray(0.9), main="Exposure-lag-response - U15")

# OVERALL
# The plots show the cumulative exposure-response association, in terms of
#    relative risks (RR) and centered in the MMT, across the 21 days of lag.
par(mar=c(5,4,3,1),mgp=c(3,1,0),las=1,cex.axis=0.9,cex.lab=1)
plot(predU_15,"overall",col="red",ylim=c(0.5,2.5),axes=T,lab=c(6,5,7),xlab=xlab,
     ylab="RR",main="Overall - Under 15 ")

layout(1)
```

```
  #dev.off()


#02 PROJECTED EXPOSURE AND HEALTH OUTCOME SERIES##########


# PROJECTED TEMPERATURE SERIES###################

# LOAD MODELLED TEMPERATURE DATA (1981-2099)
# Climate data was obtained, processed and made available by
#    the Inter-Sectoral Impact Model Intercomparison Project
#    (ISI-MIP, https://www.isimip.org/).
# It includes daily temperature series for 5 different GCMs and
#    2 (RCP2.6 and RCP8.5) climate change scenarios,
#    for the historical (1981-2015) and future periods (2016-2100).

# - ssp126 SCENARIO
load("~/Desktop/M moire/R_MEMOIRE/BM_29_09/ssp126.rda")
ssp126 = ssp126[ssp126$date <= '2099-12-31',]

# - ssp585 SCENARIO
load("~/Desktop/M moire/R_MEMOIRE/BM_29_09/ssp585.rda")
ssp585 = ssp585[ssp585$date <= '2099-12-31',]

# PLOT - FIGURE 2 TEMPERATURE TRENDS
#  The plot shows the temporal trends annual temperature averaged across
#     the 5 GCMs for each scenario (solid line), expressed as increase in
#     annual mean temperature from the historical average temperature.
#  It also shows the variability in the projected temperature across GCMs
#     (shade area).


# - COMPUTE ANNUAL AVERAGES (CENTERED)
tsyear <- as.numeric(format(ssp126$date,format="%Y"))
year <- unique(tsyear)
ssp126avg <- apply(ssp126[,-c(1,2)],2,tapply,tsyear,mean)
ssp585avg <- apply(ssp585[,-c(1,2)],2,tapply,tsyear,mean)

# - COMPUTE THE DIFFERENCE IN TEMPERATURE FROM THE HISTORICAL AVERAGE
ssp126avg <- ssp126avg-mean(ssp126avg[year%in%1981:2014,])
ssp585avg <- ssp585avg-mean(ssp585avg[year%in%1981:2014,])

ylab <- expression(paste("Temperature increase (",degree,"C)"))

col1 <- do.call(rgb,c(as.list(col2rgb("blue")),alpha=255/6,max=255))
col2 <- do.call(rgb,c(as.list(col2rgb("red")),alpha=255/6,max=255))

#pdf("Figure 2.pdf",height=5,width=5)
par(mar=c(5,4,3,1),mgp=c(2,0.8,0),las=1,cex.axis=0.8,cex.lab=1)
plot(year,rowMeans(ssp585avg),type="n",bty="l",ylab=ylab,xlab="Year",
     ylim=c(-1,8),xlim=c(1970,2110),main="")
abline(h=0)
lines(year[year<2015],rowMeans(cbind(ssp126avg,ssp126avg)[year<2015,]),lwd=1.5)
```

```
polygon(c(year[year>=2015],rev(year[year>=2015])),
        c(apply(ssp126avg,1,max)[year>=2015],rev(apply(ssp126avg,1,min)
        [year>=2015])),col=col1,border=NA)
polygon(c(year[year>=2015],rev(year[year>=2015])),
        c(apply(ssp585avg,1,max)[year>=2015],rev(apply(ssp585avg,1,min)
        [year>=2015])),col=col2,border=NA)
lines(year[year>=2015],rowMeans(ssp126avg[year>=2015,]),lwd=1.5,col=4)
lines(year[year>=2015],rowMeans(ssp585avg[year>=2015,]),lwd=1.5,col=2)
abline(v=2015,lty=3)
rect(2103-1,mean(apply(ssp126avg,1,min)[as.character(2090:2099)]),2103+1,
     mean(apply(ssp126avg,1,max)[as.character(2090:2099)]),col=4,border=NA)
rect(2106-1,mean(apply(ssp585avg,1,min)[as.character(2090:2099)]),2106+1,
     mean(apply(ssp585avg,1,max)[as.character(2090:2099)]),col=2,border=NA)
legend("top",c("Historical","ssp126","ssp585"),lwd=1.5,col=c(1,4,2),
cex=0.8,bty="n",inset=0.05)
#dev.off()



# PROJECTED MORTALITY SERIES##############################################

# DEFINE PROJECTED MORTALITY SERIES
# It is computed as the average mortality for each day of the year
#   from daily observed deaths, then repeated along the same projection period
#   of the modelled temperature series.

ssp585 = ssp585[ssp585$date >= '2000-01-01',]
ssp126 = ssp126[ssp126$date >= '2000-01-01',]


#The following step has been replicated for each age group
#   UNDER 15 ###########################################

# MODEL WITH CONSTANT MORTALITY
deathdoy_U15 <- tapply(obs$all_u_15,as.numeric
(format(obs$date,"%j")),mean,na.rm=T)[seq(365)]

while(any(isna <- is.na(deathdoy_U15)))
deathdoy_U15[isna] <- rowMeans(Lag(deathdoy_U15,c(-1,1)),na.rm=T)[isna]
deathproj_U15 <- rep(deathdoy_U15,length=nrow(ssp585))

#MODEL WITH PROJECTED MORTALITY
#load the projected deaths vector
deathdoy_U15 <- readRDS("~/Desktop/M moire/deathdoy_U15.rds")

#make vector length <=> lenght of ssp data
deathproj_U15 <- rep(deathdoy_U15,length=nrow(ssp585))


# PLOT - FIGURE 3 SEASONAL MORTALITY TRENDS
# The plot depicts the seasonal trends in daily mortality in Antananarivo
#    The grey dots are the actual number of deaths in each day of the year
#    between 2000-2015 and the blue line is the average daily mortality
```

```
#    per day of the year, which is projected along the projection period.

#pdf("Figure 3.pdf",height=5,width=6)
par(mar=c(5,4,3,1),mgp=c(2.5,1,0),las=1,cex.axis=0.8,cex.lab=1)
plot(all_u_15 ~ doy,obs,pch=19,col=grey(0.8),cex=0.5,ylab="Daily deaths (Under
    15)",xlab="Day of the year",
     main="")
lines(1:366,tapply(obs$all_u_15,obs$doy,mean),lwd=1.5,col=4)
#dev.off()


#03 BIAS-CORRECTION#################################

# LOAD BIAS CORRECTION FUNCTION
# This is a function created to apply the bias-correction method developed
#    within ISI-MIP (Hempel et al. 2013). More details on the calibration
#    procedure are described in the "fhempel.R" code.

fhempel <- function(obs ,mod, add=TRUE, mult=TRUE, output="series") {
  #
  # CHECK THE OUTPUT
  output <- match.arg(output,c("series","correction"))
  #
  # CHECK CONSISTENCY
  if(ncol(obs)!=2) stop("obs must have two variables (date and series")
  if(ncol(mod)<2) stop("mod must have at least two variables (date and series")
  if(!any(class(obs[[1]])%in%"Date") | !any(class(mod[[1]])%in%"Date"))
    stop("Class of first variable of 'obs' and 'mod' must be 'Date'")
  #
  # APPLY TO EACH MODELLED SERIES
  out <- lapply(seq(ncol(mod)-1),function(j) {
    #
    # IDENTIFY PERIOD WITH NO MISSING
    ind <- obs[[1]][obs[[1]] %in% mod[[1]]]
    notna <- complete.cases(obs[obs[[1]]%in%ind,2],mod[mod[[1]]%in%ind,j+1])
    indobs <- seq(nrow(obs))[obs[[1]]%in%ind][notna]
    indmod <- seq(nrow(mod))[mod[[1]]%in%ind][notna]
    if(length(indobs)==0) stop("no common non-missing days in 'obs' and 'mod'")
    #
    # EXTRACT MONTH AND YEAR
    month <- as.numeric(format(obs[[1]][indobs],format="%m"))
    if(length(unique(month))!=12)
      stop("some months are not reprensented in the overlapping period")
    year <- as.numeric(format(obs[[1]][indobs],format="%Y"))
    monthyear <- factor(paste(year,month,sep="-"))
    #
    # COMPUTE ADDITIVE CORRECTION
    mavgobs <- tapply(obs[[2]][indobs],month,mean,na.rm=T)
    mavgmod <- tapply(mod[[j+1]][indmod],month,mean,na.rm=T)
    C <- mavgobs - mavgmod
    if(!add) C[] <- 0
    #
    # RESIDUALS FROM MONTHLY/YEAR AVERAGES, THEN MULTIPLICATIVE CORRECTION
```

```
    myavgobs <- tapply(obs[[2]][indobs], monthyear, mean, na.rm=T)
    myavgmod <- tapply(mod[[j+1]][indmod], monthyear, mean, na.rm=T)
    resobs <- obs[[2]][indobs] - myavgobs[monthyear]
    resmod <- mod[[j+1]][indmod] - myavgmod[monthyear]
    B <- sapply(seq(12),
                function(m)
                  coef(lm(sort(resobs[month==m])~0+sort(resmod[month==m]))))
    if(!mult) B[] <- 1
    #
    # RETURN CORRECTION IF STATED
    if(output=="correction") return(matrix(c(C,B),ncol=2,
dimnames=list(unique(months(mod[,1],abbr=TRUE)),
c("add","mult"))))
    #
    # OBTAIN DAY, MONTH AND YEAR FROM DATE (ORIGINAL SERIES)
    day <- as.numeric(format(mod[[1]],format="%d"))
    month <- as.numeric(format(mod[[1]],format="%m"))
    year <- as.numeric(format(mod[[1]],format="%Y"))
    monthyear <- factor(paste(year,month,sep="-"))
    #
    # DERIVE THE QUANTITIES TO REMOVE DISCONTINUITIES FROM CORRECTION
    # (SEE Hempel et al, PAGE 228)
    nday <- tapply(mod[[j+1]],monthyear,length)
    d <- (day-1)/(nday[monthyear]-1)-0.5
    dm <- 0.5*(abs(d)-d)
    d0 <- 1-abs(d)
    dp <- 0.5*(abs(d)+d)
    #
    # DERIVE THE CORRECTIONS ACCOUNTING FOR DISCONTINUITIES
    Cm <- C[c(12,1:11)] ; Bm <- B[c(12,1:11)]
    Cp <- C[c(2:12,1)] ; Bp <- B[c(2:12,1)]
    C <- dm*Cm[month] + d0*C[month] + dp*Cp[month]
    B <- dm*Bm[month] + d0*B[month] + dp*Bp[month]
    #
    # DERIVE THE CORRECTED SERIES
    myavgout <- tapply(mod[[j+1]],monthyear,mean,na.rm=T)
    resout <- mod[[j+1]] - myavgout[monthyear]
    #
    # RETURN CORRECTED SERIES IF STATED
    return(myavgout[monthyear]+C+resout*B)
  })
  #
  # RETURN CORRECTION IF STATED
  if(output=="correction") {

    names(out) <- names(mod)[-1]
    return(out)
  }
  #
  # ADD DATE AND RENAME
  out <- cbind(mod[,1],as.data.frame(do.call(cbind,out)))
  dimnames(out) <- dimnames(mod)
  #
```

```
  # RETURN
  return(out)
}

# RE-CALIBRATE USING THE BIAS CORRECTION FUNCTION
ssp126cal <- fhempel(obs[c("date","t2m_mean")],ssp126)
ssp585cal <- fhempel(obs[c("date","t2m_mean")],ssp585)


# PLOT - FIGURE 4 CALIBRATION
# The two plots compared the distribution between the observed and the modeled
#     temperature obtained using one specific GCM, before and after applying the
#     calibration. HERE WE ARE USING MRI as it best fitted the past data.

#pdf("Figure 4.pdf",height=5,width=9)
layout(matrix(c(1,2),ncol=2,byrow=T))
par(mar=c(5,4,3,1),mgp=c(3,1,0),las=1,cex.axis=0.8,cex.lab=1)
rgbcol <- col2rgb(c(grey(0.8),"lightgreen"))
col <- apply(rgbcol,2,
             function(x) do.call(rgb,c(as.list(x),alpha=255/2,max=255)))
ind <- ssp126$date %in% obs$date
dobs <- density(obs$t2m_mean,na.rm=T)
dmod <- density(ssp126[ind,5],na.rm=T)
plot(c(obs$t2m_mean,ssp126[ind,5]),c(obs$t2m_mean,ssp126[ind,5]),type="n",bty="l",
     main="GCM: MRI",ylim=c(0,0.25),ylab="Distribution",
     xlab=expression(paste("Temperature (",degree,"C)")))
polygon(dobs,col=col[1],lty=4)
polygon(dmod,col=col[2],lty=5)
legend("topleft",c("Observed","GCM"),pch=22,pt.bg=col, cex=0.9,bty="n",
       inset=0.05)
abline(h=0)


par(mar=c(5,4,3,1),mgp=c(3,1,0),las=1,cex.axis=0.8,cex.lab=1)
ind <- ssp126$date %in% obs$date
x <- pretty(c(obs$t2m_mean,ssp126[,5]),n=100)
plot(x,ecdf(obs$t2m_mean)(x),col=1,main="",type="l",lwd=2,
     ylab="Cumulative distribution",
     xlab=expression(paste("Temperature (",degree,"C)")))
lines(x,ecdf(ssp126[ind,5])(x),col=3,lwd=2)
lines(x,ecdf(ssp126cal[ind,5])(x),col=3,lwd=2,lty=4)
legend("topleft",c("Observed","GCM","GCM calibrated"),lwd=2,lty=c(1,1,4),
       col=c(1,3,3), cex=0.9,bty="n",inset=0.05)

layout(1)
#dev.off()

# NB: run pdf() and dev.off() for saving the plot in pdf format.


# REPLACE THE ORIGINAL SERIES WITH THE RECALIBRATED
ssp126 <- ssp126cal
ssp585 <- ssp585cal
```

```
#04 05 AND 06 ########################################
# 04 EXTRAPOLATION OF THE EXPOSURE-RESPONSE CURVE
# 05 PROJECTION & QUANTIFICATION OF THE IMPACT
# 06 ENSEMBLE ESTIMATES & QUANTIFICATION OF THE UNCERTAINTY

# The three last steps of the analysis (extrapolation of the curve,
#   impact projections and quantification of the uncertainty) can be performed
#   sequentially using the following code.

# In brief, once we extrapolate the curve, we estimate the daily number of
    attributable
#   deaths (AN) in each scenario, GCM and temperature range.
# Then, we compute the sum of ANs per each 10-years period for the ensemble
#   per each RCP and temperature range. We also estimate the difference in AN
#   relative to the ANs estimated for the current days (2000-2010).
# By dividing between the total mortality, we estimate the corresponding
#   attributable fractions (AFs).
# Uncertainty of the estimated impacts is expressed in terms of empirical
#   confidence intervals, defined as the 2.5th and 97.5th percentiles of the
#   empirical distribution of the impacts across coefficients samples and GCMs.
#   The distribution is obtained through Monte Carlo simulation of the
    coefficients.


# EXTRACT COEFFICIENTS AND VCOV FROM THE MODEL IN STAGE 1
# With the crossreduce function we can reduce the fit of the bidimensional DLNM
#   (of the stage 1 using the observed temperature-mortality series)
#   to summaries defined in the exposure-response dimension. We can then
#   extract the coefficients and the covariance matrix defining the overall
#   exposure-response association.

# THE FOLLOWING CODE WAS REPLICATED FOR ALL AGE GROUPS SEQUENTIALLY. FOR FUTURE
    REFERENCE MAKE SURE TO MODIFY ALL THE NECESSARY COMPONENTS SUCH AS RIGHT
    CEN, DEATHDOY VECTOR ETC...

#   UNDER 15 ###################################
#       BASE ###################################
red <- crossreduce(cb,m_U_15,cen=cenU_15)
coef <- coef(red)
vcov <- vcov(red)

# STORE THE MORTALITY BY PERIOD
deathperiod <- sum(deathdoy_U15)*10

# CREATE TEMPORARY OBJECT TO STORE THE ESTIMATED AN
# We create an array with 6 dimensions to store the AN estimated in each
#   simulation for each period, range of temperature, gcm and rcp. An additional
#   dimension is also included to store the absolute AN (estimated directly from
#   the formula below), and the difference in AN relative to current period.

# - DEFINE THE NAMES AND NUMBER OF LEVELS PER DIMENSION (ALSO USED TO DEFINE
```

```
#      THE INDEX TO RUN THE LOOPS BELOW)

# (1) DIMENSION - 10-YEAR PERIOD
#  *LABEL THE HISTORICAL PERIOD
histperiod <- "2000-2009"

#  *LABELS THE PROJECTION PERIODS
projperiod <- paste(201:209,0,"-",substr(201:209,3,3),9,sep="")

#  *DEFINE SEQUENCE OF PERIODS FOR THE PREDICTIONS (HISTORICAL & PROJECTED)
histseqperiod <- factor(rep(histperiod,length.out=trunc
                            (365.25*length(seq(2000,2009)))))
projseqperiod <- factor(
  paste(trunc(as.numeric(format
                          (ssp126$date[ssp126$date >= as.Date("2010-01-01")]
                            , "%Y"))/10)*10,
        trunc(as.numeric
              (format(ssp126$date[ssp126$date >= as.Date("2010-01-01")]
                      , "%Y"))/10)*10+9, sep = '-')
)
seqperiod <- factor(c(as.numeric(histseqperiod)-1,as.numeric(projseqperiod)))
seqperiod <- factor(c(seqperiod, tail(seqperiod, 1)))
levels(seqperiod) <- c(histperiod,projperiod)

# (2) DIMENSION - RANGE OF TEMPERATURES
temprange <- c("tot","cold","heat")

# (3) DIMENSION - ABSOLUTE AN/DIFFERENCE IN AN
absrel <- c("abs","rel")

# (4) DIMENSION - GENERAL CIRCULATION MODELS
# *LIST OF GCMs
gcm <- c("GFDL-ESM4"="tmean_gfdl","IPSL-CM6A-LR"="tmean_ipsl",
         "MRI-ESM2-0"="tmean_mri","MPI-ESM1-2-HR"="tmean_mpi",
         "UKESM1-0-LL"="tmean_ukesm")

# (5) DIMENSION - SCENARIO DIMENSION
#  *LIST OF REPRESENTATIVE CONCENTRATION PATHWAYS SCENARIOS
rcp <- c(SSP1_RCP2.6="ssp126",SSP5_RCP8.5="ssp585")

# (6) DIMENSION - NUMBER OF ITERATION IN THE MONTE-CARLO SIMULATION
nsim <- 1000


# DEFINE THE ARRAY
ansim <- array(NA,dim=c(length(levels(seqperiod)),length(temprange),
    length(absrel),length(gcm),length(rcp),nsim+1),
    dimnames=list(levels(seqperiod),temprange,absrel,
    names(gcm),names(rcp), c("est",paste0("sim",seq(nsim)))))


# RUN LOOP PER RCP
for (i in seq(rcp)) {
```

```
# PRINT
cat("\n\n",names(rcp)[i],"\n")

# SELECTION OF THE PROJECTED TEMPERATURE SERIES FOR A SPECIFIC RCP SCENARIO
tmeanproj <- get(rcp[[i]])

# RUN LOOP PER GCM
for(j in seq(gcm)) {

  # PRINT
  cat(gcm[j],"")

  # (4) EXTRAPOLATION OF THE CURVE:
  # - DERIVE THE CENTERED BASIS USING THE PROJECTED TEMPERATURE SERIES
  #   AND EXTRACT PARAMETERS
  bvar <- do.call(onebasis,c(list(x=tmeanproj[,j+2]),argvar))
  cenvec <- do.call(onebasis,c(list(x=cenU_15),argvar))
  bvarcen <- scale(bvar,center=cenvec,scale=F)

  # INDICATOR FOR COLD/HEAT DAYS
  indheat <- tmeanproj[,j+2]>cenU_15

  # (5) IMPACT PROJECTIONS:
  # - COMPUTE THE DAILY CONTRIBUTIONS OF ATTRIBUTABLE DEATHS
  an <- (1-exp(-bvarcen%*%coef))*deathproj_U15

  # - SUM AN (ABS) BY TEMPERATURE RANGE AND PERIOD, STORE IN ARRAY BEFORE THE
      ITERATIONS
  # NB: ACCOUNT FOR NO TEMPERATURE BELOW/ABOVE CEN FOR GIVEN PERIODS
  ansim[,"tot","abs",j,i,1] <- tapply(an,seqperiod,sum)
  ansim[,"cold","abs",j,i,1] <- tapply(an[!indheat],
                                       factor(seqperiod[!indheat]),sum)
  ansim[,"heat","abs",j,i,1] <- tapply(an[indheat],
                                       factor(seqperiod[indheat]),sum)

  # (6) ESTIMATE UNCERTAINTY OF THE PROJECTED AN:
  # - SAMPLE COEF ASSUMING A MULTIVARIATE NORMAL DISTRIBUTION
  set.seed(13041975+j)
  coefsim <- mvrnorm(nsim,coef,vcov)

  # - LOOP ACROSS ITERATIONS
  for(s in seq(nsim)) {

    # COMPUTE THE DAILY CONTRIBUTIONS OF ATTRIBUTABLE DEATHS
    an <- (1-exp(-bvarcen%*%coefsim[s,]))*deathproj_U15

    # STORE THE ATTRIBUTABLE MORTALITY
    ansim[,"tot","abs",j,i,s+1] <- tapply(an,seqperiod,sum)
    ansim[,"cold","abs",j,i,s+1] <-
      tapply(an[!indheat],factor(seqperiod[!indheat]),sum)
    ansim[,"heat","abs",j,i,s+1] <-
      tapply(an[indheat],factor(seqperiod[indheat]),sum)
```

```
    }
  }
}

# ESTIMATE AN IN EACH PERIOD RELATIVE TO CURRENT DAYS (2010-19)

ansim[,,"rel",,,] <- ansim[,,"abs",,,] - ansim[rep("2000-2009",
                                  length(levels(seqperiod))),,"abs",,,]

#       SUMMARIZE THE RESULTS ###################################################

# COMPUTE AN/AF (95%CI) IN THE ENSEMBLE, BY RANGE & PERIOD & RCP

# CREATE NEW OBJECTS TO STORE RESULTS
# We now create 4 new arrays (2 arrays to store the abs and rel AN, and another
    2
#   to store the estimated rel and abs AF) with 4 dimensions each to store the
#   ensemble estimates (average impacts across GCMs) with the empirical
#   95% confidence intervals.
# In this case, the 4 dimensions correspond to the 10-year period, the point
    estimate
#   and the CI, the temperature range and the scenario.

estci <- c("est","ci.l","ci.u")

anabs <- afabs <- anrel <- afrel <- array(NA,dim=c(length(levels(seqperiod)),
                  length(estci),length(temprange),length(rcp)),
                  dimnames=list(levels(seqperiod),estci,temprange,names(rcp)))


# ATTRIBUTABLE NUMBERS
# ABSOLUTE
anabs[,"est",,"SSP1_RCP2.6"] <- apply(ansim[,,"abs",,"SSP1_RCP2.6",1],1:2,mean)
anabs[,"ci.l",,"SSP1_RCP2.6"] <- apply(ansim[,,"abs",,"SSP1_RCP2.6",-1]
                                       ,1:2,quantile,0.025)
anabs[,"ci.u",,"SSP1_RCP2.6"] <- apply(ansim[,,"abs",,"SSP1_RCP2.6",-1]
                                       ,1:2,quantile,0.975)

anabs[,"est",,"SSP5_RCP8.5"] <- apply(ansim[,,"abs",,"SSP5_RCP8.5",1],1:2,mean)
anabs[,"ci.l",,"SSP5_RCP8.5"] <- apply(ansim[,,"abs",,"SSP5_RCP8.5",-1]
                                       ,1:2,quantile,0.025)
anabs[,"ci.u",,"SSP5_RCP8.5"] <- apply(ansim[,,"abs",,"SSP5_RCP8.5",-1]
                                       ,1:2,quantile,0.975)

# RELATIVE
anrel[,"est",,"SSP1_RCP2.6"] <- apply(ansim[,,"rel",,"SSP1_RCP2.6",1],1:2,mean)
anrel[,"ci.l",,"SSP1_RCP2.6"] <- apply(ansim[,,"rel",,"SSP1_RCP2.6",-1]
                                       ,1:2,quantile,0.025)
anrel[,"ci.u",,"SSP1_RCP2.6"] <- apply(ansim[,,"rel",,"SSP1_RCP2.6",-1]
                                       ,1:2,quantile,0.975)

anrel[,"est",,"SSP5_RCP8.5"] <- apply(ansim[,,"rel",,"SSP5_RCP8.5",1],1:2,mean)
```

```
anrel[,"ci.l",,"SSP5_RCP8.5"] <- apply(ansim[,,"rel",,"SSP5_RCP8.5",-1]
                                       ,1:2,quantile,0.025)
anrel[,"ci.u",,"SSP5_RCP8.5"] <- apply(ansim[,,"rel",,"SSP5_RCP8.5",-1]
                                       ,1:2,quantile,0.975)

# ATTRIBUTABLE FRACTION
afabs[,,,] <- anabs[,,,]/deathperiod*100
afrel[,,,] <- anrel[,,,]/deathperiod*100

# REMOVE ansim
rm(ansim)


#       PLOTTING ANS ###################################################################
library(ggplot2)
library(reshape2)
library(gridExtra)

#                  SSP1_RCP2.6 ###################################################
# Extract data for SSP1_RCP2.6
ssp1_cold <- anabs[, ,"cold", "SSP1_RCP2.6"]
ssp1_heat <- anabs[, ,"heat", "SSP1_RCP2.6"]
ssp1_tot <- anabs[, ,"tot", "SSP1_RCP2.6"]

# Convert the rownames to a new column "Period"
ssp1_cold_df <- data.frame(Period = rownames(ssp1_cold), ssp1_cold)
ssp1_heat_df <- data.frame(Period = rownames(ssp1_heat), ssp1_heat)
ssp1_tot_df <- data.frame(Period = rownames(ssp1_tot), ssp1_tot)

ssp1_cold_df$ci.l <- 0
ssp1_heat_df$ci.l <- 0
ssp1_tot_df$ci.l <- 0

# Determine the common y-axis limits
y_limits <- range(c(ssp1_cold_df$est, ssp1_heat_df$est,
                    ssp1_cold_df$ci.l, ssp1_cold_df$ci.u,
                    ssp1_heat_df$ci.l, ssp1_heat_df$ci.u))

# Plot for cold
cold <- ggplot(ssp1_cold_df, aes(x = Period, y = est, group = 1)) +
  geom_line() +
  geom_ribbon(aes(ymin = ci.l, ymax = ci.u), fill = "lightblue", alpha = 0.3) +
  labs(title = "Cold: Estimated AN with Confidence Interval",
       x = "Period",
       y = "Estimated AN") +
  theme_minimal() +
  theme(axis.text.x = element_text(angle = 90, hjust = 1),
        plot.title = element_text(size = 7)) +
  ylim(y_limits)

# Plot for heat
heat <- ggplot(ssp1_heat_df, aes(x = Period, y = est, group = 1)) +
  geom_line() +
```

```
  geom_ribbon(aes(ymin = ci.l, ymax = ci.u), fill = "red", alpha = 0.3) +
  labs(title = "Heat: Estimated AN with Confidence Interval - SSP1_RCP2.6",
       x = "Period",
       y = NULL)+
  theme_minimal()+
  theme(axis.text.x = element_text(angle = 90, hjust = 1),
        plot.title = element_text(size = 7)) +
  ylim(y_limits)

# Arrange plots side by side
plot <- grid.arrange(cold, heat, ncol = 2)

ggsave("SSP1_AN+CI_U15.png", plot, width = 10, height = 5)

#                  SSP5_RCP8.5 ##################################################
# Extract data for SSP5_RCP8.5
ssp5_cold <- anabs[, ,"cold", "SSP5_RCP8.5"]
ssp5_heat <- anabs[, ,"heat", "SSP5_RCP8.5"]
ssp5_tot <- anabs[, ,"tot", "SSP5_RCP8.5"]

# Convert the rownames to a new column "Period"
ssp5_cold_df <- data.frame(Period = rownames(ssp5_cold), ssp5_cold)
ssp5_heat_df <- data.frame(Period = rownames(ssp5_heat), ssp5_heat)
ssp5_tot_df <- data.frame(Period = rownames(ssp5_tot), ssp5_tot)

ssp5_cold_df$ci.l <- 0
ssp5_heat_df$ci.l <- 0
ssp5_tot_df$ci.l <- 0

# Determine the common y-axis limits
y_limits <- range(c(ssp5_cold_df$est, ssp5_heat_df$est,
                    ssp5_cold_df$ci.l, ssp5_cold_df$ci.u,
                    ssp5_heat_df$ci.l, ssp5_heat_df$ci.u))

# Plot for cold
cold <- ggplot(ssp5_cold_df, aes(x = Period, y = est, group = 1)) +
  geom_line() +
  geom_ribbon(aes(ymin = ci.l, ymax = ci.u), fill = "lightblue", alpha = 0.3) +
  labs(title = "Cold: Estimated AN with Confidence Interval",
       x = "Period",
       y = "Estimated AN") +
  theme_minimal() +
  theme(axis.text.x = element_text(angle = 90, hjust = 1),
        plot.title = element_text(size = 7)) +
  ylim(y_limits)

# Plot for heat
heat <- ggplot(ssp5_heat_df, aes(x = Period, y = est, group = 1)) +
  geom_line() +
  geom_ribbon(aes(ymin = ci.l, ymax = ci.u), fill = "red", alpha = 0.3) +
  labs(title = "Heat: Estimated AN with Confidence Interval - SSP5_RCP8.5",
       x = "Period",
       y = NULL)+
```

```
  theme_minimal()+
  theme(axis.text.x = element_text(angle = 90, hjust = 1),
        plot.title = element_text(size = 7)) +
  ylim(y_limits)

# Arrange plots side by side
plot <- grid.arrange(cold, heat, ncol = 2)

ggsave("SSP5_AN+CI_U15.png", plot, width = 10, height = 5)


#THE FOLLOWING FIGURE WAS REPLICATED FOR SSP126 AND SSP585 FOR THE 2050-59 AND
    2090-99 HORIZON

#EXAMPLE :
#       FIGURE 5 - 2010 - 2090 SSP585############
# To obtain Figure 5 of the manuscript, we restrict the projections to one
#    RCP, one GCM (MRI-ESM2-0) and two periods ("2010-19","2050-59/2090-99").

# RESTRICT MODELLED TEMP TO 2010 AND 2050/2090, MRI-ESM2-0
tmean2010 <- ssp585cal[substr(ssp585cal$date,1,3)%in%"201",5]
tmean2090 <- ssp585cal[substr(ssp585cal$date,1,3)%in%"209",5]

# PREDICTIONS
bvar <- do.call(onebasis,c(list(x=c(tmean2010,tmean2090)),argvar))
#red <- crossreduce(cb,m,cen=19)
pred_exp <- crosspred(bvar,coef=coef,vcov=vcov,model.link="log",
                      cen=cen,by=0.1)

# RESTRICT MORTALITY DATA
death2010 <- deathproj_U15[substr(ssp585$date,1,3)%in%"201"]
death2090 <- deathproj_U15[substr(ssp585$date,1,3)%in%"209"]

# COMPUTE ATTRIBUTABLE DEATHS
breaks <- seq(min(c(tmean2010,tmean2090),na.rm=T),
              max(c(tmean2010,tmean2090),na.rm=T),length=30)
cenvec <- do.call(onebasis,c(list(x=cen),argvar))
bvar <- do.call(onebasis,c(list(x=tmean2010),argvar))
bvarcen <- scale(bvar,center=cenvec,scale=F)
anhist <- (1-exp(-bvarcen%*%coef(red)))*death2010
bvar <- do.call(onebasis,c(list(x=tmean2090),argvar))
bvarcen <- scale(bvar,center=cenvec,scale=F)
anproj <- (1-exp(-bvarcen%*%coef(red)))*death2090

# PLOT THE FIGURE
#pdf("Figure 5.pdf",height=6,width=4)
layout(matrix(1:4,ncol=1),heights=c(0.6,rep(0.3,2),0.20))

par(mar=c(0.2,5,2,1),mgp=c(3,1,0),las=1,cex.axis=0.8,cex.lab=1)

plot(pred_exp,type="n",ylim=c(0.8,3),axes=F,lab=c(6,5,7),xlab="",ylab="RR",
     main="␣")
ind1 <- pred_exp$predvar<=min(tmean2010)
```

```
ind2 <- pred_exp$predvar>=min(tmean2010) & pred_exp$predvar<=cen
ind3 <- pred_exp$predvar>=cen & pred_exp$predvar<=max(tmean2010)
ind4 <- pred_exp$predvar>=max(tmean2010)
if(any(ind1)) lines(pred_exp$predvar[ind1],pred_exp$allRRfit[ind1],
                    col=4,lwd=1.5,lty=2)
lines(pred_exp$predvar[ind2],pred_exp$allRRfit[ind2],col=4,lwd=1.5)
lines(pred_exp$predvar[ind3],pred_exp$allRRfit[ind3],col=2,lwd=1.5)
lines(pred_exp$predvar[ind4],pred_exp$allRRfit[ind4],col=2,lwd=1.5,lty=2)
axis(2,at=0:5*4*0.1+1)
abline(v=cen,lty=3)
abline(v=max(tmean2010),lty=2)

par(mar=c(0.1,5,0.3,1))

rgbcol <- col2rgb(c(grey(0.8),"lightgreen"))
col <- apply(rgbcol,2,
             function(x) do.call(rgb,c(as.list(x),alpha=255/2,max=255)))

d00 <- density(tmean2010)
d90 <- density(tmean2090)
plot(d00,type="n",bty="l",main="",axes=F,xlim=range(pred_exp$predvar),
     ylim=c(0,max(d00$y,d90$y)*1.05),ylab="Temp distribution\nSSP585",xlab="")
polygon(d00,col=col[1],lty=4)
polygon(d90,col=col[2],lty=5)
axis(2,at=pretty(c(0,max(d00$y,d90$y)*1.05),n=4))
legend("topleft",c("2000-09","2090-99"),pch=22,inset=0.005,cex=0.9,bty="n",
       pt.bg=col)
abline(v=cen,lty=3)
abline(v=max(tmean2010),lty=2)
abline(h=0)

w00 <- abs(anhist)/sum(death2010)
d00 <- density(tmean2010,weights=w00/sum(w00))
w90 <- abs(anproj)/sum(death2090)
d90 <- density(tmean2090,weights=w90/sum(w90))
plot(d00,type="n",bty="l",main="",axes=F,xlim=range(pred_exp$predvar),
     ylim=c(0,max(d00$y,d90$y)*1.05),ylab="Excess mortality (%)",xlab="")
axis(2,at=pretty(c(0,max(d00$y,d90$y)*1.05),n=4))
polygon(d00,col=col[1],lty=4)
polygon(d90,col=col[2],lty=5)
abline(v=cen,lty=3)
abline(v=max(tmean2010),lty=2)
abline(h=0)

par(mar=c(4,5,0,1),mgp=c(2.5,1,0))

plot(pred_exp$predvar,rep(0,length(pred_exp$predvar)),type="n",yaxt="n",ylab="",
     xlab=xlab,frame.plot=F)
axis(1,at=-50:50,tck=0,labels=F)

layout(1)
#dev.off()
```

```
# NB: uncomment pdf() and dev.off() for saving the plot in pdf format.

#                    REPRESENT CHANGE IN AF
    ##############################################
# AFREL= RELATIVE AF (relative to 2000-2009 period)
# AFABS= ABSOLUTE AF

# HEAT
afrel["2090-99",,"heat","SSP5_RCP8.5"]
afabs["2090-99",,"heat","SSP5_RCP8.5"]

# COLD
afrel["2090-99",,"cold","SSP5_RCP8.5"]
afabs["2090-99",,"cold","SSP5_RCP8.5"]
```

0.3 Exponential Projections

The following code is our method for projecting mortality. This is an example of our code which was replicated for each age group.

```
# Load required libraries
library(ggplot2)
library(dplyr)

# Set working directory and load the data
setwd("/Users/EmmaKuijt/Desktop/M moire")
load("~/Desktop/M moire/UNDER_15_4PROJ.Rda")

#############################################################
#YEARLY PROJECTIONS
#############################################################

# Convert 'date' column to Date type and extract the year
under15_deaths$date <- as.Date(under15_deaths$date)
under15_deaths$year <- format(under15_deaths$date, "%Y")

# Sum deaths by year
yearly_deaths <- under15_deaths %>%
  group_by(year) %>%
  summarise(total_deaths = sum(all))

# Use data from 2000 to 2015 for the model
past_data <- filter(yearly_deaths, as.numeric(year) >= 2000 &
    as.numeric(year) < 2016)
```

```r
# Perform log transformation
past_data$log_total_deaths <- log(past_data$total_deaths)

# Fit linear regression model
past_linear_model <- lm(log_total_deaths ~ as.numeric(year), data =
    past_data)

# Calculate R-squared for the past model
past_r_squared <- summary(past_linear_model)$r.squared
cat("R-squared for the model from 2000 to 2015:", past_r_squared, "\n")

# Get the coefficients for projection
intercept <- coef(past_linear_model)[1]
slope <- coef(past_linear_model)[2]

# Population base in 2015
pop_base_2015 <- exp(predict(past_linear_model, newdata = data.frame(year
    = 2015)))

# Project future deaths
projection_years <- 2016:2099
r <- slope  # Growth rate
projected_deaths <- data.frame(
  year = projection_years,
  projected_deaths = pop_base_2015 * exp(r * (projection_years - 2015))
)

# Combine past recorded deaths and projected deaths
combined_deaths <- merge(yearly_deaths, projected_deaths, by = "year",
    all = TRUE)
combined_deaths <- combined_deaths[combined_deaths$year >= '2000-01-01',]

# Plot past recorded deaths and projected deaths
PROJ_under15_deaths <- ggplot(combined_deaths, aes(x = as.numeric(year)))
    +
  geom_point(aes(y = total_deaths), color = "blue", na.rm = TRUE) +
  geom_line(aes(y = projected_deaths), color = "red") +
  labs(title = "Exponential Projection of Under 15 Deaths (2016-2099)",
       x = "Year", y = "Total Deaths") +
  theme_minimal()

ggsave("PROJ_under15_deaths.jpeg", plot = PROJ_under15_deaths, width =
    10, height = 6, units = "in", dpi = 300)
```

```
# Print out a summary to validate everything
summary(past_linear_model)


# Extract residuals from the linear regression model
residuals <- residuals(past_linear_model)

# Create a data frame containing year and residuals
residual_data <- data.frame(year = as.numeric(past_data$year), residuals
    = residuals)

# Plot residuals
residual_plot <- ggplot(residual_data, aes(x = year, y = residuals)) +
  geom_point(color = "blue") +
  geom_hline(yintercept = 0, linetype = "dashed", color = "red") +
  labs(title = "Residuals of Linear Regression Model for under 15 years
      old deaths",
       x = "Year", y = "Residuals") +
  theme_minimal()

# Save the plot as an image
ggsave("residual_plot_U15.jpeg", plot = residual_plot, width = 10, height
    = 6, units = "in", dpi = 300)


#######################################################
#DAILY REPARTITION + SEASONALITY
#######################################################

#######################################################
# ACCOUNTS FOR LEAP AND NON_LEAP YEARS

#convert past data in appropriate format
under15_deaths$date <- as.Date(under15_deaths$date)

# regroup data for the day of the year
grouped_deaths <- aggregate(all ~ doy + year, data = under15_deaths, FUN
    = mean)

#compute mean deaths
mean_daily_deaths_past <- aggregate(all ~ doy, data = grouped_deaths, FUN
    = mean)


# Filter data for leap years and non-leap years
leap_years <- unique(subset(under15_deaths,
```

```
    as.integer(format(as.Date(under15_deaths$date), "%Y")) %% 4 == 0 &
                  (as.integer(format(as.Date(under15_deaths$date), "%Y"))
                     %% 100 != 0 |
                  as.integer(format(as.Date(under15_deaths$date), "%Y")) %%
                     400 == 0))$year)

nonleap_years <- unique(subset(under15_deaths,
    as.integer(format(as.Date(under15_deaths$date), "%Y")) %% 4 != 0 |
                  (as.integer(format(as.Date(under15_deaths$date), "%Y"))
                     %% 100 == 0 &
                  as.integer(format(as.Date(under15_deaths$date), "%Y")) %%
                     400 != 0))$year)

# Calculate mean daily deaths for leap years
mean_daily_deaths_leap <- aggregate(all ~ doy, data =
    subset(under15_deaths, year %in% leap_years), FUN = mean)

# Calculate mean daily deaths for non-leap years
mean_daily_deaths_nonleap <- aggregate(all ~ doy, data =
    subset(under15_deaths, year %in% nonleap_years), FUN = mean)

################################################

deces_annuels <- projected_deaths$projected_deaths
annees <- projected_deaths$year
annees_projetees <- projected_deaths$year

################################################
# Function to attribute daily deaths while accounting for seasonality

# Set leap year
leap_year <- 366

# Function to determine if a year is a leap year
is_leap_year <- function(year) {
  year %% 4 == 0 & (year %% 100 != 0 | year %% 400 == 0)
}


# Calculate mean daily deaths for leap years
repartir_deces_journaliers_saisonnalite <- function(deces_annuels,
    mean_daily_deaths_leap, mean_daily_deaths_nonleap, annees) {
  # Function to determine if a year is a leap year
  is_leap_year <- function(year) {
    year %% 4 == 0 & (year %% 100 != 0 | year %% 400 == 0)
  }
```

```
  # Initialise an empty vector to store the daily deaths
  deces_journaliers <- numeric(0)

  for (i in seq_along(annees)) {
    # Determine if the current year is a leap year
    is_leap <- is_leap_year(annees[i])

    # Determine the number of days in the current year
    jours_par_an <- ifelse(is_leap, 366, 365)

    # Convert daily death seasonality to proportion of deaths per day of
        the year
    if (is_leap) {
      daily_proportions <- mean_daily_deaths_leap /
          sum(mean_daily_deaths_leap)
    } else {
      daily_proportions <- mean_daily_deaths_nonleap /
          sum(mean_daily_deaths_nonleap)
    }

    # Distribute annual deaths into daily deaths for each day of the
        projected year
    deces_journaliers_year <- deces_annuels[i] * daily_proportions

    # Append the vector for the current year to the overall vector
    deces_journaliers <- c(deces_journaliers, deces_journaliers_year)
  }

  # Return the vector of daily deaths
  return(deces_journaliers)
}

##############################################
#There is a missing value in dates : resolving the issue :

# Create a dataframe with the complete sequence of dates
complete_dates <- data.frame(date = seq.Date(min(under15_deaths$date),
    max(under15_deaths$date), by = "day"))

# Merge the complete dates dataframe with the original dataframe
under15_deaths_complete <- merge(complete_dates, under15_deaths, by =
    "date", all = TRUE)

# Replace all other variables with NA for the missing dates
under15_deaths_complete[is.na(under15_deaths_complete)] <- 0
```

```
# Print the resulting dataframe
print(under15_deaths_complete)



##########################################
#call the function and merge with past data
# Call the function to distribute annual deaths into daily deaths
deces_journaliers_projetes <-
    repartir_deces_journaliers_saisonnalite(deces_annuels,
    mean_daily_deaths_leap$all, mean_daily_deaths_nonleap$all,
    annees_projetees)

under15_from1990 <- under15_deaths_complete[under15_deaths_complete$date
    >= '2000-01-01',]

# Combine the projected daily deaths with the historical data
combined_daily_deaths <- c(under15_from1990$all,
    deces_journaliers_projetes)


# Update deathdoy vector
deathdoy <- combined_daily_deaths


saveRDS(deathdoy, file = "deathdoy_U15.rds")
```

0.4 Recoding ICD 9 codes to larger groups

The following code details the different ICD9 codes which we aggregated into different groups.

```
rm(list=ls(all=TRUE))

# ICD 9 codes to chapters
    ######################################################
#Creating new larger sub groups based on the
    ARTICLE#############################

load("~/Desktop/M moire/R_MEMOIRE/main.rda")
```

```r
library(dplyr)

# Function to map ICD codes to chapters

map_icd_to_chapter <- function(ICD9) {
  # Check if ICD9 is missing
  if (is.na(ICD9)) {
    return(0)
  }

  # Convert ICD9 to character to handle cases like "E" and "V"
  icd_char <- as.character(ICD9)

  if (grepl("^E", icd_char)) {
    return(19)
  } else if (grepl("^V", icd_char)) {
    return(18)
  }

  # Convert ICD9 to numeric
  icd_num <- as.numeric(ICD9)

  # Check if the conversion was successful
  if (!is.na(icd_num)) {
    if (icd_num < 1) {
      return(0)
    } else if (icd_num >= 1 && icd_num < 140) {
      return(1)
    } else if (icd_num >= 140 && icd_num < 240) {
      return(2)
    } else if (icd_num >= 240 && icd_num < 260) {
      return(3)
    } else if (icd_num >= 260 && icd_num < 270) {
      return(3.5)
    } else if (icd_num >= 270 && icd_num < 280) {
      return(3.75)
    } else if (icd_num >= 280 && icd_num < 290) {
      return(4)
    } else if (icd_num >= 290 && icd_num < 320) {
      return(5)
    } else if (icd_num >= 320 && icd_num < 390) {
      return(6)
    } else if (icd_num >= 390 && icd_num < 460) {
      return(7)
    } else if (icd_num >= 460 && icd_num < 520) {
      return(8)
```

```
    } else if (icd_num >= 520 && icd_num < 580) {
      return(9)
    } else if (icd_num >= 580 && icd_num < 630) {
      return(10)
    } else if (icd_num >= 630 && icd_num < 680) {
      return(11)
    } else if (icd_num >= 680 && icd_num < 710) {
      return(12)
    } else if (icd_num >= 710 && icd_num < 740) {
      return(13)
    } else if (icd_num >= 740 && icd_num < 760) {
      return(14)
    } else if (icd_num >= 760 && icd_num < 780) {
      return(15)
    } else if (icd_num >= 780 && icd_num < 800) {
      return(16)
    } else if (icd_num >= 800 && icd_num < 1000) {
      return(17)
    } else {
      return(NA)
    }
  } else {
    return(NA)
  }
}

# Applying the function + labelling
extract <- extract %>%
  mutate(ICD9_Chap = sapply(ICD9, map_icd_to_chapter),
         Chapter_Label = case_when(
           ICD9_Chap == 0 ~ "Missing ICD Code",
           ICD9_Chap == 1 ~ "Infectious and Parasitic Diseases",
           ICD9_Chap == 2 ~ "Neoplasms",
           ICD9_Chap == 3 ~ "Endocrine Diseases",
           ICD9_Chap == 3.5 ~ "Nutritional Disorders",
           ICD9_Chap == 3.75 ~ "Metabolic Diseases, And Immunity
               Disorders",
           ICD9_Chap == 4 ~ "Diseases Of The Blood And Blood-Forming
               Organs",
           ICD9_Chap == 5 ~ "Mental Disorders",
           ICD9_Chap == 6 ~ "Diseases Of The Nervous System And Sense
               Organs",
           ICD9_Chap == 7 ~ "Diseases Of The Circulatory System",
           ICD9_Chap == 8 ~ "Diseases Of The Respiratory System",
           ICD9_Chap == 9 ~ "Diseases Of The Digestive System",
           ICD9_Chap == 10 ~ "Diseases Of The Genitourinary System",
```

```
            ICD9_Chap == 11 ~ "Complications␣Of␣Pregnancy,␣Childbirth,␣And␣
                The␣Puerperium",
            ICD9_Chap == 12 ~ "Diseases␣Of␣The␣Skin␣And␣Subcutaneous␣
                Tissue",
            ICD9_Chap == 13 ~ "Diseases␣Of␣The␣Musculoskeletal␣System␣And␣
                Connective␣Tissue",
            ICD9_Chap == 14 ~ "Congenital␣Anomalies",
            ICD9_Chap == 15 ~ "Certain␣Conditions␣Originating␣In␣The␣
                Perinatal␣Period",
            ICD9_Chap == 16 ~ "Symptoms,␣Signs,␣And␣Ill-Defined␣
                Conditions",
            ICD9_Chap == 17 ~ "Injury␣And␣Poisoning",
            ICD9_Chap == 18 ~ "Supplementary␣Classification␣Of␣Factors␣
                Influencing␣Health␣Status␣And␣Contact␣With␣Health␣
                Services",
            ICD9_Chap == 19 ~ "Supplementary␣Classification␣Of␣External␣
                Causes␣Of␣Injury␣And␣Poisoning",
            TRUE ~ "Unknown␣Chapter"
          ))

# Function to recode ICD-9 chapters ACCORDING TO ARTICLE
recode_icd_chapters <- function(chapter) {
  case_when(
    chapter %in% c(1) ~ "Infectious␣Diseases",
    chapter %in% c(2) ~ "Neoplasms",
    chapter %in% c(3) ~ "Endocrine␣Diseases",
    chapter %in% c(3.5) ~ "Nutritional␣Disorders",
    chapter %in% c(7) ~ "Cardiovascular␣Diseases",
    chapter %in% c(8) ~ "Diseases␣of␣the␣respiratory␣system",
    chapter %in% c(3.75, 4, 5, 6, 9, 10, 11, 12, 13, 14, 15, 17, 19) ~
        "Others",
    chapter %in% c(16, 18) ~ "Garbage",
    chapter %in% c(0, NA) ~ "Missing",
    TRUE ~ "Unknown␣Category"
  )
}


# Applying the function to create a new column 'ICD_Category'
extract <- extract %>%
  mutate(CoD_article = recode_icd_chapters(ICD9_Chap))



# Filter data for children below 5 years old
bet_15_59 <- extract %>%
```

```
  filter(agedece < 60)
bet_15_59 <- bet_15_59 %>%
  filter(agedece >=15)

# adolescents
bet_5_14 <- extract %>%
  filter(agedece < 15)
bet_5_14 <- bet_5_14 %>%
  filter(agedece >=5)

# Filter data for children below 5 years old
under5 <- extract %>%
  filter(agedece < 5)

# infs
infants <- extract %>%
  filter(agedece < 1)

# Filter over 60
over60 <- extract %>%
  filter(agedece >= 60)



save(extract, file="Alldeaths_lit.Rda")
save(infants, file="Infantdeaths_lit.Rda")
save(over60, file="Over60deaths_lit.Rda")
save(under5, file="Under5deaths_lit.Rda")
save(bet_5_14, file ="Between5&14_lit.Rda")
save(bet_15_59, file ="Between15&59_lit.Rda")

# GRAPHICAL REPRESENTATION OF THE VARIATIONS OF THESE CODs
   ######################

coD_order <- c("Neoplasms", "Cardiovascular␣Diseases", "Endocrine␣
    Diseases", "Diseases␣of␣the␣respiratory␣system" ,"Infectious␣
    Diseases", "Nutritional␣Disorders", "Others", "Missing", "Garbage")

# Convert CoD_large to factor with defined order
extract$CoD_article <- factor(extract$CoD_article, levels = coD_order)

extract <- extract %>%
  mutate(Year = lubridate::year(datedece),
         Month = lubridate::month(datedece, label = TRUE, abbr = FALSE))

extract <- extract %>%
```

```
  mutate(Year = as.factor(year(datedece)))

# Bar chart :

pdf("evol_all_deaths_BASED_ON_ARTICLE.pdf")

ggplot(extract, aes(x = Year, fill = CoD_article)) +
  geom_bar(position = "fill", stat = "count") +
  scale_y_continuous(labels = scales::percent_format(scale = 100,
      accuracy = 1), breaks = seq(0, 1, 0.25),
                     name = "Percentage") +
  scale_fill_manual(values = c("Infectious Diseases" =
      "#009b1d","Nutritional Disorders" =  "#ca0020", "Diseases of the
      respiratory system" = "#d88087", "Cardiovascular Diseases" =
      "#0571b0", "Neoplasms" = "#008897", "Endocrine Diseases" =
      "#009b90", "Others" = "#808080", "Garbage" = "#fdae61", "Missing" =
      "#d0d0d0"),name = "CoD Category") +
  labs(title = "Distribution of Mortality according to Broad Causes of
      Death\nfrom 1990 to 2015 in Antananarivo",
       x = "Year",
       y = "Percentage")+
  theme_minimal() +
  theme(legend.position = "top",
        legend.text = element_text(size = 6),  # Adjust legend text size
        legend.title = element_text(size = 6),  # Adjust legend title size
        plot.title = element_text(size = 12, hjust = 0.5),  # Adjust
            title size
        axis.text.x = element_text(angle = 90, vjust = 0.5, hjust = 1),
        axis.title = element_text(size = 10)) +  # Adjust axis title size
  geom_vline(xintercept = which(levels(extract$Year) == "2000"), linetype
      = "dashed", color = "black")

dev.off()
```

Key words: climate change, projections, mortality, LLMICs, DLNMs

Abstract

Background: The well-established effect of global warming on human health underscores the urgency of addressing this relation on the most vulnerable populations. However, the scarcity of studies in highly vulnerable regions, such as Low and Lower Middle-Income Countries (LLMICs), raises methodological questions about measuring this association using methods that have mostly been applied in different epidemiological and demographic contexts.

Methods: Using death notification data from Antananarivo from 2000 to 2015 and daily mean temperatures, we conducted multiple sensitivity tests for our chosen Distributed Lag Non-Linear Model (DLNMs). These tests aimed to assess variations in the temperature-mortality association by age, cause of death and temperature data choice. Additionally, we controlled for changing mortality rates and confusion from the seasonal patterns in the model.

Results: We observed marked disparities in the temperature-mortality association for different age groups, although with a high degree of uncertainty. Projected changes in mortality rates, resulting from epidemiological and demographic transitions, appeared to contribute more to variations in the numbers attributed to non-optimal temperatures than climate change itself. The measured association varied markedly for different causes of deaths, depending on the inclusion of seasonality as a confounder and the choice of the exposure variable.

Conclusions: Contextualised studies measuring the effects of temperature on health are necessary to understand the burden of climate change. Our findings underscore the importance of considering population structure and health profile when using DLNMs in LLMICs. While our study has limitations, we express its relevance, especially for providing a basis for future research to assess potential adaptation.

UNIVERSITÉ CATHOLIQUE DE LOUVAIN
Faculté des sciences économiques, sociales, politiques et de communication
École des sciences politiques et sociales (PSAD)

Place Montesquieu, 1 bte L2.08.05, 1348 Louvain-la-Neuve, Belgique | **www.uclouvain.be/psad**